In vitro induction and *in vivo* engraftment of lung bud tip progenitor cells derived from human pluripotent stem cells

Alyssa J. Miller[1,2], Melinda S. Nagy[2], David R. Hill[2], Yu-Hwai Tsai[2], Yoshiro Aoki[4], Briana R. Dye[5], Alana M. Chin[2], Sha Huang[2], Michael A.H. Ferguson[2], Felix Zhou[2], Eric S. White[2], Vibha Lama[4], Jason R. Spence[1,2,3*]

1. Program in Cellular and Molecular Biology
2. Department of Internal Medicine
3. Department of Cell and Developmental Biology
4. Division of Pulmonary and Critical Care Medicine
University of Michigan Medical School, Ann Arbor, Michigan 48109

5. Department of Biomedical Engineering
University of Michigan College of Engineering, Ann Arbor, Michigan 48109

* Author for correspondence:
Email: spencejr@umich.edu
ORCID: http://orcid.org/0000-0001-7869-3992

Author Contributions: AJM and JRS conceived the study. AJM, MSN, BRD, YHT, SH, MAHF, YA, AMC, and ESW conducted experiments. AJM, DRH, BRD, YHT, MAHF, SH, MSN, YA, AMC, FZ, VL and JRS analyzed and interpreted results. ESW also provided critical materials and reagents. AJM and JRS wrote the manuscript. All authors read, edited and approved the final content of the manuscript.

Conflicts of Interest: The authors have no conflicts to declare.

Abbreviations:
Bone Morphogenic Protein, BMP
Fibroblast Growth Factor, FGF
All-Trans Retinoic Acid, RA
Human Lung Organoid, HLO

Summary:

In the current study, we identified that FGF7, CHIR-99021 and RA maintained isolated mouse and human lung bud tip progenitor cells in a multipotent state *in vitro*, and induced the differentiation of 3-dimensional lung-like epithelium from human pluripotent stem cells (hPSCs). These hPSC-derived lung organoids were initially patterned, with airway-like interior domains and bud tip-like progenitor domains at the periphery. Bud tip-like domains could be isolated, expanded and maintained as a nearly homogeneous population by serial passaging. *In situ* hybridization, immunostaining and transcriptome-wide analysis showed that hPSC-derived bud tip progenitors were remarkably similar to human fetal bud tip progenitors. hPSC-derived bud tip progenitors retained multilineage differentiation capabilities *in vitro*, survived *in vitro* for over 16 weeks and could be easily frozen and thawed. Furthermore, hPSC-derived bud tip progenitors successfully engrafted into the proximal airways of immunocompromised NSG mouse lungs, where they began to express markers of mature proximal lung cells.

Introduction:

During development, the lung undergoes branching morphogenesis, where a series of stereotyped epithelial bifurcations give rise to the branched, tree-like architecture of the adult lung (Metzger et al., 2008). A population of rapidly proliferating progenitor cells resides at the tips of the epithelium throughout the branching process (the 'bud tip progenitors') (Branchfield et al., 2015; Rawlins et al., 2009). This population, which expresses *Id2* and *Sox9* in mice, has the capability to differentiate into both mature airway and alveolar cell types; at early stages of branching morphogenesis, this population of progenitors gives rise to proximal airway cells, while at later time points these progenitors give rise to mature alveolar cells (Rawlins, 2009).

Studies utilizing genetic mouse models have shown that lung branching morphogenesis and proximal-distal patterning are regulated by a series of complex mesenchymal-epithelial interactions that involve multiple signaling events, transcription factors, and dynamic regulation of the physical environment (Domyan and Sun, 2010; Hines and Sun, 2014; Kim and Nelson, 2012; Morrisey and Hogan, 2010; Morrisey et al., 2013; Rawlins, 2010; Rock and Hogan, 2011; Varner and Nelson, 2014). These studies have identified major roles for several signaling pathways in these processes, including Wnt, Fibroblast Growth Factor (Fgf), Bone Morphogenic Protein (Bmp), Sonic Hedgehog (Shh), Retinoic Acid (RA) and Hippo signaling among others (Abler et al., 2009; Bellusci et al., 1997a; Bellusci et al., 1997b; Bellusci et al., 1996; Cornett et al., 2013; Desai et al., 2006; Desai et al., 2004; Domyan et al., 2011; Goss et al., 2009; Harris-Johnson et al., 2009; Herriges et al., 2015; Lange et al., 2015; Lu et al., 2009; Mahoney et al., 2014; Motoyama et al., 1998; Sekine et al., 1999; Shu et al., 2005; Weaver et al., 2000; White et al., 2006; Yin et al., 2011; Yin et al., 2008; Zhang et al., 2016; Zhao et al., 2014). However, due to the complex and intertwined nature of these signaling networks, perturbations in one pathway often affect signaling activity of others (Hines and Sun, 2014; Morrisey et al., 2013; Ornitz and Yin, 2012). To date, how multiple signaling networks interact to generate, maintain, and prompt cell fate decisions in bud tip progenitors remains poorly understood. Furthermore, emerging evidence suggests that there are significant differences in gene expression between the developing human and mouse lungs (Chen et al., 2017), and thus it remains unknown whether interactions governing murine lung development are mirrored in human lung organogenesis.

Our aforementioned understanding of murine lung development has been used as a guide to successfully direct differentiation of human pluripotent stem cells into differentiated lung lineages and 3-dimensional lung organoids (Chen et al., 2017; Dye et al., 2016b; Dye et al., 2015; Firth et al., 2014; Ghaedi et al., 2013; Gilpin et al., 2014; Gotoh et al., 2014; Huang et al., 2013; Konishi et al., 2015; Longmire et al., 2012; McCauley et al., 2017). However, specifically inducing and maintaining the bud tip progenitor cell population from hPSCs has remained elusive. For example, our own studies have shown that hPSCs can be differentiated into human lung organoids (HLOs) that possess airway-like

epithelial structures and alveolar cell types; however, it was not clear if HLOs passed through bud tip progenitor-like stage, mimicking the normal developmental events *in vivo* (Dye et al. 2015). More recent evidence from others has demonstrated that putative bud tip progenitor cells can be induced from hPSCs; however, these cells were rare, had low cloning efficiency, and their multilineage differentiation potential was not assessed (Chen et al., 2017). Thus, generation of a nearly homogenous population of bud tip progenitor cells from hPSCs would shed additional mechanistic light on how these cells are regulated, would provide a platform for further investigation into mechanisms of lung lineages cell fate specification, and would add a layer of control to existing directed differentiation protocols allowing them to pass through this developmentally important progenitor transition.

The current work aimed to increase our understanding of how growth factor signaling networks cooperate to promote *in vitro* expansion and maintenance of bud tip progenitors in an undifferentiated state in isolated embryonic mouse and human tissue, and to determine if this signaling environment was sufficient to induce bud tip progenitors in hPSC-derived lung organoid cultures.

Our results demonstrated that FGF7 promoted an initial expansion of both embryonic mouse and human bud tip progenitors, but could not maintain these cells in an undifferentiated state. In both mouse and human tissue, FGF signaling (FGF7) plus CHIR-99021 (a GSK3β inhibitor that acts to stabilize β-catenin) and All-trans Retinoic Acid (RA) (3-Factor conditions, herein referred to as '3F') led to growth/expansion of organoids that maintained a bud tip progenitor identity, expressing markers including *SOX9, ID2,* and *NMYC.* Our results also confirmed recent studies showing that bud tip progenitor cells in the developing human lung express SOX2, which is exclusively expressed in the proximal airway in the embryonic mouse lung, and we identified novel markers of this population in human tissue (Chen et al., 2017; Hashimoto et al., 2012; Que et al., 2007).

When applied to hPSC-derived foregut spheroid cultures, we observed that 3F conditions promoted growth into larger organoid structures with a patterned epithelium that had airway-like and bud tip-like domains. Bud tip-like domains possessed SOX9/SOX2+ cells with molecular profile similar to human fetal bud tip organoids. Bud tip progenitors could be further enriched and expanded by serial passage and underwent multilineage differentiation *in vitro*. Transplantation studies revealed that hPSC-derived bud tip progenitors could engraft into the epithelium of immunocompromised mice, differentiate, and respond to systemic factors. Taken together, these studies provide an improved mechanistic understanding of human lung bud tip progenitor cell regulation, and highlight the importance of using developing tissues to provide a framework for improving differentiation of hPSCs into specific lineages.

Results:

Isolation and *in vitro* culture of murine distal lung bud epithelium

During branching morphogenesis, the distal epithelial bud tips are comprised of progenitor cells that remain in the progenitor state until the branching program is complete (Chang et al., 2013) and will give rise to all the mature cell types of the lung epithelium (Rawlins et al., 2009). In mice, this population of progenitor cells is known to express several transcription factors, including *Sox9*, *Nmyc* and *Id2* (Chang et al., 2013; Moens et al., 1992; Okubo et al., 2005; Perl et al., 2005; Rawlins et al., 2009; Rockich et al., 2013). In order to identify conditions that could maintain mouse bud tip progenitors *in vitro*, epithelial buds were isolated from lungs of embryonic day (E) 13.5 *Sox9*-eGFP mice and cultured in a Matrigel droplet (Figure 1- Figure Supplement 1A). Isolated *Sox9*-eGFP lung bud tips were shown to express GFP, and to have the same level of *Sox9* mRNA as their wild type (WT) counterparts by QRT-PCR analysis (Figure 1- Figure Supplement 1B,C).

FGF7 promotes growth of murine distal epithelial lung buds

We sought to identify culture conditions that could support the *in vitro* growth of isolated bud tips with the goal of identifying culture conditions that could subsequently be used to grow human fetal bud tip progenitors and/or induce bud tip progenitors in hPSC cultures (all mouse data presented in Figure 1, Figure Supplements 1-5).

To this end, we performed a low-throughput screen to identify factors implicated in normal lung development that could promote growth of bud tips in culture. Signaling pathways examined included FGF, WNT, BMP and RA signaling (Bellusci et al., 1997b; Cardoso et al., 1997; Min et al., 1998; Nyeng et al., 2008; Sekine et al., 1999; Volckaert et al., 2013)the screen included FGF7, FGF10, BMP4, All Trans Retinoic Acid (hereafter referred to as 'RA') and CHIR-99021 (a GSK3β inhibitor that acts to stabilize β-catenin) (Figure 1- Figure Supplement 1D). Treating isolated E13.5 mouse bud tips with no growth factors (basal media, control) or individual growth factors showed that FGF7 robustly promoted growth, expansion and survival of isolated buds for up to two weeks (Figure 1- Figure Supplement 1D). We also conducted an experiment in which all 5 factors (5F) were combined together, with one factor removed at a time (Figure 1- Figure Supplement 3A). Buds grew robustly in 5F media, whereas removing FGF7 from the 5F media (5F -FGF7) led to a loss of growth, even after 5 days in culture (Figure 1- Figure Supplement 3A). It was interesting to note that the same concentration of FGF7 and FGF10 did not have the same effect on lung bud outgrowth. To test the possibility that ligand activity may explain experimental differences, we treated buds with a 50-fold excess of FGF10 (500ng/mL, compared to 10ng/mL). A high concentration of FGF10 led to modest growth of

buds and was sufficient to keep buds alive in culture, but cultures did not exhibit robust growth seen with low levels of FGF7 (Figure 1- Figure Supplement 1E).

Initial experimental conditions used FGF7 concentrations based on previous literature (Huang et al., 2013) (10ng/mL; Figure 1 – Figure Supplement 1D-E). We tested if FGF7 affected growth in a concentration dependent manner by treating isolated buds with increasing concentrations of FGF7 and performing an EdU incorporation assay (Figure 1- Figure Supplement 1F-G). After one week, Fluorescence Activated Cell Sorting of cultures pulsed with EdU showed that 50-100 ng/mL of FGF7 increased proliferation significantly above lower concentrations, but led to a dense, compact phenotype. Expansion of buds in 10ng/mL FGF7 was more robust than 1ng/mL, and cultures appeared less compact and dense compared to higher doses (Figure 1 – Figure Supplement 1F). Based on these results, FGF7 was used at a concentration of 10 ng/mL for the remainder of our experiments.

FGF7 alone does not maintain *Sox9* in culture.

In order to determine if FGF7 was promoting expansion of *Sox9*+ distal progenitors cells, we performed a lineage trace utilizing *Sox9*-Cre^{ER};*Rosa26*^{Tomato} mice. Tamoxifen was given to timed pregnant dams at E12.5, and epithelial lung buds were isolated 24 hours later, at E13.5 (Figure 1 - Figure Supplement 1H). Isolated distal buds were placed *in vitro* in basal media (control) or with FGF7. The *Sox9*-Cre^{ER};*Rosa26*^{Tomato} lineage labeled population expanded over time (Figure 1 - Figure Supplement 1H). After two weeks in culture, FGF7-grown cultures were dense and contained cells that stained for mature markers of both alveolar cell types (AECI - AQP5; AECII - SFTPB) and airway cell types (Clara cells – SCGB1A1; multi-ciliated cells - Acetylated Tubulin; basal stem cells – P63) although the tissue, appeared to lack spatial organization and did not demonstrate functionally mature cells as we did not observe beating cilia or secreted mucous within cultures (Figure 1 – Figure Supplement 2A). Many of these cell types in culture had similar morphologies as cells found at postnatal day 0 of the *in vivo* mouse lung (Figure 1 – Figure Supplement 2B). However, Aqp5+ cells lacked the normal elongated morphology of AECI cells in the native mouse lung. We examined the changes of differentiation marker expression over time using QRT-PCR and observed that the length of time in culture led to significant increases in differentiated cell markers *Scgb1a1*, *Aqp5* and *SftpB*, and a significant reduction in the bud tip progenitor marker, *Sox9* (Figure 1 – Figure Supplement 2C). Additionally, levels of the proximal marker Sox2 were undetected by protein stain and had nearly undetectable mRNA levels by qRT-PCR (Figure 1 – Figure Supplement 4 C,E). Collectively, this data suggests that FGF7 promoted an initial growth of *Sox9*+ bud tip progenitor cells that subsequently began expressing markers of differentiated cell types with longer times in culture.

FGF7, CHIR-99021 and RA are sufficient to maintain the expression of distal progenitor markers in mouse lung buds *in vitro*

Given that FGF7 promoted robust expansion of bud tips *in vitro* but was also permissive for differentiation, we sought to identify additional growth factors that interacted with FGF signaling to maintain the undifferentiated SOX9+ distal progenitor cell state *in vitro.* To do this, we grew bud tips in 5F media, and removed one growth factor at a time to examine the effect on growth and expression of *Sox9* and *Sox2* as well as genes expressed in differentiated cell types (Figure 1 – Figure Supplement 3). Bud tips were grown in 5F-1 media for two weeks in culture. Removing FGF10, CHIR-99021, RA or BMP4 from 5F culture media did not affect the ability of isolated buds to expand (Figure 1-Figure Supplement 3A), although these culture conditions led to an interesting variety of morphological phenotypes that will be the focus of future studies. However, QRT-PCR analysis of buds after 5 days in culture showed that removing BMP4 led to a statistically significant increase in *Sox9* mRNA expression levels when compared to other culture conditions (Figure 1 - Figure Supplement 3B), and led to gene expression levels that were closest in expression levels of freshly isolated WT E13.5 lung buds (Figure 1 - Figure Supplement 3B). Removal of RA also led towards higher *Sox9* mRNA expression, however, this was a non-statically significant finding (Figure 1 – Figure Supplement 3E) compared with buds grown with 5F-BMP4. *Sox2* gene expression was generally low in isolated E13.5 lung buds, and in all culture conditions after 5 days *in vitro* (Figure 1- Figure Supplement 3C). We also assessed markers for several genes expressed in differentiated cells (Figure 1 - Figure Supplement 3D-E). Collectively, this data suggested that removing BMP4 from the media was ideal for supporting an environment with low expression proximal airway markers and high expression of the distal progenitor marker *Sox9*.

Based on our data that FGF7 is critical for *in vitro* expansion of isolated murine bud tips, and that BMP4 led to a decrease in *Sox9* expression, we screened combinations of the remaining factors (FGF7 plus combinations of FGF10, CHIR-99021, RA) to determine a minimal set that helped to maintain the SOX9+ identity of bud tip progenitor cells (Figure 1 – Figure Supplement 4). We found that all conditions supported robust growth (Figure 1- Figure Supplement 4A) and expression of *Sox9*, *Id2* and *Nmyc*, while maintaining low levels of *Sox2* (Figure 1- Figure Supplement 4C-E). To demonstrate that *Sox9+* progenitors are expanded over time *in vitro*, lineage tracing experiments utilizing *Sox9*-Cre^{ER};$Rosa26^{Tomato}$ mice, in which Tamoxifen was administered to timed pregnant dams at E12.5 and epithelial lung buds were isolated at E13.5, showed an expansion of labeled progenitors over the 2 week period in culture (Figure 1-Figure Supplement 4B). We noted that cultured buds treated with 4-factor '4F' or 3-Factor conditions ('3F'; FGF7, CHIR-99021, RA) maintained *Sox9* mRNA expression at the highest levels, similar to those expressed in freshly isolated epithelial buds at E13.5 (Figure 1 – Figure Supplement 4E). Additional QRT-PCR

analysis of differentiation markers further suggested that 3F and 4F conditions promoted optimal expression of distal progenitor identity markers while keeping proximal airway marker gene expression low (Figure 1- Figure Supplement 4E-G). Immunofluorescence and whole mount immunostaining of buds after 2 weeks in culture supported QRT-PCR data and showed that 3F and 4F conditions supported robust SOX9 protein expression (Figure 1- Figure Supplement 4C, D).

To determine whether murine bud tip progenitors that were expanded in 4F media retained multilineage differentiation potential, buds were grown in 4F and subsequently transitioned to media with FGF7 only for 4 days (Figure 1 - Figure Supplement 5A). Cultures exposed to FGF7 only exhibited a reduction of SOX9 protein and mRNA expression compared to progenitors grown in 4F for the duration of the experiment (Figure 1- Figure Supplement 5B, C). We noted that tissue grown in FGF7 lost SOX9 expression and began to take on protein expression patterns that closely matched that of mature alveolar cell types, suggesting differentiation towards a more mature AECI or AECII-like cell lineage (Figure 1- Figure Supplement 5B), and mRNA levels of mature alveolar markers remained high (Figure 5 – Figure Supplement 5D). Expression patterns of differentiated proximal cell types remained low in both conditions (Figure 5 – Figure Supplement 5E). Collectively, the experiments conducted in isolated mouse bud tips suggest that 3 factors (FGF7, CHIR-99021, RA) are sufficient to allow growth of bud tip progenitor cells and to maintain markers characteristic of the undifferentiated progenitor cell state *in vitro.* These screens are the foundation for our subsequent experiments aimed at culturing human fetal bud tip progenitors and inducing this population of cells in hPSC-derived lung cultures.

In vitro growth and maintenance of human fetal distal epithelial lung progenitors

Given that almost nothing is known about the functional regulation of human fetal epithelial bud tip progenitor cells, we asked if conditions supporting mouse bud tip progenitors also supported growth and expansion of human bud tip progenitors *in vitro*. Distal epithelial lung buds were enzymatically and mechanically isolated from the lungs of 3 different biological samples at 12 weeks of gestation (84-87 days; n=3) and cultured in a Matrigel droplet (Figure 1A-B), where they formed cystic organoid structures that will hereafter be referred to as 'fetal progenitor organoids' (Figure 1E; Figure 1 – Figure Supplement 7A). Consistent with recent reports (Chen et al., 2017), whole mount immunostaining revealed that human bud tip epithelial progenitors express both SOX9 and SOX2 at 12 weeks (Figure 1C). This is in stark contrast to mice, where SOX9 is exclusively expressed in the bud tip epithelium and SOX2 is exclusively expressed in the proximal airway epithelium (Perl et al., 2005; Rockich et al., 2013). Further investigation of fetal lungs ranging from 10-19 weeks of gestation revealed that SOX2/SOX9 double-positive cells are present in bud tips until about 16 weeks gestation (Figure 1D; Figure 1 - Figure Supplement 6A). By 16 weeks, SOX9 and SOX2 became localized to the distal and proximal

epithelium, respectively, and were separated by a SOX9/SOX2-negative transition zone, which continued to lengthen throughout development (Figure 1 - Figure Supplement 6A). This data suggests that progenitors co-expressing SOX9/SOX2 will represent a developmental time up to 16 weeks in gestation, and are not likely to represent later stage progenitors, such as bipotential alveolar progenitors (Treutlein et al., 2014). Based on this this difference between mice and humans, we further characterized protein expression in human fetal lungs from 8-20 weeks gestation (Figure 1 – Figure Supplement 6B-D). Staining showed that Pro-SFTPC was co-expressed with SOX9, consistent with expression in the embryonic mouse lung (Rockich et al., 2013), but Pro-SFTPC expression was also observed in SOX9-negative epithelial cells (Figure 1H; Figure 1 – Figure Supplement 6D). The canonical AECI marker, PDPN, is present at 8 weeks in cells directly adjacent to SOX9+ bud tips, but is excluded from the bud tip region at all developmental time points analyzed (Figure 1 - Figure Supplement 6B). Similarly, the canonical AECI marker, RAGE, is detectable by 14 weeks and begins to exhibit membrane localization by 16 weeks, but is also excluded from SOX9+ bud tips and is expressed in cells adjacent to this domain at least until 20 weeks gestation (Figure 1 - Figure Supplement 6B-C). The canonical AECII marker, ABCA3, is also present in PDPN+ epithelial cells adjacent to bud tip regions by 16 weeks (Figure 1 -Figure Supplement 6C).

When experiments were carried out culture of human bud tips *in vitro*, similar to isolated mouse lung bud cultures, we observed that FGF7 promoted an initial expansion of tissue *in vitro* after 2 and 4 weeks, but structures began to collapse by 6 weeks in culture (Figure 1 - Figure Supplement 7A). All other groups tested permitted expansion and survival of buds in culture for 6 weeks or longer (Figure 1 - Figure Supplement 7A). Immunofluorescence demonstrated that human fetal progenitor organoids exposed to 3F or 4F supported robust protein expression of both SOX2 and SOX9, and QRT-PCR showed that these organoids expressed high levels of the distal progenitor markers *SOX9, SOX2, ID2 and NMYC* (Figure 1 - Figure Supplement 7B-C). In contrast, culture in only 2 factors (FGF7+CHIR-99021, or FGF7+RA) did not support robust bud tip progenitor marker expression (Figure 1 - Figure Supplement 7B-C). QRT-PCR also showed that fetal progenitor organoids cultured in 3F or 4F media expressed very low levels of the proximal airway markers *P63, FOXJ1* and *SCGB1A1* and the AECI marker HOPX at levels similar to the fetal lung (Figure 1 - Figure Supplement 7D-E). Consistent with low mRNA expression, protein staining was not detected in fetal progenitor organoids treated for 4 weeks in 3F media for P63, FOXJ1, SCGB1A1, MUC5AC, HOPX, RAGE, and SFTPB (n=8; negative data not shown). On the other hand, SOX2 and pro-SFTPC was robustly expressed in human bud tip progenitor organoids, as demonstrated by immunofluorescence in sections or by whole mount staining, consistent with expression in human fetal bud tips earlier than 16 weeks of gestation (Figure 1F-H; Figure 1 - Figure Supplement 7B-C).

Lastly, to confirm our immunofluorescence and QRT-PCR data, we performed bulk RNA-sequencing on tissue from the distal portion of fetal lungs (epithelium plus mesenchyme) (n=3), on freshly isolated bud tips (n=3) and on 3F grown human fetal bud tip progenitor organoids after 4 weeks in culture (n=2). Analysis revealed a high degree of similarity in gene expression between these samples with respect to progenitor gene expression (Figure 1I). We also observed that whole lungs and freshly isolated bud tips showed robust expression of genes expressed in the mesenchyme, indicating that our isolation procedures did not remove all of the mesenchyme (Figure 1I). However, after 4 weeks in culture; the mesenchymal gene expression signature was markedly reduced, indicating that the mesenchyme did not expand significantly in culture (Figure 1I).

Finally, we tested if fetal progenitor organoid cells could engraft into the airways of injured NSG mice (Figure 1 - Figure Supplement 8A). Adult male mice were injured with naphthaline, which severely damaged the lung epithelium within 24 hours (Figure 1- Figure Supplement 8B). Fetal progenitor organoids were digested into single cells and delivered by intratracheal gavage of mice 24 hours after injury (n=6 mice injected). Seven days after the cells were injected, patches of human cells that had engrafted into the proximal mouse airway in 3 out of the 4 surviving mice as determined by expression of a human specific mitochondrial marker (HuMito, Figure 1 - Figure Supplement 8D)(Dye et al., 2016a). Compared to human fetal lung bud organoids, which robustly expressed SOX9 and SOX2 on the day of injection (Figure 1 - Figure Supplement 8C), engrafted NKX2.1+ human cells did not express SOX9 or Pro-SFTPC but maintained expression of SOX2 (Figure 1 - Figure Supplement 8D; negative Pro-SFTPC staining not shown). Protein staining for differentiated cell markers indicated that engrafted human cells did not express detectable levels of proximal airway markers SCGB1A1, MUC5AC, FOXJ1, CHGA and P63, nor differentiated alveolar cell markers SFTPB, ABCA3, HOPX, RAGE and PDPN, suggesting that these cells had not taken on a differentiated cell fate by 7 days post injection (negative data not shown).

3F media induces a bud tip progenitor-like population of cells in hPSC-derived lung organoids

Given the robustness by which 3F media supported mouse and human lung bud progenitor growth and maintenance *in vitro*, we sought to determine whether these culture conditions could promote a lung bud tip progenitor-like population from hPSCs. NKX2.1+ ventral foregut spheroids were generated as previously described (Dye et al., 2015; Dye et al., 2016b), and were cultured in a droplet of Matrigel and overlaid with serum-free media containing 3F media (FGF7, CHIR-99021, RA). Spheroids were considered to be “day 0” on the day they were placed in Matrigel. Foregut spheroids cultured in 3F media generated organoids (hereafter referred to as 'hPSC-derived patterned lung organoids'; PLOs) that passed through stereotyped phases of epithelial morphogenesis (Figure 2A, Figure 2- Figure Supplement 1C). These organoids grew robustly, survived for

over 16 weeks in culture, and could be frozen and re-cultured (Figure 2- Figure Supplement 1A-D). At 2, 6 and 16 weeks, PLOs were shown to co-express NKX2.1 and SOX2 in >99% of all cells at 2 ad 6 weeks (99.41 +/- 0.82% and 99.06 +/- 0.83%, respectively), while older PLOs had slightly reduced NKX2.1/SOX2 co-expression (93.7 +/- 4.6%) at 16 weeks, but we note that PLOs did not appear as healthy or to grow as quickly at this later time point (Figure 2B-C). In order to passage patterned lung organoids, the organoids were manually removed from their Matrigel droplets and replated in fresh matrigel every two weeks, allowing their structure to remain intact.

Patterned lung organoids were examined for mesenchymal cell markers by immunofluorescence (VIMENTIN, α-SMOOTH MUSCLE ACTIN, PDGFRα;); however at 2, 6 or 16 weeks in culture mesenchyme was not detected in the cultures (negative immunostaining data not shown). PLOs exhibited epithelial folding around 3 weeks in culture; after which regions in the periphery began to form budded structures that underwent repeated rounds of outgrowth and apparent bifurcation (Figure 2A, D, asterisks mark bifurcating buds in D). In 100% of analyzed PLOs (n=8) Peripheral budded regions contained cells that co-stained for SOX9 and SOX2, whereas interior regions of the PLOs contained cells that were positive only for SOX2, suggesting these organoids had proximal-like and distal-like regions corresponding to airway and bud tip progenitor regions in the developing human lung (Figure 2E-F). Budded regions of PLOs contained SOX9+ cells that also expressed low levels of pro-SFTPC, similar to what is seen in human fetal bud tip cells (Figure 2H; Figure 1- Figure Supplement 6B). SOX9+/SOX2+ bud tip regions persisted within PLOs for over 100 days in culture (~16 weeks, the longest time examined) (Figure 2I). QRT-PCR analysis showed that *SOX2*, *NMYC*, and *ID2* expression levels are similar between whole fetal human lung and 54 day PLOs, while SOX9 mRNA was expressed at lower levels in PLOs (Figure 2- Figure Supplement 3A). Comparison of freshly isolated 12 week human fetal bud tips and microdissected bud regions from PLOs demonstrated that PLO buds have similar expression of *SOX9, SOX2, ID2* and *NMYC* (Figure 2 - Figure Supplement 3B), while expression of differentiation markers are significantly lower in PLOs compared to whole human fetal lungs (Figure 2- Figure Supplement 2G-H).

Interior regions of PLOs contained a small proportion of cells that showed positive immunostaining for the club cell marker SCGB1A1 and the goblet cell marker MUC5AC, with similar morphology to adult human proximal airway secretory cells (Figure 2J-M). Approximately 1% of cells were marked by MUC5AC while approximately 9% of cells were marked by SCGB1A1 (Figure 2L-M). Some apical staining of acetylated tubulin was present in the cells within the interior regions of PLOs, but no *bona fide* cilia were noted and FOXJ1 was not detected by protein stain in any PLOs (Figure 2J). Additionally, the basal cell marker P63 was absent from PLOs (Figure 2J), as was staining for markers of lung epithelial cell types including HOPX, RAGE, PDPN, ABCA3, SFTPB, and CHGA (negative data not shown).

In addition to patterned lung organoids, which were made up exclusively of lung-like epithelium with a clear lumen, we also observed that 21.5% of organoids grown in 3F media exhibited a 'dense' phenotype that did not exhibit the patterned epithelial structure or possess a clear lumen (Figure 2- Figure Supplement 2A-B; n=275 organoids). These 'dense' organoids contained cells that stained positive for NKX2.1 as well as the AECI cell markers HOPX and PDPN but did not express ECAD (Figure 2- Figure Supplement 2C-E), consistent with adult human AECI cells (Kaarteenaho et al., 2010). However, these cells did not exhibit classic elongated morphology nor did they express the AECI marker RAGE, and some cells still expressed high levels of nuclear SOX9, suggesting that these cells might represent an immature AECI-like cell. No staining for the mature AECII marker SFTPB was observed in dense structures, and immunofluorescence for mesenchymal cells types was also not observed (Figure 2- Figure Supplement 2C; negative data not shown). Because we were primarily concerned with investigating cell fate decisions by SOX9+ bud tip progenitors, we chose to focus the remainder of our studies on patterned lung organoids.

Expansion of bud tip progenitor-like cells from patterned lung organoids

Patterned lung organoids could be passaged by mechanically shearing the epithelial structures using a 27-gauge needle, followed by embedding in fresh Matrigel and growth in 3F media (Figure 3A-B). Following needle shearing, many small cysts were re-established and could be serially passaged every 7-10 days (Figure 3C). Interestingly, we noted that patterned structures were not re-established following passaging. The cysts that formed after needle passaging were NKX2.1+ (Figure 3 – Figure Supplement 1A) and most cells co-expressed nuclear SOX2 and SOX9 (Figure 3D,E), therefore these cysts were called ‘bud tip organoids.’ When compared to PLOs, bud tip organoids possessed a much higher proportion of SOX9+ cells (42.5% +/- 6.5%, n=5; vs. 88.3% +/- 2.3%, n=9; Figure 3E). When proliferation was examined by KI67 immunofluorescence, we observed that bud tip organoids contained significantly higher number of proliferating cells when compared to PLOs (38.24% +/- 4.7%, n=9 for bud tip organoids vs. 4.9% +/- 0.6%, n=5 for PLOs; Figure 3F-I). In PLOs, we noted that proliferation was largely restricted to SOX9+ budded regions, but only a small proportion of SOX9+ cells co-expressed (8.1% +/- 0.9%, n=5), whereas bud tip organoids had a much higher proportion of proliferative SOX9+ cells (40.2% +/- 4.3%, n=9) (Figure 3I). Bud tip organoids were further characterized and compared to the bud tips in human fetal lungs using *in situ* hybridization and immunofluorescence (Figure 3 – Figure Supplement 1). Bud tip organoids exhibited protein staining patterns consistent with 15-16 week fetal lungs, including co-staining of SOX9 and pro-SFTPC (Figure 3 - Figure Supplement 1B). We also noted that all epithelial cells in bud tip organoids and in the human fetal epithelium were positive for *ID2* based on *in situ hybridization* (Figure 3 - Figure supplement 1E). In the developing human fetal lung, bud tip regions were

negative for AECI markers HOPX, RAGE and PDPN, similar to what was observed in the bud tip organoid epithelium (Figure 3 - Figure Supplement 1C-D). Furthermore, no positive protein staining was evident for mature proximal airway markers P63, FOXJ1, AC-TUB, MUC5AC, SCGB1A1 or CHGA (negative data not shown). Interestingly, we noted that low levels of the AECII marker ABCA3 were expressed in human fetal bud tips by 16 weeks of gestation, and we also observed low levels of ABCA3 expression in bud tip organoids (Figure 3 - Figure Supplement 1D). Transmission electron microscopy further revealed that the ultrastructures of bud tip organoids were similar to 14 week old human fetal buds tip cells, including the presence of infrequent, small lamellar bodies (Figure 3 - Figure Supplement 1F). Together, this data suggested that bud tip organoids have a high degree of molecular similarity to native human fetal lung bud tips.

In addition to targeted analysis comparing bud tip organoids and the human fetal lung, we also conducted and unbiased comparison using RNA-sequencing by comparing: hPSC-derived bud tip organoids; whole peripheral (distal) human fetal lung tissue; freshly isolated fetal bud tips; human fetal lung progenitor organoids; undifferentiated hPSCs; and hPSC-derived lung spheroids. Principal component analysis revealed the highest degree of similarity between hPSC-derived bud tip organoids, patterned lung organoids and human fetal organoids (Figure 3J). Interestingly, freshly isolated bud tips and whole distal human fetal lungs had a high degree of similarity, but were separated from both fetal and hPSC-derived organoids. These transcriptional differences are likely due to the mesenchymal populations present in the whole distal lung and freshly isolated buds, and due to molecular changes that are induced in the tissue culture environment compared to the environment of the native lung (Figure 1J).

hPSC-derived bud tip organoids maintain multilineage potential *in vitro*

To test whether hPSC-derived bud tip organoid cells had multilineage potential *in vitro*, we asked whether removal of CHIR-99021 and RA from culture media would be permissive for differentiation of bud tip-like cells, since FGF7 alone was permissive for differentiation of mouse lung bud tip cells (Figure 1 - Figure Supplement 2). Bud tip organoids (generated from a previously published line, iPSC20-1 (Spence et al., 2011)) were cultured for 35 days with 3F media and subsequently underwent needle passaging every two weeks. Bud tip organoids continued to receive 3F media and needle passages for an additional 23 days or they received media with FGF7 alone ('differentiation media') for 23 days, with no needle passage (Figure 4A). At the end of the experiment, control bud tip organoids maintained a clear, thin epithelium with visible a lumen whereas FGF7 treated organoids appeared as large dense cysts, some of which contained a dark and opaque lumen (Figure 4B). Cystic bud tip organoids maintained in 3F media remained SOX9/SOX2 positive, and did not display evidence of differentiation (negative for MUC5AC, FOXJ1, SCGB1A1; Figure 5 – Figure Supplement 1). After 23 days of FGF7 treatment, all cells remained

NKX2.1+/ECAD+, signifying that they retained a lung epithelial identity (Figure 4C). Protein staining revealed cells that expressed both alveolar and proximal airway markers were present in cultures grown in differentiation media. Although no *bona fide* alveolar structures were observed, a subset of cells expressed the AECI markers PDPN (8.6% of total cells) and HOPX (5.9% of total cells), with some cells exhibiting elongated nuclei similar to AECI cell morphology in vivo (Figure 4D, H-I) Approximately ~45% of all counted cells stained positive for AECII markers SFTPB and pro-SFTPC, with overlapping punctate staining clearly seen (Figure 4D, H-I). Transmission electron microscopy also revealed cells with lamellar bodies suggestive of differentiation into AECII-like cells (Figure 4F). Interestingly, only 6.3% of cells stained positive for ABCA3, a marker of mature AECII cells (Figure 4D, H). This may suggest that AECII-like cells did not reach full maturity *in vitro.* Another 43.2% of cells stained positive for nuclear SOX2 (Figure 4G, H-I), a marker of the proximal airway, but did not express nuclear SOX9 (Figure 4H-I). 26.8% of cells stained positive for the goblet cell marker MUC5AC, and secreted MUC5AC was detected within the lumens of almost all differentiated organoids (Figure 4E). Transmission electron microscopy confirmed the presence of mucous filled vacuoles within cells (Figure 4F, 'M' marks mucous). 7% of cells were positive for the club cell marker SCGB1A1 (Figure 4E, H-I). Apical acetylated tubulin staining was present in 2.5% of cells, although these cells did not appear to possess fully formed multiciliated structures, no beating cilia were observed in culture, and FOXJ1 staining was absent (Figure 4E, H-I). Additionally, 2.0% of cells expressed very clear staining for Chromagranin A (CHGA), a marker for neuroendocrine cells. These cells morphologically looked similar to native neuroendocrine cells in the adult lung and sat on the basal side of epithelial structures (Figure 4E). No positive staining was detected for basal cell marker P63 (Figure 4E).

Together, this data suggests that SOX2+/SOX9+ bud tip organoids maintained the ability to undergo multilineage differentiation, and could give rise to both alveolar-like and airway-like cell lineages *in vitro*.

Engraftment of hPSC-derived bud tip progenitor cells into the injured mouse airway.

We next sought to explore the potential of hPSC-derived bud tip progenitor organoids to contribute to injury repair by determining whether bud tip organoid cells could engraft into the airways of injured mouse lungs (Figure 5A). We reasoned that damaging the lung epithelium would create additional niches for injected cells to engraft. Sixteen male immunocompromised NSG mice (8 control, 8 treatment group) were given an i.p. injection of 300 mg/kg Naphthaline to induce proximal airway injury (Karagiannis et al., 2012). The lung epithelium was severely damaged 24 hours after naphthaline injury but largely recovered by 7 days after injury (Figure 5B). Bud tip organoids were generated from the iPSC20.1 line, which was transduced with a doxycycline inducible GFP (tet-O-GFP) lentivirus (Chen et al., 2014). iPSC20.1 bud tip organoids were digested to

a single cell suspension and 600,000 cells were intratracheally administed to 8 NSG mice 24 hours following Naphthalene injury (Figure 5A). iPSC20.1 bud tip organoids from the same cohort that were injected were also collected for comparison on the day of injection (Figure 5, Figure Supplement 1). Starting 24 hours after delivery of the cells, mice were given doxycycline in the drinking water for 7 days to determine whether any engrafted human cells could receive a systemic signal from the bloodstream, and animals were sacrificed 8 days after injury. Mice were injected with BrdU 1 hour before sacrifice to assess cell proliferation (Figure 5A). 75% of mice that received iPSC20.1 bud tip progenitor cells survived to 8 days post injury, compared with only 50% of animals that received an injury but no cells, although this survival benefit was not statistically significant (Figure 5C).

The lungs of all surviving animals were analyzed, and 4/6 surviving mice that received human cells had clear patches of engrafted cells as determined by protein staining for HuMITO or NuMA within the proximal airways (Figure 5D). No human cells were found within the alveolar spaces. Human cell engraftment was assessed in each lung by counting the number of patches in a histological section of lung stained with HuMITO or NuMA and with one or more human cells flanked by mouse epithelial cells within the airway. Individual mice possessed cell patches ranging from 3.1 (+/- 0.5) to 9.8 (+/-2.1) cells per patch, depending on the individual mouse; although it is noteworthy to point out that some grafts were as large as 45 cells (Figure 5E). Engrafted human cells retained NKX2.1 expression after integration (Figure 5F). Many human cells found within the airway were positive for BrdU, showing that engrafted lung bud progenitors were actively proliferating after 8 days (Figure 5G). KI67 protein staining further confirmed that 52.8% of engrafted human cells within the mouse airway were proliferating at the time of sacrifice (Figure 5H-I). Interestingly, 7 days post injection of the cells, 79% of human cells in the mouse airway were still co-labeled by nuclear SOX2 and nuclear SOX9 (Figure 5J). However, the protein stain for SOX9 appeared weaker and exhibited some cytoplasmic staining patterns in these cells as compared to *in vitro* grown bud tip organoids (Figure 5-Figure Supplement 1C), suggesting that engrafted cells may be transitioning to a SOX2+, SOX9- state.

Immunofluorescent staining for proximal cell markers revealed that of the SOX2+ cells, 42.8% expressed the club cell marker SCGB1A1, and 25% of cells expressed the goblet cell marker MUC5AC (Figure 5L-O). Markers of multiiliated cells FOXJ1 (Figure 5N) and Acetylated Tubulin (negative data not shown) were not observed, nor was the basal cell marker P63 (negative data not shown). Immunofluorescent staining for differentiated alveolar cell markers (AECI: HOPX, PDPN, RAGE; AECII: Pro-SFTPC, SFTPB, ABCA3) were not observed in any engrafted human cells (data not shown).

Staining for ECAD demonstrated that human cells possessed basal and lateral cellular membranes in continuity with the mouse airway (Figure 5L, P).

Furthermore, we observed that 35% of all human cells expressed GFP, indicating that engrafted human cells had access to systemic factors delivered by the host bloodstream, and indicating that these cells can respond to orally administered drugs. Taken together, our data indicates that hPSC-derived bud tip progenitor cells may hold a therapeutic benefit to repopulate lung epithelium that may be dysfunctional, such as with cystic fibrosis, or lost to disease or immune attack, such as with complications from lung transplantation.

Discussion:

The ability to study human lung development, homeostasis and disease is limited by our ability to carry out functional experiments in human tissues. This has led to the development of many different *in vitro* model systems using primary human tissue, and using cells and tissues derived from hPSCs (Dye et al., 2016c; Miller and Spence, 2017). Current approaches to differentiate hPSCs have used many techniques, including the stochastic differentiation of lung-specified cultures into many different lung cell lineages (Chen et al., 2017; Huang et al., 2013; Wong et al., 2012), FACS based sorting methods to purify lung progenitors from mixed cultures followed by subsequent differentiation (Gotoh et al., 2014; Konishi et al., 2015; Longmire et al., 2012; McCauley et al., 2017), and by expanding 3-dimensional ventral foregut spheroids into lung organoids (Dye et al., 2015; Dye et al., 2016b). During normal development, early lung progenitors transition through a SOX9+ distal bud tip progenitor cell state on their way to terminal differentiation, and it is assumed that in many hPSC-differentiation studies, NKX2.1-positive cells specified to the lung lineage also transition through a SOX9+ distal epithelial progenitor state prior to differentiating; however, this has not been shown definitively. For example, studies have identified methods to sort and purify lung epithelial progenitor cells from a mixed population (Gotoh et al., 2014; Konishi et al., 2015; McCauley et al., 2017). However, whether or not these populations represents a true bud tip epithelial progenitor or is representative of an earlier stage lung progenitor is unknown.

Capturing the bud tip progenitor state in vitro has remained elusive, in part, because the complex signaling networks required to induce and/or maintain this progenitor cell state are not well understood. A more recent study observed putative SOX9+/SOX2+ human bud tip progenitor cells, but these cells were rare, were not easily expanded in culture and their multipotent ability was not tested (Chen et al., 2017). The current study aimed to elucidate the signaling interactions that are required to maintain and expand the bud tip progenitor population in mouse and human fetal lungs, and to induce, expand and maintain a nearly homogenous population of these cells from hPSCs. Passing through a distal progenitor cell state is a critical aspect of normal lung epithelial development *en route* to becoming an alveolar or airway cell type (Rawlins et al., 2009), and so achieving this with hPSC-derived models is an important step toward faithfully modeling the full complement of developmental events that take

place during lung organogenesis *in vivo*. Moreover, capturing this cell state *in vitro* will facilitate future studies aimed at understanding the precise mechanisms by which progenitor cells make cell fate choices in order to differentiate into mature cell types.

Our study has identified a minimum core group of signaling events that synergize to efficiently support the maintenance of mouse and human bud tip progenitor cells cultured *ex vivo*, and we have used the resulting information to differentiate multipotent lung bud tip-like progenitor cells from hPSCs. The ability to induce, *de novo*, populations of cells from hPSCs suggest that biologically robust experimental findings can be used in a manner that predicts how a naïve cell will behave in the tissue culture dish with a high degree of accuracy, and across multiple cell lines (D'Amour et al., 2005; Green et al., 2011; Spence et al., 2011). Thus, the robustness of our results culturing and expanding isolated mouse and human bud tip progenitors is highlighted by the ability to use this information in a predictive manner in order to accurately induced a bud tip-like population of cells from hESCs and iPSCs. Using isolated embryonic tissue side-by-side with *in vitro* hPSC differentiation highlights the power of using the embryo as guide, but also shows the strength of hPSC-directed differentiation. In this context, hPSCs and embryos can be viewed as complementary models that, when paired together, are a powerful platform of discovery and validation.

Our studies also identified significant species-specific differences between the human and fetal mouse lung. Differences included both gene/protein expression differences, as well as functional differences when comparing how cells responded to diverse signaling environments *in vitro.* For example, in mice, SOX9 is exclusively expressed in the bud tip progenitors and SOX2 is exclusively expressed in the proximal airway. In contrast, the bud tip progenitors in the human fetal lung robustly co-express SOX2 and SOX9 until around 16 weeks of gestation. Others have noted similar differences with regards to expression Hedgehog signaling machinery (Zhang et al., 2010). These mouse-human differences highlight the importance of validating observations made in hPSC-derived tissues by making direct comparisons with human tissues, as predictions or conclusions about human cell behavior based on results generated from the developing mouse lung may be misleading.

Significantly, our studies also suggest that hPSC derived lung epithelium may have therapeutic potential, especially for chronic and fatal diseases such as cystic fibrosis or bronchiolitis obliterans, which occurs following lung transplantation. The present study has shown that lung bud tip progenitors derived from iPSCs are able to successfully engraft into the airway of an injured host mammalian lung, integrate into an existing epithelial layer, proliferate, differentiate into multiple cell types, and can respond to systemic circulating drugs and nutrients (Doxycycline, BrdU). While this result is promising, a significant amount of future work is needed to determine whether engrafted cells survive long-term in the host airway, whether they eventually reduce proliferation

and avoid tumor formation, and how they interact with the host lung neuronal and vascular networks. In the future, an deepened mechanistic understanding of how a hPSC-derived lung bud tip progenitor gives rise to any one specific lung lineage may allow cell based therapies that rely less on progenitors, and more on specific cell populations.

Our experimental findings, in combination with previously published work, have also raised new questions that may point to interesting avenues for future mechanistic studies to determine how specific cell types of the lung are born. Previously, we have shown that lung organoids grown in high concentrations of FGF10 predominantly give rise to airway-like tissues, with a small number of alveolar cell types and a lack of alveolar structure (Dye et al., 2015; Dye et al., 2016b). Here, our results suggest that high concentrations of FGF10 alone do not play a major role in supporting robust growth bud tip progenitor cells. When comparing our previously published work and our current work, we also note that lung organoids grown in high FGF10 possess abundant P63+ basal-like cells (Dye et al., 2015), whereas bud tip organoids grown in 3F media lack this population. Similarly, lung organoids grown in high FGF10 lacked secretory cells (Dye et al., 2015), whereas we find evidence for robust differentiation of club and goblet cells in patterned lung organoids grown in 3F media. This data suggests that FGF10 may have different functional roles in the human fetal lung or that there are still unappreciated roles for FGF7 and FGF10 during lung morphogenesis. These findings may also suggest that we still do not fully appreciate how these signaling pathways interact to control cell fate decisions. Additionally, one unique element of the currently described bud tip organoids is that they lack mesenchymal cells, yet they undergo complex epithelial budding and branching-like events, confirming previous in vitro results suggesting the mesenchyme is not essential for branching (Varner et al., 2015). The lack of mesenchyme also presents a powerful opportunity to explore questions related to the role of specific growth factors, cell types, mechanical forces, vascular or neuronal factors that may influence cell fate or lung development. Collectively, these observations lay the groundwork for many future studies.

Taken together, our current work has identified that multiple signals are integrated into a network that is critical *in vitro* tissue growth, expansion and maintenance of mouse and human distal bud tip epithelial progenitors, and we have utilized this information to generate and expand*, de novo*, a population of lung bud tip-like progenitor cells from hPSCs. These conditions generated patterned lung organoids that underwent complex epithelial budding and branching, in spite of a complete absence of mesenchyme. They contained mature secretory cells, and maintained a bud tip progenitor domain for over 115 days in culture. Regular needle passaging allowd us to expand a nearly homogenous population of proliferative bud tip-like progenitor cells for over 16 weeks in culture, which maintained a multipotent lineage capability *in vitro* and which were able to engraft into injured mouse lungs and respond to systemic factors. We believe the result of the current studies, as well as the predictive

approach incorporating primary mouse and human tissue to inform differentiation of hPSCs will be a valuable tool to more carefully understand how specific elements of an environment control the differentiation of hPSCs.

Methods:

EXPERIMENTAL MODEL AND SUBJECT DETAILS

Mouse models:

All animal research was approved by the University of Michigan Committee on Use and Care of Animals. Lungs from Sox9-eGFP (MGI ID:3844824), Sox9CreER;Rosa$^{Tomato/Tomato}$ (MGI ID:5009223 and 3809523)(Kopp et al., 2011), or wild type lungs from CD1 embryos (Charles River) were dissected at embryonic day (E) 13.5, and buds were isolated as described below and as previously described (del Moral and Warburton, 2010). 8-10 week old Immunocompromised NSG *scid* mice (Jackson laboratories 0005557) were used for engraftment studies. Pilot studies identified that females had a more severe reaction and died at a higher rate from naphthalene injection, therefore male mice were used for engraftment experiments.

Human fetal lung tissue:

All research utilizing human fetal tissue was approved by the University of Michigan institutional review board. Normal human fetal lungs were obtained from the University of Washington Laboratory of Developmental Biology, and epithelial bud tips were dissected as described below. All tissues were shipped overnight in Belzer's solution at 4 degrees Celsius and were processed and cultured within 24 hours of obtaining the specimen. Experiments to evaluate the effect on progenitor maintenance in culture by media conditions were repeated using tissues from 3 individual lung specimens; (1) 84 day post fertilization of unknown gender, (2), 87 day post fertilization male, and (3), 87 day post fertilization of unknown gender. RNAseq experiments utilized tissue from 2 additional individual lungs; (4) 59 day male and (5) 87 day of unknown gender. Fetal progenitor organoids grown from sample (5) were injected into injured mouse lungs to assess engraftment.

Cell lines and culture conditions:

Mouse and human primary cultures:

Isolated mouse bud tips were cultured in 4-6 µl droplets of matrigel, covered with media, and kept at 37 degrees Celsius with 5% CO2. Isolated human fetal lung bud tips were cultured in 25-50 µl droplets of matrigel, covered with media, and kept at 37 degrees Celsius with 5% CO2. Cultures were fed every 2-4 days.

Generation and culture of hPSC-derived lung organoids:

The University of Michigan Human Pluripotent Stem Cell Research Oversight (hPSCRO) Committee approved all experiments using human embryonic stem

cell (hESC) lines. Patterned lung organoids were generated from 4 independent pluripotent cell lines in this study: hESC line UM63-1 (NIH registry #0277) was obtained from the University of Michigan and hESC lines H9 and H1 (NIH registry #0062 and #0043, respectively) were obtained from the WiCell Research Institute. iPSC20.1 was previously described (Spence et al., 2011). ES cell lines were routinely karyotyped to ensure normal karyotype and ensure the sex of each line (H9 - XX, UM63-1 – XX, H1 - XY). All cell lines are routinely monitored for mycoplasma infection monthly using the MycoAlert Mycoplasma Detection Kit (Lonza). Stem cells were maintained on hESC-qualified Matrigel (Corning Cat# 354277) using mTesR1 medium (Stem Cell Technologies). hESCs were maintained and passaged as previously described (Spence et al., 2011) and ventral foregut spheroids were generated as previously described (Dye et al., 2015; Dye et al., 2016b). Following differentiation, free-floating foregut spheroids were collected from differentiated stem cell cultures and plated in a matrigel droplet on a 24-well tissue culture grade plate.

METHOD DETAILS

Isolation and culture of mouse lung epithelial buds

Mouse buds were dissected from E13.5 embryos. For experiments using Sox9CreER;Rosa$^{Tomato/Tomato}$ mice, 50 ug/g of tamoxifen was dissolved in corn oil and given by oral gavage on E12.5, 24 hours prior to dissection. Briefly, in a sterile environment, whole lungs were placed in 100% dispase (Corning Cat# 354235) on ice for 30 minutes. Lungs were then transferred using a 25uL wiretrol tool (Drummond Scientific Cat# 5-000-2050) to 100% FBS (Corning Cat#35-010-CV) on ice for 15 minutes, and then transferred to a solution of Dulbecco's Modified Eagle Medium: Nutrient Mixture F12 (DMEM/F12, ThermoFisher SKU# 12634-010) with 10% FBS and 1x Pennicillin-Streptomycin (ThermoFisher Cat# 15140122) on ice. To dissect buds, a single lung or lung lobe was transferred by wiretrol within a droplet of media to a 100mm sterile petri dish. Under a dissecting microscope, the mesenchyme was carefully removed and epithelial bud tips were torn away from the bronchial tree using tungsten needles (Point Technologies, Inc.). Care was taken to remove the trachea and any connective tissue from dissected lungs. Isolated bud tips were picked up using a p20 pipette and added to an eppendorf tube with cold Matrigel (Corning Ref# 354248) on ice. The buds were picked up in a p20 pipette with 4-6 uL of Matrigel and plated on a 24-well tissue culture well (ThermoFisher Cat# 142475). The plate was moved to a tissue culture incubator and incubated for 5 minutes at 37 degrees Celsius and 5% CO2 to allow the Matrigel droplet to solidify. 500uL of media was then added to the dish in a laminar flow hood. Media was changed every 2-3 days.

Isolation and culture of human fetal lung epithelial buds

Distal regions of 12 week fetal lungs were cut into ~2mm sections and incubated with dispase, 100% FBS and then 10% FBS as described above, and moved to a sterile petri dish. Mesenchyme was removed by repeated pipetting of distal lung pieces after dispase treatment. Buds were washed with DMEM until

mesenchymal cells were no longer visible in the media. Buds were then moved to a 1.5 mL eppendorf tube containing 200uL of Matrigel, mixed using a p200 pipette, and plated in ~20uL droplets in a 24 well tissue culture plate. Plates were placed at 37 degrees Celsius with 5% CO2 for 20 minutes while droplets solidified. 500uL of media was added to each well containing a droplet. Media was changed every 2-4 days.

EdU quantification by Flow Cytometry

Epithelial lung buds were dissected from e13.5 CD1 mice and plated in a matrigel droplet as described above. 3-4 individual buds from one mouse were placed in each droplet and were pooled to serve as a single biological replicate. Three droplets (corresponding to 3 independent biological samples) were assigned to each experimental group, receiving either 1, 10, 50 or 100 ng/mL of FGF7 for 7 days. Media was changed every 2-3 days. Cells were incubated with EdU for 1 hour and stained with the Click-It EdU Alexa Fluor 488 system (ThermoFisher Cat# C10337) according to the manufacturer's instructions. As a control, wells that received 10 ng/mL of FGF7 for 7 days were taken through the EdU steps but were not stained were used to set the gates. For analysis, lung buds were broken into a single cell suspension. 1mL of accutase (Sigma Cat# A6964) was added to a 15mL conical tube containing pooled epithelial buds and cells were incubated at 37 degrees Celsius with frequent visual inspection until clumps of cells were no longer visible. 3mL of basal media (see below) was added to each tube, and cells were centrifuged at 300g for 5 minutes at 4 degrees Celsius. The supernatant was then withdrawn, and cells were resuspended with 1 mL sterile PBS, filtered through a 70 uM strainer to remove any cell clumps and transferred to a cell sorting tube. Flow cytometric analysis was performed on a BD FACSARIA III cell sorter (BD biosciences).

RNA-sequencing and Bioinformatic Analysis

RNA was isolated using the mirVana RNA isolation kit, following the "Total RNA" isolation protocol (Thermo-Fisher Scientific, Waltham MA). RNA sequencing library preparation and sequencing was carried out by the University of Michigan DNA Sequencing Core and Genomic Analysis Services (https://seqcore.brcf.med.umich.edu/). 50bp single end cDNA libraries were prepared using the Truseq RNA Sample Prep Kit v2 (Illumina), and samples were sequenced on an Illumina HiSeq 2500. Transcriptional quantitation analysis was conducted using 64-bit Debian Linux stable version 7.10 ("Wheezy"). Pseudoalignment of RNA-sequencing reads was computed using kallisto v0.43.0 and a normalized data matrix of pseudoaligned sequences (Transcripts Per Million, TPM) and differential expression was calculated using the R package DEseq2 (Bray et al., 2016; Love et al., 2014). Data analysis was performed using the R statistical programming language (http://www.R-project.org/) and was carried out as previously described (Dye et al., 2015; Finkbeiner et al., 2015; Tsai et al., 2016). The complete sequence alignment, expression analysis and all corresponding scripts can be found at https://github.com/hilldr/Miller_Lung_Organoids_2017 (in process). All raw data files generated by RNA-sequencing have been deposited to the EMBL-EBI ArrayExpress database (In process).

Naphthaline injury

Naphthaline (Sigma #147141) was dissolved in corn oil at a concentration of 40 mg/ml. NSG *scid* males (8-10 weeks of age) were given i.p. injections at a dose of 300 mg/kg weight.

Intratracheal injection of fetal progenitor organoids and hPSC-derived bud tip organoid cells into immunocompromised mouse lungs

Generating single cells from organoid tissues

2-3 matrigel droplets containing organoid tissues were removed from the culture plate and combined in a 1.5mL eppendorf tube with 1mL of room temperature Accutase (Sigma #A6964). The tube was laid on its side to prevent organoids from settling to the bottom. Tissue was pipetted up and down 15-20 times with a 1mL tip every 5 minutes for a total of 20 minutes. Single cell status was determined by hemocytometer. Cells were diluted to a concentration of 500,000-600,000 cells per 0.03 mL in sterile PBS.

Intratracheal injection of cells

Injection of cells into the mouse trachea was performed as previously described (Badri et al., 2011; Cao et al., 2017). Briefly, animals were anesthetized and intubated. Animals were given 500,000-600,000 single cells in 30-35 uL of sterile PBS through the intubation cannula.

Culture media, growth factors and small molecules

Low-serum basal media

All mouse bud, human fetal bud, and hPSC-derived human lung organoids were grown in low-serum basal media (basal media) with added growth factors. Basal media consisted of Dulbecco's Modified Eagle Medium: Nutrient Mixture F12 (DMEM/F12, ThermoFisher SKU# 12634-010) supplemented with 1X N2 supplement (ThermoFisher Catalog# 17502048) and 1X B27 supplement (ThermoFisher Catalog# 17504044), along with 2mM Glutamax (ThermoFisher Catalog# 35050061), 1x Pennicillin-Streptomycin (ThermoFisher Cat# 15140122) and 0.05% Bovine Serum Albumin (BSA; Sigma product# A9647). BSA was weighed and dissolved in DMEM F/12 media before being passed through a SteriFlip 0.22 uM filter (Millipore Item# EW-29969-24) and being added to basal media. Media was stored at 4 degrees Celsius for up to 1 month. On the day of use, basal media was aliquoted and 50ug/mL Ascorbic acid and 0.4 uM Monothioglycerol was added. Once ascorbic acid and monothioglycerol had been added, media was used within one week.

Growth factors and small molecules

Recombinant Human Fibroblast Growth Factor 7 (FGF7) was obtained from R&D systems (R&D #251-KG/CF) and used at a concentration of 10 ng/mL unless otherwise noted. Recombinant Human Fibroblast Growth Factor 10 (FGF10) was

obtained either from R&D systems (R&D #345-FG) or generated in house (see below), and used at a concentration of 10 ng/mL (low) or 500 ng/mL (high) unless otherwise noted. Recombinant Human Bone Morphogenic Protein 4 (BMP4) was purchased from R&D systems (R&D Catalog # 314-BP) and used at a concentration of 10 ng/mL. All-trans Retinoic Acid (RA) was obtained from Stemgent (Stemgent Catalog# 04-0021) and used at a concentration of 50 nM. CHIR-99021, a GSK3β inhibitor that stabilizes β-CATENIN, was obtained from STEM CELL technologies (STEM CELL Technologies Catalog# 72054) and used at a concentration of 3 uM. Y27632, a ROCK inhibitor (APExBIO Cat# A3008) was used at a concentration of 10uM.

Generation and Isolation of human recombinant FGF10

Recombinant human FGF10 was produced in-house. The recombinant human FGF10 (rhFGF10) expression plasmid pET21d-FGF10 in *E. coli* strain BL21*trxB*(DE3) was a gift from James A. Bassuk at the University of Washington School of Medicine(Bagai et al., 2002). *E. coli* strain was grown in standard LB media with peptone derived from meat, carbenicillin and glucose. rhFGF10 expression was induced by addition of isopropyl-1-thio-β-D-galactopyranoside (IPTG). rhFGF10 was purified by using a HiTrap-Heparin HP column (GE Healthcare, 17040601) with step gradients of 0.5M to 2M LiCl. From a 200 ml culture, 3 mg of at least 98% pure rFGF-10 (evaluated by SDS-PAGE stained with Coomassie Blue R-250) was purified. rFGF10 was compared to commercially purchased human FGF10 (R&D Systems) to test/validate activity based on the ability to phosphorylate ERK1/2 in an A549 alveolar epithelial cell line (ATCC Cat#CCL-185) as assessed by western blot analysis.

RNA extraction and quantitative RT-PCR analysis

RNA was extracted using the MagMAX-96 Total RNA Isolation System (Life Technologies). RNA quality and concentration was determined on a Nanodrop 2000 spectrophotometer (Thermo Scientific). 100 ng of RNA was used to generate a cDNA library using the SuperScript VILO cDNA master mix kit (Invitrogen) according to manufacturer's instructions. qRT-PCR analysis was conducted using Quantitect SYBR Green Master Mix (Qiagen) on a Step One Plus Real-Time PCR system (Life Technologies). Expression was calculated as a change relative to GAPDH expression using arbitrary units, which were calculated by the following equation: [2^(GAPDH Ct - Gene Ct)] x 10,000. A Ct value of 40 or greater was considered not detectable. A list of primer sequences used can be found in Table 1.

Tissue preparation, Immunohistochemistry and imaging

Paraffin sectioning and staining

Mouse bud, human bud, and HLO tissue was fixed in 4% Paraformaldehyde (Sigma) for 2 hours and rinsed in PBS overnight. Tissue was dehydrated in an alcohol series, with 30 minutes each in 25%, 50%, 75% Methanol:PBS/0.05%

Tween-20, followed by 100% Methanol, and then 100% Ethanol. Tissue was processed into paraffin using an automated tissue processor (Leica ASP300). Paraffin blocks were sectioned 5-7 uM thick, and immunohistochemical staining was performed as previously described (Spence et al., 2009). A list of antibodies, antibody information and concentrations used can be found in Table 2. PAS Alcian blue staining was performed using the Newcomer supply Alcian Blue/PAS Stain kit (Newcomer Supply, Inc.) according to manufacturer's instructions.

Whole mount staining

For whole mount staining tissue was placed in a 1.5mL eppendorf tube and fixed in 4% paraformaldehyde (Sigma) for 30 minutes. Tissue was then washed with PBS/0.05% Tween-20 (Sigma) for 5 hours, followed by a 2.5-hour incubation with blocking serum (PBS-Tween-20 plus 5% normal donkey serum). Primary antibodies were added to blocking serum and tissue was incubated for at least 24 hours at 4 degrees Celcius. Tissue was then washed for 5 hours with several changes of fresh PBS-Tween-20. Secondary antibodies were added to fresh blocking solution and tissue was incubated for 12-24 hours, followed by 5 hours of PBS-Tween-20 washes. Tissue was then dehydrated to 100% methanol and carefully moved to the center of a single-well EISCO concave microscope slide (ThermoFisher Cat# S99368) using a glass transfer pipette. 5-7 drops of Murray's clear (2 parts Benzyl alcohol, 1 part Benzyl benzoate [Sigma]) were added to the center of the slide, and slides were coverslipped and sealed with clear nail polish.

In situ hybridization

In situ hybridization for ID2 was performed using the RNAscope 2.5 HD manual assay with brown chromogenic detection (Advanced Cell Diagnostics, Inc.) according to manufacturers instructions. The human 20 base pair ID2 probe was generated by Advanced Cell Diagnostics targeting 121-1301 of ID2 (gene accession NM_002166.4) and is commercially available.

Imaging and image processing

Images of fluorescently stained slides were taken on a Nikon A-1 confocal microscope. When comparing groups within a single experiment, exposure times and laser power were kept consistent across all images. All Z-stack imaging was done on a Nikon A-1 confocal microscope and Z-stacks were 3-D rendered using Imaris software. Brightness and contrast adjustments were carried out using Adobe Photoshop Creative Suite 6 and adjustments were made uniformly among all images.

Brightfield images of live cultures were taken using an Olympus S2X16 dissecting microscope. Image brightness and contrast was enhanced equally for all images within a single experiment using Adobe Photoshop. Images were cropped where noted in figure legends to remove blank space surrounding buds or cultures. Brightfield images of Alcian Blue stains were taken using an Olympus DP72 inverted microscope.

Quantification and Statistical Analysis

All plots and statistical analysis were done using Prism 6 Software (GraphPad Software, Inc.). For statistical analysis of qRT-PCR results, at least 3 biological replicates for each experimental group were analyzed and plotted with the standard error of the mean. If only two groups were being compared, a two-sided student's T-test was performed. In assessing the effect of length of culture with FGF7 on gene expression in mouse buds (Figure 1G), a one-way, unpaired Analysis of Variance (ANOVA) was performed for each individual gene over time. The mean of each time point was compared to the mean of the expression level for that gene at day 0 of culture. If more than two groups were being compared within a single experiment, an unpaired one-way analysis of variance was performed followed by Tukey's multiple comparison test to compare the mean of each group to the mean of every other group within the experiment. For all statistical tests, a significance value of 0.05 was used. For every analysis, the strength of p values is reported in the figures according the following: $P > 0.05$ ns, $P \leq 0.05$ *, $P \leq 0.01$ **, $P \leq 0.001$ ***, $P \leq 0.0001$ ****. Details of statistical tests can be found in the figure legends.

Acknowledgements:
JRS is supported by the NIH-NHLBI (R01 HL119215). AJM is supported by the NIH Cellular and Molecular Biology training grant at Michigan (T32 GM007315), and by the Tissue Engineering and Regeneration Training Grant (DE00007057-40). The University of Washington Laboratory of Developmental Biology was supported by NIH Award Number 5R24HD000836 from the Eunice Kennedy Shriver National Institute of Child Health & Human Development.

KEY RESOURCES TABLES

TABLE 1: qRT-PCR primer sequences

Species	Gene Target	Forward Primer Sequence	Reverse Primer Sequence
Mouse	aqp5	TAGAAGATGGCTCGGAGCAG	CTGGGACCTGTGAGTGGTG
Mouse	foxj1	TGTTCAAGGACAGGTTGTGG	GATCACTCTGTCGGCCATCT
Mouse	gapdh	TGTCAGCAATGCATCCTGCA	CCGTTCAGCTCTGGGATGAC
Mouse	id2	AGAAAAGAAAAAGTCCCCAAATG	GTCCTTGCAGGCATCTGAAT
Mouse	nmyc	AGCACCTCCGGAGAGGATA	TCTCTACGGTGACCACATCG
Mouse	p63	AGCTTCTTCAGTTCGGTGGA	CCTCCAACACAGATTACCCG
Mouse	Scgb1a1	ACTTGAAGAAATCCTGGGCA	CAAAGCCTCCAACCTCTACC
Mouse	sftp-b	ACAGCCAGCACACCCTTG	TTCTCTGAGCAACAGCTCCC
Mouse	sox2	AAAGCGTTAATTTGGATGGG	ACAAGAGAATTGGGAGGGGT
Mouse	sox9	TCCACGAAGGGTCTCTTCTC	AGGAAGCTGGCAGACCAGTA
Human	Foxj1	CAACTTCTGCTACTTCCGCC	CGAGGCACTTTGATGAAGC
Human	gapdh	AATGAAGGGGTCATTGATGG	AAGGTGAAGGTCGGAGTCAA
Human	hopx	GCCTTTCCGAGGAGGAGAC	TCTGTGACGGATCTGCACTC
Human	id2	GACAGCAAAGCACTGTGTGG	TCAGCACTTAAAAGATTCCGTG
Human	muc5ac*	GCACCAACGACAGGAAGGATGAG	CACGTTCCAGAGCCGGACAT
Human	nkx2.1	CTCATGTTCATGCCGCTC	GACACCATGAGGAACAGCG
Human	nmyc	CACAGTGACCACGTCGATTT	CACAAGGCCCTCAGTACCTC
Human	p63	CCACAGTACACGAACCTGGG	CCGTTCTGAATCTGCTGGTCC
Human	scgb1a1	ATGAAACTCGCTGTCACCCT	GTTTCGATGACACGCTGAAA
Human	sftp-b	CAGCACTTTAAAGGACGGTGT	GGGTGTGTGGGACCATGT
Human	sox2	GCTTAGCCTCGTCGATGAAC	AACCCCAAGATGCACAACTC
Human	sox9	GTACCCGCACTTGCACAAC	ATTCCACTTTGCGTTCAAGG
Human	sp-c	AGCAAAGAGGTCCTGATGGA	CGATAAGAAGGCGTTTCAGG

Note: All primer sequences were obtained from http://primerdepot.nci.nih.gov (human) or http://mouseprimerdepot.nci.nih.gov (mouse) unless otherwise noted. All annealing temperatures are near 60°C.

*MUC5AC Huang, SX et al. Efficient generation of lung and airway epithelial cells from human pluripotent stem cells. Nature Biotechnol. 1–11 (2013). doi:10.1038/nbt.2754

Table 2: Antibody information

Primary Antibody	Source	Catalog #	Used for Species	Dilution (Sections)	Dilution (Whole mount)	Clone
Goat anti-CC10 (SCGB1A1)	Santa Cruz Biotechnology	sc-9770	Mouse, Human	1:200		C-20
Goat anti-Chromogranin A (CHGA)	Santa Cruz Biotechnology	sc-1488	Human	1:100		C-20
Goat anti-SOX2	Santa Cruz Biotechnology	Sc-17320	Mouse, Human	1:200	1:100	polyclonal
Mouse anti-ABCA3	Seven Hills Bioreagents	WMAB-17G524	Human	1:500		17-H5-24
Mouse anti-Acetylated Tubulin (ACTTUB)	Sigma-Aldrich	T7451	Mouse, Human	1:1000		6-11B-1

Mouse anti-E-Cadherin (ECAD)	BD Transduction Laboratories	610181	Mouse, Human	1:500		36/E-Cadherin
Mouse anti- human mitochondria	Millipore	MAB1273	Human	1:500		113-1
Mouse anti-human nuclear matrix protein-22 (NuMA)	Thermofisher	PA5-22285	Human	1:500		polyclonal
Mouse anti-Surfactant Protein B (SFTPB)	Seven Hills Bioreagents	Wmab-1B9	Mouse, Human	1:250		monoclonal
Rabbit anti-Aquaporin 5 (Aqp5)	Abcam	Ab78486	Mouse	1:500		polyclonal
Rabbit anti-Clara Cell Secretory Protein (CCSP; SCGB1A1)	Seven Hills Bioreagents	Wrab-3950	Mouse, Human	1:250		polyclonal
Rabbit anti-HOPX	Santa Cruz Biotechnology	Sc-30216	Human	1:250		polyclonal
Rabbit anti-NKX2.1	Abcam	ab76013	Human	1:200		EP1584Y
Rabbit anti-PDPN	Santa Cruz Biotechnology	Sc-134482	Human	1:500		polyclonal
Rabbit anti-Pro-Surfactant protein C (Pro-SFTPC)	Seven Hills Bioreagents	Wrab-9337	Human, Mouse	1:500		polyclonal
Rabbit anti-P63	Santa Cruz Biotechnology	sc-8344	Mouse, Human	1:200		H-129
Rabbit anti-SOX9	Millipore	AB5535	Mouse, Human	1:500	1:250	polyclonal
Rat anti-KI67	Biolegend	652402	Mouse	1:100		16A8
*Biotin-Mouse anti MUC5AC	Abcam	ab79082	Human	1:500		Monoclonal
Secondary Antibody	**Source**	**Catalog #**		**Dilution**		
Donkey anti-goat 488	Jackson Immuno	705-545-147		1:500		
Donkey anti-goat 647	Jackson Immuno	705-605-147		1:500		
Donkey anti-goat Cy3	Jackson Immuno	705-165-147		1:500		
Donkey anti-mouse 488	Jackson Immuno	715-545-150		1:500		
Donkey anti-mouse 647	Jackson Immuno	415-605-350		1:500		
Donkey anti-mouse Cy3	Jackson Immuno	715-165-150		1:500		
Donkey anti-rabbit 488	Jackson Immuno	711-545-152		1:500		
Donkey anti-rabbit 647	Jackson Immuno	711-605-152		1:500		
Donkey anti-rabbit Cy3	Jackson Immuno	711-165-102		1:500		
Donkey anti-goat 488	Jackson Immuno	705-545-147		1:500		
Donkey anti-goat 647	Jackson Immuno	705-605-147		1:500		
Donkey anti-goat Cy3	Jackson Immuno	705-165-147		1:500		
Donkey anti-mouse 488	Jackson Immuno	715-545-150		1:500		
Donkey anti-mouse 647	Jackson Immuno	415-605-350		1:500		
Donkey anti-mouse Cy3	Jackson Immuno	715-165-150		1:500		
Donkey anti-rabbit 488	Jackson Immuno	711-545-152		1:500		
Donkey anti-rabbit 647	Jackson Immuno	711-605-152		1:500		
Donkey anti-rabbit Cy3	Jackson Immuno	711-165-102		1:500		
Streptavidin 488	Jackson Immuno	016-540-084		1:500		

References:

Abler, L. L., Mansour, S. L. and Sun, X. (2009). Conditional gene inactivation reveals roles for Fgf10 and Fgfr2 in establishing a normal pattern of epithelial branching in the mouse lung. *Dev. Dyn.* **238**, 1999–2013.

Badri, L., Walker, N. M., Ohtsuka, T., Wang, Z., Delmar, M., Flint, A., Peters-Golden, M., Toews, G. B., Pinsky, D. J., Krebsbach, P. H., et al. (2011). Epithelial Interactions and Local Engraftment of Lung-Resident Mesenchymal Stem Cells. *American Journal of Respiratory Cell and Molecular Biology* **45**, 809–816.

Bagai, S., Rubio, E., Cheng, J.-F., Sweet, R., Thomas, R., Fuchs, E., Grady, R., Mitchell, M. and Bassuk, J. A. (2002). Fibroblast growth factor-10 is a mitogen for urothelial cells. *J. Biol. Chem.* **277**, 23828–23837.

Bellusci, S., Furuta, Y., Rush, M. G., Henderson, R., Winnier, G. and Hogan, B. L. (1997a). Involvement of Sonic hedgehog (Shh) in mouse embryonic lung growth and morphogenesis. *Development* **124**, 53–63.

Bellusci, S., Grindley, J., Emoto, H., Itoh, N. and Hogan, B. L. (1997b). Fibroblast growth factor 10 (FGF10) and branching morphogenesis in the embryonic mouse lung. *Development* **124**, 4867–4878.

Bellusci, S., Henderson, R., Winnier, G., Oikawa, T. and Hogan, B. L. (1996). Evidence from normal expression and targeted misexpression that bone morphogenetic protein (Bmp-4) plays a role in mouse embryonic lung morphogenesis. *Development* **122**, 1693–1702.

Branchfield, K., Li, R., Lungova, V., Verheyden, J. M., McCulley, D. and Sun, X. (2015). A three-dimensional study of alveologenesis in mouse lung. *Developmental Biology*.

Bray, N. L., Pimentel, H., Melsted, P. and Pachter, L. (2016). Near-optimal probabilistic RNA-seq quantification. *Nat Biotechnol* **34**, 525–527.

Cao, P., Aoki, Y., Badri, L., Walker, N. M., Manning, C. M., Lagstein, A., Fearon, E. R. and Lama, V. N. (2017). Autocrine lysophosphatidic acid signaling activates β-catenin and promotes lung allograft fibrosis. *Journal of Clinical Investigation* **127**, 1517–1530.

Cardoso, W. V., Itoh, A., Nogawa, H., Mason, I. and Brody, J. S. (1997). FGF-1 and FGF-7 induce distinct patterns of growth and differentiation in embryonic lung epithelium. *Dev. Dyn.* **208**, 398–405.

Chang, D. R., Martinez Alanis, D., Miller, R. K., Ji, H., Akiyama, H., McCrea, P. D. and Chen, J. (2013). Lung epithelial branching program antagonizes alveolar differentiation. *Proceedings of the National Academy of Sciences*.

Chen, Y.-J., Finkbeiner, S. R., Weinblatt, D., Emmett, M. J., Tameire, F., Yousefi, M., Yang, C., Maehr, R., Zhou, Q., Shemer, R., et al. (2014). De Novo Formationof Insulin-Producing "'Neo-b Cell Islets'" from Intestinal Crypts. *Cell Rep* 1–13.

Chen, Y.-W., Huang, S. X., de Carvalho, A. L. R. T., Ho, S.-H., Islam, M. N., Volpi, S., Notarangelo, L. D., Ciancanelli, M., Casanova, J.-L., Bhattacharya, J., et al. (2017). A three-dimensional model of human lung development and disease from pluripotent stem cells. *Nat. Cell Biol.* **19**, 542–549.

Cornett, B., Snowball, J., Varisco, B. M., Lang, R., Whitsett, J. and Sinner, D. (2013). Wntless is required for peripheral lung differentiation and pulmonary vascular development. *Developmental Biology* **379**, 38–52.

D'Amour, K. A., Agulnick, A. D., Eliazer, S., Kelly, O. G., Kroon, E. and Baetge, E. E. (2005). Efficient differentiation of human embryonic stem cells to definitive endoderm. *Nat Biotechnol* **23**, 1534–1541.

del Moral, P.-M. and Warburton, D. (2010). Explant culture of mouse embryonic whole lung, isolated epithelium, or mesenchyme under chemically defined conditions as a system to evaluate the molecular mechanism of branching morphogenesis and cellular differentiation. *Methods Mol. Biol.* **633**, 71–79.

Desai, T. J., Chen, F., Lü, J., Qian, J., Niederreither, K., Dollé, P., Chambon, P. and Cardoso, W. V. (2006). Distinct roles for retinoic acid receptors alpha and beta in early lung morphogenesis. *Developmental Biology* **291**, 12–24.

Desai, T. J., Malpel, S., Flentke, G. R., Smith, S. M. and Cardoso, W. V. (2004). Retinoic acid selectively regulates Fgf10 expression and maintains cell identity in the prospective lung field of the developing foregut. *Developmental Biology* **273**, 402–415.

Domyan, E. T. and Sun, X. (2010). Patterning and plasticity in development of the respiratory lineage. *Dev. Dyn.* **240**, 477–485.

Domyan, E. T., Ferretti, E., Throckmorton, K., Mishina, Y., Nicolis, S. K. and Sun, X. (2011). Signaling through BMP receptors promotes respiratory identity in the foregut via repression of Sox2. *Development* **138**, 971–981.

Dye, B. R., Dedhia, P. H., Miller, A. J., Nagy, M. S., White, E. S., Shea, L. D. and Spence, J. R. (2016a). A bioengineered niche promotes in vivo engraftment and maturation of pluripotent stem cell derived human lung organoids. *Elife* **5**, e19732.

Dye, B. R., Dedhia, P. H., Miller, A. J., Nagy, M. S., White, E. S., Shea, L. D., Spence, J. R. and Rossant, J. (2016b). A bioengineered niche promotes in vivo engraftment and maturation of pluripotent stem cell derived human lung organoids. *Elife* **5**, e19732.

Dye, B. R., Hill, D. R., Ferguson, M. A., Tsai, Y.-H., Nagy, M. S., Dyal, R., Wells, J. M., Mayhew, C. N., Nattiv, R., Klein, O. D., et al. (2015). In vitro generation of human pluripotent stem cell derived lung organoids. *Elife* **4**.

Dye, B. R., Miller, A. J. and Spence, J. R. (2016c). How to Grow a Lung: Applying Principles of Developmental Biology to Generate Lung Lineages from Human Pluripotent Stem Cells. *Curr Pathobiol Rep* 1–11.

Finkbeiner, S. R., Hill, D. R., Altheim, C. H., Dedhia, P. H., Taylor, M. J., Tsai, Y.-H., Chin, A. M., Mahe, M. M., Watson, C. L., Freeman, J. J., et al. (2015). Transcriptome-wide Analysis Reveals Hallmarks of Human Intestine Development and Maturation In Vitro and In Vivo. *Stem Cell Reports* **4**, 1140–1155.

Firth, A. L., Dargitz, C. T., Qualls, S. J., Menon, T., Wright, R., Singer, O., Gage, F. H., Khanna, A. and Verma, I. M. (2014). Generation of multiciliated cells in functional airway epithelia from human induced pluripotent stem cells. *Proceedings of the National Academy of Sciences* **111**, E1723–30.

Ghaedi, M., Calle, E. A., Mendez, J. J., Gard, A. L., Balestrini, J., Booth, A., Bove, P. F., Gui, L., White, E. S. and Niklason, L. E. (2013). Human iPS cell-derived alveolar epithelium repopulates lung extracellular matrix. *J. Clin. Invest.* **123**, 4950–4962.

Gilpin, S. E., Ren, X., Okamoto, T., Guyette, J. P., Mou, H., Rajagopal, J., Mathisen, D. J., Vacanti, J. P. and Ott, H. C. (2014). Enhanced lung epithelial specification of human induced pluripotent stem cells on decellularized lung matrix. *Ann. Thorac. Surg.* **98**, 1721–9– discussion 1729.

Goss, A. M., Tian, Y., Tsukiyama, T., Cohen, E. D., Zhou, D., Lu, M. M., Yamaguchi, T. P. and Morrisey, E. E. (2009). Wnt2/2b and β-Catenin Signaling Are Necessary and Sufficient to Specify Lung Progenitors in the Foregut. *Developmental Cell* **17**, 290–298.

Gotoh, S., Ito, I., Nagasaki, T., Yamamoto, Y., Konishi, S., Korogi, Y., Matsumoto, H., Muro, S., Hirai, T., Funato, M., et al. (2014). Generation of alveolar epithelial spheroids via isolated progenitor cells from human pluripotent stem cells. *Stem Cell Reports* **3**, 394–403.

Green, M. D., Chen, A., Nostro, M.-C., d'Souza, S. L., Schaniel, C., Lemischka, I. R., Gouon-Evans, V., Keller, G. and Snoeck, H.-W. (2011). Generation of anterior foregut endoderm from human embryonic and induced pluripotent stem cells. *Nat Biotechnol* 1–7.

Harris-Johnson, K. S., Domyan, E. T., Vezina, C. M. and Sun, X. (2009). beta-Catenin promotes respiratory progenitor identity in mouse foregut. *Proceedings of the National Academy of Sciences* **106**, 16287–16292.

Hashimoto, S., Chen, H., Que, J., Brockway, B. L., Drake, J. A., Snyder, J. C., Randell, S. H. and Stripp, B. R. (2012). β-Catenin-SOX2 signaling regulates the fate of developing airway epithelium. *Journal of Cell Science* **125**, 932–942.

Herriges, J. C., Verheyden, J. M., Zhang, Z., Sui, P., Zhang, Y., Anderson, M. J., Swing, D. A., Zhang, Y., Lewandoski, M. and Sun, X. (2015). FGF-Regulated ETV Transcription Factors Control FGF-SHH Feedback Loop in Lung Branching. *Developmental Cell* **35**, 322–332.

Hines, E. A. and Sun, X. (2014). Tissue crosstalk in lung development. *J Cell Biochem* **115**, 1469–1477.

Huang, S. X. L., Islam, M. N., O'Neill, J., Hu, Z., Yang, Y.-G., Chen, Y.-W., Mumau, M., Green, M. D., Vunjak-Novakovic, G., Bhattacharya, J., et al. (2013). efficient generation of lung and airway epithelial cells from human pluripotent stem cells. *Nat Biotechnol* 1–11.

Kaarteenaho, R., Lappi-Blanco, E. and Lehtonen, S. (2010). Epithelial N-cadherin and nuclear β-catenin are up-regulated during early development of human lung. *BMC Dev Biol* **10**, 113.

Karagiannis, T. C., Li, X., Tang, M. M., Orlowski, C., El-Osta, A., Tang, M. L. and Royce, S. G. (2012). Molecular model of naphthalene-induced DNA damage in the murine lung. *Human & Experimental Toxicology* **31**, 42–50.

Kim, C. F. B., Jackson, E. L., Woolfenden, A. E., Lawrence, S., Babar, I., Vogel, S., Crowley, D., Bronson, R. T. and Jacks, T. (2005). Identification of bronchioalveolar stem cells in normal lung and lung cancer. *Cell* **121**, 823–835.

Kim, H. Y. and Nelson, C. M. (2012). Extracellular matrix and cytoskeletal dynamics during branching morphogenesis. *Organogenesis* **8**, 56–64.

Konishi, S., Gotoh, S., Tateishi, K., Yamamoto, Y., Korogi, Y., Nagasaki, T., Matsumoto, H., Muro, S., Hirai, T., Ito, I., et al. (2015). Directed Induction of Functional Multi-ciliated Cells in Proximal Airway Epithelial Spheroids from Human Pluripotent Stem Cells. *Stem Cell Reports* **0**.

Kopp, J. L., Dubois, C. L., Schaffer, A. E., Hao, E., Shih, H. P., Seymour, P. A., Ma, J. and Sander, M. (2011). Sox9+ ductal cells are multipotent progenitors throughout development but do not produce new endocrine cells in the normal or injured adult pancreas. *Development* **138**, 653–665.

Lange, A. W., Sridharan, A., Xu, Y., Stripp, B. R., Perl, A.-K. and Whitsett, J. A. (2015). Hippo/Yap signaling controls epithelial progenitor cell proliferation and differentiation in the embryonic and adult lung. *Journal of Molecular Cell Biology* **7**, 35–47.

Longmire, T. A., Ikonomou, L., Hawkins, F., Christodoulou, C., Cao, Y., Jean, J. C., Kwok, L. W., Mou, H., Rajagopal, J., Shen, S. S., et al. (2012). Efficient derivation of purified lung and thyroid progenitors from embryonic stem cells. *Cell Stem Cell* **10**, 398–411.

Love, M. I., Huber, W. and Anders, S. (2014). Moderated estimation of fold change and dispersion for RNA-seq data with DESeq2. *Genome Biol.* **15**, 31–21.

Lu, B. C., Cebrian, C., Chi, X., Kuure, S., Kuo, R., Bates, C. M., Arber, S., Hassell, J., MacNeil, L., Hoshi, M., et al. (2009). Etv4 and Etv5 are required downstream of GDNF and Ret for kidney branching morphogenesis. *Nat Genet* **41**, 1295–1302.

Mahoney, J. E., Mori, M., Szymaniak, A. D., Varelas, X. and Cardoso, W. V. (2014). The Hippo Pathway Effector Yap Controls Patterning and Differentiation of Airway Epithelial Progenitors. *Dev. Cell* 1–14.

McCauley, K. B., Hawkins, F., Serra, M., Thomas, D. C., Jacob, A. and Kotton, D. N. (2017). Efficient Derivation of Functional Human Airway Epithelium from Pluripotent Stem Cells via Temporal Regulation of Wnt Signaling. *Cell Stem Cell*.

Metzger, R. J., Klein, O. D., Martin, G. R. and Krasnow, M. A. (2008). The branching programme of mouse lung development. *Nature* **453**, 745–750.

Miller, A. J. and Spence, J. R. (2017). In Vitro Models to Study Human Lung Development, Disease and Homeostasis. *Physiology (Bethesda)* **32**, 246–260.

Min, H., Danilenko, D. M., Scully, S. A., Bolon, B., Ring, B. D., Tarpley, J. E., DeRose, M. and Simonet, W. S. (1998). Fgf-10 is required for both limb and lung development and exhibits striking functional similarity to Drosophila branchless. *Genes & Development* **12**, 3156–3161.

Moens, C. B., Auerbach, A. B., Conlon, R. A., Joyner, A. L. and Rossant, J. (1992). A targeted mutation reveals a role for N-myc in branching morphogenesis in the embryonic mouse lung. *Genes Dev.* **6**, 691–704.

Morrisey, E. E. and Hogan, B. L. M. (2010). Preparing for the First Breath: Genetic and Cellular Mechanisms in Lung Development. *Developmental Cell* **18**, 8–23.

Morrisey, E. E., Cardoso, W. V., Lane, R. H., Rabinovitch, M., Abman, S. H., Ai, X., Albertine, K. H., Bland, R. D., Chapman, H. A., Checkley, W., et al. (2013). Molecular determinants of lung development. *Ann Am Thorac Soc* **10**, S12–6.

Motoyama, J., Liu, J., Mo, R., Ding, Q., Post, M. and Hui, C. C. (1998). Essential function of Gli2 and Gli3 in the formation of lung, trachea and oesophagus. *Nat Genet* **20**, 54–57.

Nyeng, P., Norgaard, G. A., Kobberup, S. and Jensen, J. (2008). FGF10 maintains distal lung bud epithelium and excessive signaling leads to progenitor state arrest, distalization, and goblet cell metaplasia. *BMC Dev Biol* **8**, 2.

Okubo, T., Knoepfler, P. S., Eisenman, R. N. and Hogan, B. L. M. (2005). Nmyc plays an essential role during lung development as a dosage-sensitive regulator of progenitor cell proliferation and differentiation. *Development* **132**, 1363–1374.

Ornitz, D. M. and Yin, Y. (2012). Signaling Networks Regulating Development of the Lower Respiratory Tract. *Cold Spring Harb Perspect Biol* **4**, a008318–a008318.

Perl, A.-K. T., Kist, R., Shan, Z., Scherer, G. and Whitsett, J. A. (2005). Normal lung development and function after Sox9 inactivation in the respiratory epithelium. *genesis* **41**, 23–32.

Que, J., Okubo, T., Goldenring, J. R., Nam, K. T., Kurotani, R., Morrisey, E. E., Taranova, O., Pevny, L. H. and Hogan, B. L. M. (2007). Multiple dose-dependent roles for Sox2 in the patterning and differentiation of anterior foregut endoderm. *Development* **134**, 2521–2531.

Rawlins, E. L. (2010). The building blocks of mammalian lung development. *Dev. Dyn.* **240**, 463–476.

Rawlins, E. L., Clark, C. P., Xue, Y. and Hogan, B. L. M. (2009). The Id2+ distal tip lung epithelium contains individual multipotent embryonic progenitor cells. *Development* **136**, 3741–3745.

Rock, J. R. and Hogan, B. L. M. (2011). Epithelial Progenitor Cells in Lung Development, Maintenance, Repair, and Disease. *Annu. Rev. Cell Dev. Biol.* **27**, 493–512.

Rockich, B. E., Hrycaj, S. M., Shih, H.-P., Nagy, M. S., Ferguson, M. A. H., Kopp, J. L., Sander, M., Wellik, D. M. and Spence, J. R. (2013). Sox9 plays multiple roles in the lung epithelium during branching morphogenesis. *Proceedings of the National Academy of Sciences*.

Sekine, K., Ohuchi, H., Fujiwara, M., Yamasaki, M., Yoshizawa, T., Sato, T., Yagishita, N., Matsui, D., Koga, Y., Itoh, N., et al. (1999). Fgf10 is essential for limb and lung formation. *Nat Genet* **21**, 138–141.

Shu, W., Guttentag, S., Wang, Z., Andl, T., Ballard, P., Lu, M. M., Piccolo, S., Birchmeier, W., Whitsett, J. A., Millar, S. E., et al. (2005). Wnt/beta-catenin signaling acts upstream of N-myc, BMP4, and FGF signaling to regulate proximal-distal patterning in the lung. *Dev Biol* **283**, 226–239.

Spence, J. R., Lange, A. W., Lin, S.-C. J., Kaestner, K. H., Lowy, A. M., Kim, I., Whitsett, J. A. and Wells, J. M. (2009). Sox17 Regulates Organ Lineage Segregation of Ventral Foregut Progenitor Cells. *Developmental Cell* **17**, 62–74.

Spence, J. R., Mayhew, C. N., Rankin, S. A., Kuhar, M. F., Vallance, J. E., Tolle, K., Hoskins, E. E., Kalinichenko, V. V., Wells, S. I., Zorn, A. M., et al. (2011). Directed differentiation of human pluripotent stem cells into intestinal tissue in vitro. *Nature* **470**, 105–109.

Treutlein, B., Brownfield, D. G., Wu, A. R., Neff, N. F., Mantalas, G. L., Espinoza, F. H., Desai, T. J., Krasnow, M. A. and Quake, S. R. (2014). Reconstructing lineage hierarchies of the distal lung epithelium using single-cell RNA-seq. *Nature* **509**, 371–375.

Tsai, Y.-H., Hill, D. R., Kumar, N., Huang, S., Chin, A. M., Dye, B. R., Nagy, M. S., Verzi, M. P. and Spence, J. R. (2016). LGR4 and LGR5 Function Redundantly During Human Endoderm Differentiation. *Cell Mol Gastroenterol Hepatol* **2**, 648–662.e8.

Varner, V. D. and Nelson, C. M. (2014). Cellular and physical mechanisms of branching morphogenesis. *Development* **141**, 2750–2759.

Varner, V. D., Gleghorn, J. P., Miller, E., Radisky, D. C. and Nelson, C. M. (2015). Mechanically patterning the embryonic airway epithelium. *Proceedings of the National Academy of Sciences* 201504102.

Volckaert, T., Campbell, A., Dill, E., Li, C., Minoo, P. and De Langhe, S. (2013). Localized Fgf10 expression is not required for lung branching morphogenesis but prevents differentiation of epithelial progenitors. *Development* **140**, 3731–3742.

Weaver, M., Dunn, N. R. and Hogan, B. L. (2000). Bmp4 and Fgf10 play opposing roles during lung bud morphogenesis. *Development* **127**, 2695–2704.

White, A. C., Xu, J., Yin, Y., Smith, C., Schmid, G. and Ornitz, D. M. (2006). FGF9 and SHH signaling coordinate lung growth and development through regulation of distinct mesenchymal domains. *Development* **133**, 1507–1517.

Wong, A. P., Bear, C. E., Chin, S., Pasceri, P., Thompson, T. O., Huan, L.-J., Ratjen, F., Ellis, J. and Rossant, J. (2012). Directed differentiation of human pluripotent stem cells into mature airway epithelia expressing functional CFTR protein. *Nat Biotechnol*.

Yin, Y., Wang, F. and Ornitz, D. M. (2011). Mesothelial- and epithelial-derived FGF9 have distinct functions in the regulation of lung development. *Development* **138**, 3169–3177.

Yin, Y., White, A. C., Huh, S.-H., Hilton, M. J., Kanazawa, H., Long, F. and Ornitz, D. M. (2008). An FGF–WNT gene regulatory network controls lung mesenchyme development. *Developmental Biology* **319**, 426–436.

Zhang, M., Wang, H., Teng, H., Shi, J. and Zhang, Y. (2010). Expression of SHH signaling pathway components in the developing human lung. *Histochem. Cell Biol.* **134**, 327–335.

Zhang, Y., Yokoyama, S., Herriges, J. C., Zhang, Z., Young, R. E., Verheyden, J. M. and Sun, X. (2016). E3 ubiquitin ligase RFWD2 controls lung branching through protein-level regulation of ETV transcription factors. *Proceedings of the National Academy of Sciences* 201603310.

Zhao, R., Fallon, T. R., Saladi, S. V., Pardo-Saganta, A., Villoria, J., Mou, H., Vinarsky, V., Gonzalez-Celeiro, M., Nunna, N., Hariri, L. P., et al. (2014). Yap tunes airway epithelial size and architecture by regulating the identity, maintenance, and self-renewal of stem cells. *Developmental Cell* **30**, 151–165.

Figure legends:

Figure 1. FGF7, CHIR-99021 and RA are sufficient to maintain human fetal bud tip progenitor cells cultured *ex vivo.*

(A-B) Distal epithelial lung bud tips were collected from 3 human fetal lungs ((1) 84 day post fertilization of unknown gender, (2), 87 day post fertilization male, and (3), 87 day post fertilization of unknown gender) and cultured in Matrigel droplets. Scalebar in (B) represents 500um.

(C) Freshly isolated buds from an 87 post-fertilization fetal lung were immunostained for SOX9, SOX2, ECAD and DAPI and wholemount imaged. Z-stacks were 3D rendered, and resulting images demonstrated overlapping SOX2 and SOX9 expression at bud tips. Scalebar represents 100um.

(D) Overlapping SOX9/SOX2 protein expression at distal bud tips was confirmed in formalin fixed, paraffin embedded sections from a 14 week old human fetal lung specimen.

(E) Isolated human fetal lung buds were cultured for over 6 weeks in serum-free media supplemented with FGF7, CHIR-99021 and RA ('3-factor', or '3F' media). Organoids grown from isolated human fetal lung bud tips are called ‘fetal progenitor organoids’. Scale bar represents 500um.

(F) Protein staining of tissue sections shows that almost all cells in fetal progenitor organoids grown in 3F media were double positive for both SOX2 and SOX9. Scale bar represents 100um.

(G) Whole mount staining, confocal Z-stack imaging and 3D rendering demonstrating co-expression of SOX2 and SOX9 in 3F grown fetal progenitor organoids. Scale bar represents 100um.

(H) Distal human lung epithelial cells, including bud tip cells, are positive for pro-Surfactant Protein C (Pro-SFTPC) by 16 weeks gestation. Similarly, fetal progenitor organoids express Pro-SFTPC at 4 weeks in culture. Scale bars represent 100um at lower magnification and 25um at higher magnification.

(I) Heatmap of key genes expressed during lung development in the epithelium and mesenchyme based on RNA-sequencing from peripheral (distal) portion of whole fetal lung tissue (n=4, 59-125 days post fertilization), freshly isolated uncultured fetal lung buds (n=2, 59 and 89 days post fertilization) and fetal progenitor organoids cultured for 2 weeks (n=2, 59 and 89 days post fertilization).

Figure 1 - Figure supplement 1: FGF7 is sufficient to promote growth of mouse SOX9+ bud tip progenitors *ex vivo*

(A) Schematic of *Sox9*-eGFP distal lung buds dissected at E13.5 and cultured in a Matrigel droplet.

(B) Low magnification images of isolated lung buds under brightfield (left) or showing *Sox9*-eGFP expression (right). Scale bar represents 200um.

(C) Isolated E13.5 embryonic mouse lung buds from wild type versus *Sox9*-eGFP mice did not have significantly different levels of Sox9 transcript as shown by qPCR. Each data point represents an independent biological replicate. Error bars plot the standard error of the mean. The mean of each group was compared

using a two-sided student's T-test with a significance level of 0.05. P > 0.05 ns, P ≤ 0.05 *, P ≤ 0.01 **, P ≤ 0.001 ***, P ≤ 0.0001 ****.

(D) Isolated buds were cultured in basal media or individually with different factors (10ng/mL FGF7, 10ng/mL FGF10, 10ng/mL BMP4, 50nM RA, 3uM CHIR-99021) and imaged at Day 0, Day 5 and Day 14 in culture to assess the ability of each factor to support growth and survival in culture. Scale bar represents 200um.

(E) Mouse lung buds were growth with FGF7 or with a 50-fold increase in the concentration of FGF10 to test whether FGF10 could provide the same growth support as 10ng/mL of FGF7. After 5 days in culture, buds grown with 500ng/mL of FGF10 were not as large and did not exhibit branched structures. Scale bar represents 200um.

(F) Lung buds were grown in increasing concentrations of FGF7 and examined after 3 days and 5 days *in vitro.* 0ng/mL (basal media) did not induce bud growth, whereas 1ng/mL induced very modest growth, and all other conditions supported robust growth for 5 days *in vitro*. Scale bar represents 200um.

(G) Cultured buds were pulse labeled for 1 hour with EdU and the percent of total cell labeled was quantified by Flow Cyotometry. Low doses of FGF7 (1-10ng/mL) had a similar proportion of cells labeled whereas treatment with 50-100 ng/mL resulted in a significant increase in labeled cells. Each data point represents an independent biological replicate. An unpaired one-way analysis of variance was performed followed by Tukey's multiple comparison test to compare the mean of each group to the mean of every other group within the experiment. A significance value of 0.05 was used. P > 0.05 ns, P ≤ 0.05 *, P ≤ 0.01 **, P ≤ 0.001 ***, P ≤ 0.0001 ****.

(H) *Sox9*-Cre^{ER};Rosa26^{Tomato} lungs were induced with Tamoxifen 24 hours prior to isolation of the buds, which were isolated and cultured at E13.5. Lineage labeled buds demonstrated that labeled cells expanded in culture over the course of two weeks. Asterisks (*) mark air bubbles within Matrigel droplets that were auto-fluorescent, and arrowheads point to day 0 isolated lung buds. Scale bar represents 200um.

Figure 1 - Figure supplement 2: FGF7 is permissive for differentiation of cultured mouse bud tip progenitors.

(A-B) FGF7 cultured tissue was interrogated for differentiation after 2 weeks of *in vitro* culture (A) and was compared to the developing mouse lung *in vivo* (B). Low magnification images (top row in A,B) or at high magnification (bottom row in A,B). Differentiation markers examined include AQP5 (AECI), SFTPB (AECII), SCGB1A1 (club cell), Acetylated-TUBULIN (Ac-Tub; multiciliated cells), P63 (Basal cells). Scale bars in the top and bottom rows represent 50um.

(C) QRT-PCR across time in culture with 10 ng/ml of FGF7 to examine cell differentiation markers *Scgb1a1*, *Sftpb* and *Aqp5*, and *Sox9*. Each data point represents the mean (+/- SEM) of 3 independent biological replicates (n=3). Statistical significance was determined by a one-way, unpaired Analysis of Variance (ANOVA) for each individual gene over time. The mean of each time

point was compared to the mean of the expression level for that gene at day 0 of culture. P > 0.05 ns, P ≤ 0.05 *, P ≤ 0.01 **, P ≤ 0.001 ***, P ≤ 0.0001 ****.

Figure 1 - Figure supplement 3: Removal of BMP4 from media increases SOX9 expression.
(A) E13.5 isolated mouse lung bud tips cultured with a combination of 5 growth factors in serum free media (10ng/mL FGF7, 10ng/mL FGF10, 10ng/mL BMP4, 50nM RA, 3uM CHIR-99021) with single growth factors removed.
(B) Removing BMP4 from the 5F media (5F-BMP4) led to a significant increase in *Sox9* expression after 5 days when compared to the full 5F media.
(C) *Sox2* expression is shown for all groups.
(D-E) Gene expression for differentiation markers of alveolar cell types, including *Aqp5* (AECI), *Sftpb* (AECII) **(D)** and airway cell types, including *p63* (basal cell), *Foxj1* (multiciliated cells), *Scgb1a1* (club cells) **(E)**. Each data point represents an independent biological replicate and graphs indicate the mean +/- the standard error of the mean for each experimental group.

Figure 1 - Figure supplement 4: Synergistic activity of FGF7, CHIR-99021 and RA maintains SOX9 and progenitor markers of mouse bud tip cells *in vitro.*
(A) E13.5 mouse bud tips grown with different combinations of growth factors, including '4F' media (FGF7/FGF10/CHIR-99021/RA) or '3F' media (FGF7/CHIR-99021/RA), in addition to FGF7/CHIR-99021 and FGF7/RA.
(B) E13.5 bud tips isolated from *Sox9*-Cre^{ER};Rosa26^{Tomato} lungs that were induced with Tamoxifen 24 hours prior to isolation. Scale bar represents 200um.
(C-D) Section and whole mount immunohistochemical staining for SOX9 and SOX2 on various growth conditions. Asterisks marks areas within cultures that contained debris with non-specific staining for DAPI.
(E) *Sox9, Id2, Nmyc* and *Sox2* mRNA expression levels from E13.5 isolated bud tips and from various growth conditions as assessed by QRT-PCR. Each data point in (E) represents an independent biological replicate.
(F) Isolated bud tips and various growth conditions were assessed for proximal airway cell-specific markers by QRT-PCR analysis. Each data point in (F) represents an independent biological replicate.
(G) Isolated bud tips and various growth conditions were assessed for alveolar cell-specific markers by QRT-PCR analysis. Each data point in (G) represents an independent biological replicate.

Figure 1 - Figure supplement 5: Mouse bud tip cells grown in 3F media maintain the ability to express differentiated cell markers.
(A) Isolated bud tips were grown for 5 days in 4F media and then either maintained for an additional 4 days in 4F media or switched to FGF7 alone. Scale bar represents 200um.
(B) Protein staining for SOX9, Pro-SFTPC and AQP5 was carried out (top row), and staining was compared to *in vivo* developing lungs at E16.5 and P0 (bottom row). Scale bar represents 50um.

(C-E) QRT-PCR analysis after 9 days in culture (as shown in (A)) for *Sox9* and *Sox2* (C); *Aqp5* and *Sftpb* (D); *Scgb1a, p63, Foxj1* (E). Each data point in (C-E) represents an independent biological replicate and graphs indicate the mean +/- the standard error of the mean for each experimental group. Statistically significant variation between the means of experimental groups within each experiment was determined by an unpaired, one-way analysis of variance in which the mean of each group was compared to the mean of every other group. A significance level of 0.05 was used. Significance is shown on the graph according to the following: P > 0.05 ns, P ≤ 0.05 *, P ≤ 0.01 **, P ≤ 0.001 ***, P ≤ 0.0001 ****.

Figure 1 - Figure supplement 6: Assessing protein expression in bud tips of human fetal lungs.

(A) SOX9 and SOX2 co expression was assessed in paraffin sections from human fetal lung specimens from 10-20 weeks gestation. Scale bar represents 50um.

(B) The AECI markers PDPN and RAGE, along with the bud tip progenitor marker SOX9 was assessed in paraffin sections from human fetal lung specimens from 10-20 weeks gestation. Scale bar represents 50um.

(C) The AECII marker ABCA3 and PDPN were co-stained in paraffin sections from human fetal lung specimens from 10-20 weeks gestation. Scale bar represents 50um.

(D) Pro-surfactant protein C (Pro-SFTPC) was co-stained with SOX9 in paraffin sections from human fetal lung specimens from 10-20 weeks gestation. Scale bar represents 50um.

Figure 1 - Figure supplement 7: FGF7, CHIR-99021 and RA maintain the highest levels of progenitor markers in cultured human fetal bud tips.

(A) Bright field image of human fetal bud tips cultured in a droplet of matrigel, overlayed with different media combinations, and examined at 2, 4 and 6 weeks. Scale bar represents 500um.

(B) Immunofluorescent co-expression of SOX9 and SOX2 was examined in different media combinations tested. Scalebar represents 50 um.

(C) QRT-PCR analysis of human fetal bud tips after 4 weeks *in vitro* examining expression of *SOX9*, *SOX2, NMYC* and *ID2*. Each data point represents an independent biological replicate and graphs indicate the mean +/- the standard error of the mean for each experimental group. An unpaired, one-way analysis of variance was performed for each experiment followed by Tukey's multiple comparison to compare the mean of each group to the mean of every other group within the experiment. A significance level of 0.05 was used. Significance is shown on the graph according to the following: P > 0.05 ns, P ≤ 0.05 *, P ≤ 0.01 **, P ≤ 0.001 ***, P ≤ 0.0001 ****.

(D-E) QRT-PCR analysis of human fetal bud tips after 4 weeks *in vitro* examining expression of airway cell markers *P63, FOXJ1, SCGB1A1* (D) and alveolar markers *SFTPB* and *HOPX (*E). Each data point represents an independent

biological replicate and graphs indicate the mean +/- the standard error of the mean for each experimental group. An unpaired, one-way analysis of variance was performed for each experiment followed by Tukey's multiple comparison to compare the mean of each group to the mean of every other group within the experiment. A significance level of 0.05 was used. Significance is shown on the graph according to the following: $P > 0.05$ ns, $P \leq 0.05$ *, $P \leq 0.01$ **, $P \leq 0.001$ ***, $P \leq 0.0001$ ****.

Figure 1 - Figure supplement 8: Cultured fetal progenitor organoids successfully engraft into injured mouse airway epithelium

(A) Experimental schematic. 5 male NSG mice were injected with 300 mg/kg of Naphthaline to induce injury to the airway epithelium. 24 hours after injury, mice were given intratracheal injections of 500,000 single cells of fetal progenitor organoids that had been grown in 3F media. Lungs were harvested after 7 days to assess engraftment.

(B) Naphthaline injured lungs exhibit epithelial cell shedding and severe injury in the proximal airway. Scale bar represents 50um.

(C) Brightfield, SOX9 and SOX2 co-expression in fetal progenitor organoids harvested on the day of injection. Fetal progenitor organoids had been grown for 4 weeks in 3F media in culture and were derived from the same sample that was used for cell injection studies. Brightfield scale bare represents 500um; immunofluorescent scale bars represent 100um.

(D) Cell-injected lungs were examined for Human mitochondira (HuMITO), SOX2, SOX9, NKX2.1 and the epithelial marker β–catenin (bCAT). Low magnification cale bars represent 50um; high magnification scale bars represent 25um.

Figure 2: FGF7, CHIR-99021 and RA generate patterned epithelial lung organoids from hPSCs

(A) Brightfield images of hPSC-derived foregut spheroids cultured in 3F media (FGF7, CHIR-99021 and RA) and grown *in vitro.* Images taken at 2, 3, 5, 6 or 10 weeks. Scale bars represent 200um.

(B) Immunostaining for NKX2.1 and SOX2 in PLOs at 2, 6 and 16 weeks, respectively. Scale bars represent 50um.

(C) Quantitative analysis of cells co-expressing NKX2.1 and SOX2 in PLOs at 2, 6 and 16 weeks, as shown in (B). Each data point represents an independent biological replicate, and the mean +/- the standard error of the mean is shown for each group.

(D) The same organoid was imaged from day 39 through day 46. Asterisks identify buds undergoing apparent bifurcation. Scale bars represent 200um.

(E) Patterned lung organoids co-stained for NKX2.1 and ECAD. Inset shows high magnification of the boxed, interior region of the organoid. Scale bars represent 100um, and 200um for the brightfield image.

(F) Patterned lung organoids were co-stained for SOX9+/SOX2+ expression by immunofluorescence. Inset shows high magnification of boxed region. Scale bar represents 100um.
(G) Schematic representing a patterned lung organoid, highlighting bud tip region and and interior regions of patterned lung organoids.
(H) Low and high magnification immunofluorescent images of Pro-SFTPC and SOX9 co-expression in bud tip region of patterned lung organoids. Scale bars represent 50um.
(I) SOX9 and SOX2 co-expression in bud-tip region of patterned lung organoids after more than 16 weeks (115 days) in vitro. Scale bar represents 100um.
(J) Interior regions of patterned lung organoids (top) and adult human airway (bottom) co-stained for SCGB1A1, Acetylated Tubulin (AC-TUB) and P63. Scale bars represent 100um (left panels, low magnification) or 50um (right panels, high magnification).
(K) Interior regions of patterned lung organoids (top) and adult human airway (bottom) co-stained for MUC5AC and β–catenin (bCAT). Scale bars represent 100um (left panels, low magnification) or 50um (right panels, high magnification).
(L-M) Percent of cells expressing cell specific markers MUC5AC or SCGB1A1, plotted as aggregate data ((J); # cells positive in all organoids/total cells counted in all organoids) and for each individual patterned lung organoid counted ((K); # cells positive in individual organoid/all cells counted in individual organoid).

Figure 2 - Figure supplement 1: Patterned lung organoids grown from hPSCs exhibit robust and stereotyped growth
(A) Representative low magnification image of many foregut spheroids on day 1 plated in a Matrigel droplet, and cultured in 3F media for 7 days. Dashed line outlines the Matrigel droplet. Scale bar represents 1mm.
(B) Each experiment yielded many wells of spheroids plated in a 24 well plate on day 1, which were subsequently split into multiple 24 well plates to allow sufficient space for growth by day 35, and each well contained many organoids .
(C) During early stages of growth (day 23-30 shown), epithelial organoids undergo epithelial 'folding', which typically occurs from weeks 3-5. Scale bar represents 200um.
(D) Patterned lung organoids were frozen and stored in liquid nitrogen, then thawed and grown in 3F media. After thawing, organoids were split as whole intact structures, they were passaged through a 27-gauge needle to generate cystic bud tip organoids.

Figure 2 - Figure supplement 2: A portion of lung organoids grown in 3F media exhibited a 'dense' phenotype
(A) hPSC-derived lung organoids exhibited 2 major phenotypes when grown in 3F media, termed ‘patterned' (as characterized in Figures 2 and Figure 2 - supplement 1-2) and ‘dense’. 'Dense' phenotype organoids contained regions that did not have obvious lumens. Scale bar represents 200um.

(B) 45% of organoids grown in 3F media exhibited a purely epithelial 'patterned' phenotype, 35% contained mixed regions of epithelium along with 'dense' regions, and 20% were appeared 'dense.'
(C-D) After 42 days *in vitro,* dense organoids were assessed by immunofluorescence and consisted predominantly of cells expressing the markers HOPX, SFTPB (C) and SOX9, PDPN (D). Notably, dense 3F HLOs did not express SFTPB (C), but maintained expression of SOX9 in some cells (D). Scale bars in C-D represents 50um.
(E) Dense organoids maintained expression of the lung epithelial marker NKX2.1. Scale bar represents 50 um.
(F-H) After 42 days *in vitro,* dense 3F HLOs were compared to patterned lung organoids and whole fetal lung tissue by QRT-PCR to examine expression of progenitor markers, *SOX2, SOX2* and *ID2*, *NMYC* and *NKX2.1* (F), airway differentiation markers *MUC5AC, SCGB1A1, P63* (G), and alveolar markers *SFTPB, SFTPC* and *HOPX* (H), Each data point represents an independent biological replicate, and the mean +/- the standard error of the mean is shown for each group. An unpaired one-way analysis of variance was performed followed by Tukey's multiple comparison test to compare the mean of each group to the mean of every other group for each target. A significance value of 0.05 was used. P > 0.05 ns, P ≤ 0.05 *, P ≤ 0.01 **, P ≤ 0.001 ***, P ≤ 0.0001 ****.

Figure 2 - Figure supplement 3: Patterned lung organoids show similarities between fetal lung and cultured fetal progenitor organoids
(A) QRT-PCR comparison of patterned lung organoids show examining expression of the progenitor markers *SOX9*, *SOX2*, *NMYC* and *ID2.* Each data point represents an independent biological replicate and graphs indicate the mean +/- the standard error of the mean for each experimental group. An unpaired, Student's T test was performed for each gene. A significance level of 0.05 was used. Significance is shown on the graph according to the following: P > 0.05 ns, P ≤ 0.05 *, P ≤ 0.01 **, P ≤ 0.001 ***, P ≤ 0.0001 ****.
(B) QRT-PCR comparison between undifferentiated hPSCs (H9 hESC line), Foregut (FG) Spheroids, human fetal progenitor organoids and patterned organoids was performed to examine mRNA levels of *SOX9, SOX2, NMYC* and *ID2*. Each data point represents an independent biological replicate and graphs indicate the mean +/- the standard error of the mean for each experimental group. An unpaired, one-way analysis of variance was performed for each gene followed by Tukey's multiple comparison to compare the mean of each group to the mean of every other group within the experiment. A significance level of 0.05 was used. Significance is shown on the graph according to the following: P > 0.05 ns, P ≤ 0.05 *, P ≤ 0.01 **, P ≤ 0.001 ***, P ≤ 0.0001 ****.

Figure 3: A highly enriched population of proliferative SOX9+/SOX2+ progenitors can expanded from patterned lung organoids
(A) hPSC-derived epithelial patterned lung organoids were passaged through a 27-gague needle 2-3 times to break them apart.

(B) Epithelial fragments were replated in a fresh Matrigel droplet and formed cystic structures, called bud tip organoids. Scale bar represents 1mm.
(C) Quantitative assessment of organoid passaging and expansion. One single patterned lung organoid was needle passaged into 6 wells (passage 1), generating 75 new bud tip organoids in total (average 12.5 per well). A single well of the resulting bud tip organoids were then passaged into 6 new wells after 2 weeks in culture (1:6 split ratio), generating 200 new organoids in total (average 33 per well). This 1:6 passaging was carried out two additional times, every 1-2 weeks for up to 4 passages before growth slowed. 3 biological replicates were performed for expansion experiments; graph plots the mean +/- the SEM.
(D) Immunostaining for SOX9 and SOX2 in bud tip organoids. Scale bar represents 50um.
(E) Quantitation of the percent of SOX9+ cells in patterned lung organoids versus bud tip organoids (# SOX9+ cells/total cells). Each data point represents an independent biological replicate and graphs indicate the mean +/- the standard error of the mean for each experimental group. An unpaired, one-way analysis of variance was performed for each gene followed by Tukey's multiple comparison to compare the mean of each group to the mean of every other group within the experiment. A significance level of 0.05 was used. Significance is shown on the graph according to the following: $P > 0.05$ ns, $P \leq 0.05$ *, $P \leq 0.01$ **, $P \leq 0.001$ ***, $P \leq 0.0001$ ****.
(F-G) Immunostaining for KI67 and SOX9 in patterned lung organoids (F) and bud tip organoids (G). Scale bar represents 100um.
(H) Quantitation of the percent of all cells that were KI67+ in patterned and bud tip organoids (# KI67+ cells /total cells).
(I) Quantitation of the percent of proliferating SOX9+ cells in patterned and bud tip organoids (# KI67+/SOX9+ cells/total cells). For (H) and (I), each data point represents an independent biological replicate and graphs indicate the mean +/- the standard error of the mean for each experimental group. Significance was determined by an unpaired Student's T test. A significance value of 0.05 was used. $P > 0.05$ ns, $P \leq 0.05$ *, $P \leq 0.01$ **, $P \leq 0.001$ ***, $P \leq 0.0001$ ****.
(J) RNA-sequencing was conducted to compare the global transcriptome of hPSCs, foregut spheroids, hPSC-derived patterned lung organoids, hPSC-derived bud tip organoids, whole peripheral (distal) fetal lung, freshly isolated (uncultured) fetal lung buds and fetal progenitor organoids. Principal component analysis (PCA) is shown for the first 3 principal components (PC1-3).
(K) Heatmap of key genes expressed during lung development in the epithelium based on RNA-sequencing from freshly isolated (uncultured) fetal lung buds (n=2 , 59 and 89 days post fertilization) and fetal progenitor organoids cultured for 2 weeks (n=2, 59 and 89 days post fertilization).

Figure 3 - Figure supplement 1: Comparison of hPSC-derived bud tip organoids to human fetal bud tips.
(A) ECAD and NKX2.1 immunofluorescence in bud tip organoids. Scale bar represents 50um.

(B) Protein localization for Pro- Pro-SFTPC, SFTPB and SOX9 in bud tip organoids and 15 week human fetal lungs. Scale bar represents 50 um.
(C) Protein localization of HOPX and RAGE in bud tip organoids and 15 week human fetal lungs. Scale bar represents 50um.
(D) Protein localization of PDPN and ABCA3 in bud tip organoids and 15 week human fetal lungs. Scale bar represents 50um.
(E) In situ hybridization for ID2 in bud tip organoids and 12 week human fetal lungs (brown dots indicate positive staining). Scale bar represents 50um.
(F) Transmission electron microscopy (TEM) of bud tip progenitor cells in the 14 week human fetal lung and in bud tip organoid cells. Scale bar represents 2 um.

Figure 4: Bud tip organoids retain multilineage potential *in vitro*
(A) Schematic of experimental setup. iPSC20-1 bud tip organoids were initially cultured in 3F media and subsequently grown in 3F media or media containing FGF7 alone ('differentiation media') for 24 days.
(B) Brightfield images of bud tip organoids growing in 3F media (left) and FGF7 alone (right). Scale bar represents 500 um.
(C) NKX2.1 immunofluorescence of bud tip organoids grown in FGF7 for 24 days. Scale bar represents 50 um.
(D) Immunostaining for AECI (PDPN, HOPX, RAGE) and AECII cells (ABCA3, Pro-SFTPC, SPB) in alveolar regions of the native human adult lung (left panels) and in hPSC-derived bud tip organoids exposed to differentiation media (right panels). Scale bar represents 50 um.
(E) Immunostaining for airway cell types (MUC5AC, FOXJ1, SCGB1A1, P63, SOX2, Ac-TUB, CHGA) in bronchiolar regions of the native human adult lung (left panels) and in hPSC-derived bud tip organoids exposed to differentiation media (right panels). Scale bar represents 50 um.
(F) Transmission Electron Microscopy (TEM) was performed on hPSC-derived bud tip organoids exposed to differentiation media. Mucous containing vessicles were observed (marked "M") and lamellar bodies were seen in many cells (marked "LB").
(G) Immunostaining for SOX9 and SOX2 in bud tip organoids grown in differentiation media. Scale bar represents 50 um.
(H-I) Quantitation of cell type markers in bud tip organoids grow in differentiation media plotted as aggregate data ((H) numbers at top of bars represent positive cells/total cells counted across 5 individual organoids), and as individual data per organoid ((I) number of positive cells per organoid). Each data point in (I) represents an independent biological replicate and graphs indicate the mean +/- the standard error of the mean.

Figure 5: hPSC-derived bud tip progenitor cells fully engraft into the mouse airway and express differentiated proximal airway cell markers
(A) Schematic of experimental design. 16 immunocompromised NSG male mice were injected with 300mg/kg of Naphthalene. 24 hours post-injury, mice were randomly assigned (8 per group) to receive an intratracheal injection of 600,000 single cells isolated from bud tip organoids maintained, or no injection of cells.

Doxycycline (1mg/ml) was added to the drinking water for all mice starting on day 2 post-injury. 8 days post-injury, animals were injected with BrdU to assess cell proliferation and sacrificed one hour later.

(B) H&E staining showing the kinetics of Naphthalene injury in NSG mice, before injury and 24 hours and 7 days post-injury. Scale bar represents 50um.

(C) Mouse survival data. 75% (6/8) of animals that received Naphthalene and an injection of cells survived until the day of harvest, compared with 50% (4/8) of animals that did not receive cells (not statistically significant, log-rank test $p>0.05$).

(D-E) Characterization of surviving cell-injected mice. Engraftment was assessed based on human specific antibodies (NuMA, huMITO) in 3 independent histological sections from each surviving mouse. (D) Engraftment was observed in 4/6 animals. (E) Quantitation of the number of human cells in each engrafted cell 'patch'. Each data point represents the number of cells in a single patch of cells.

(F) Immunostaining for the human specific mitochondrial marker, HuMITO and NKX2.1 in transplanted lungs. Scale bar represents 50um.

(G) Immunostaining for human nuclear specific antibody (NuMA) and BrdU in transplanted lungs . Low magnification (top) and high magnification (bottom) images are shown. Scale bars represent 50um.

(H-I) Immunostaining for HuMito and KI67 demonstrates proliferating human cells in transplanted lungs (H). Low magnification (top) and high magnification (bottom) images are shown. Scale bars represent 50um. (I) Quantitation of human cells that co-express the proliferation marker KI67 comparing proliferation *in vitro* bud tip organoids (day 0) and following *in vivo* engraftmet (day 7). Aggregate data is plotted showing total number of cells positive for KI67, and the total number of cells counted from 3 non-serial sections from 3 different mice is plotted for day 7.

(J-K) Immunostaining for HuMITO, SOX9 and SOX2 in transplanted lungs(J). Low magnification (top) and high magnification (bottom) images are shown. Scale bars represent 50um. (K) shows quantification of immunostaining, comparing *in vitro* bud tip organoids (day 0) and following *in vivo* engraftmet (day 7). Aggregate data from 3 non-serial sections from 3 mice is plotted for day 7.

(L-M) Immunostaining for NuMA and MUC5AC in transplanted lungs (L). Low magnification (top) and high magnification (bottom) images are shown. Scale bars represent 50um. (M) shows quantification of immunostaining, comparing *in vitro* bud tip organoids (day 0) and following *in vivo* engraftmet (day 7). Aggregate data from 3 non-serial sections from 3 mice is plotted for day 7.

(N-O) Immunostaining for NuMA, SCGB1A1 and FOXJ1 in transplanted lungs (N). Low magnification (top) and high magnification (bottom) images are shown. Note that he FOXJ1+ cell shown is assumed to be of murine origin, since it does not express NuMA. Scale bars represent 50um. (O) shows quantification of immunostaining, comparing *in vitro* bud tip organoids (day 0) and following *in vivo* engraftmet (day 7). Aggregate data from 3 non-serial sections from 3 mice is plotted for day 7.

(P-Q) Immunostaining for NuMA, ECAD and GFP in transplanted lungs (P). Low magnification (top) and high magnification (bottom) images are shown. Scale bars represent 50um. (Q) shows quantification of GFP+ cells following *in vivo* engraftmet and dox induction for (day 7). Aggregate data from 3 non-serial sections from 3 mice is plotted for day 7.

Figure 5 - figure supplement 1: Characterization of bud tip organoids generated from iPSC20-1 on the day of transplantation into the injured mouse airway

(A) Bud tip organoids immunostained for NKX2.1 and HuMITO. Scale bar represents 50 um.

(B) Bud tip organoids immunostained for KI67 and HuMITO. Scale bar represents 50 um.

(C) Bud tip organoids immunostained or HuMITO, SOX9 and SOX2 at low magnification (top) and high magnification (bottom). Scale bar for all images represents 50 um.

(D) Bud tip organoids immunostained or NuMA, MUC5AC and ECAD at low magnification (top) and high magnification (bottom). Positive staining for MUC5AC is not observed. Images taken at the same scale as shown in (C).

(E) Bud tip organoids immunostained or FOXJ1 and SCGB1A1. Positive staining was not observed. Scale bar represents 50 um.

(F) Bud tip organoids from untreated cultures (no Doxycycline added to media) immunostained or GFP. Positive staining was not observed. Scale bar represents 50 um.

Figure 1

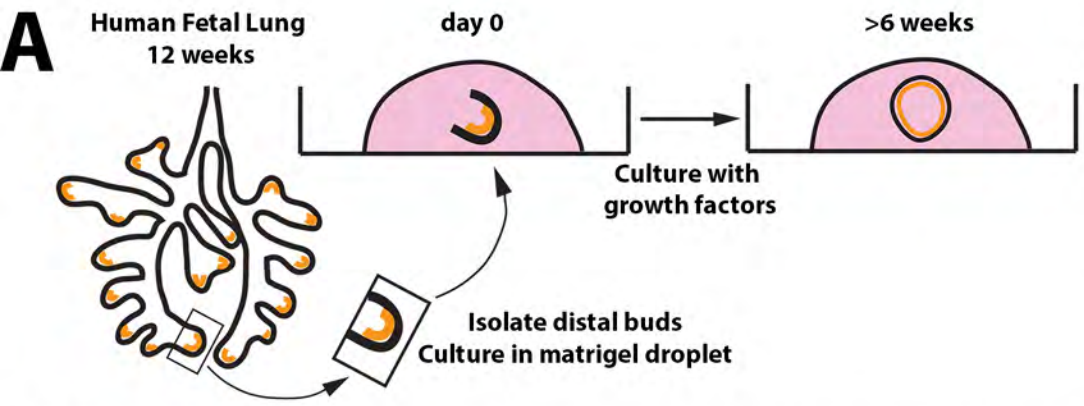

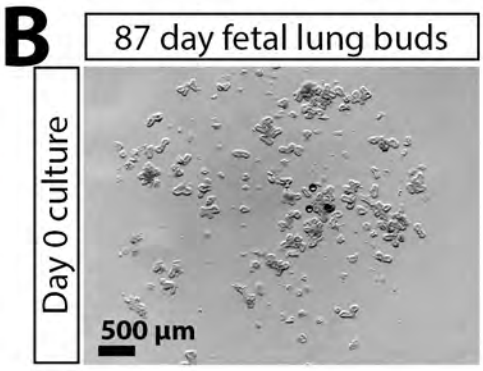

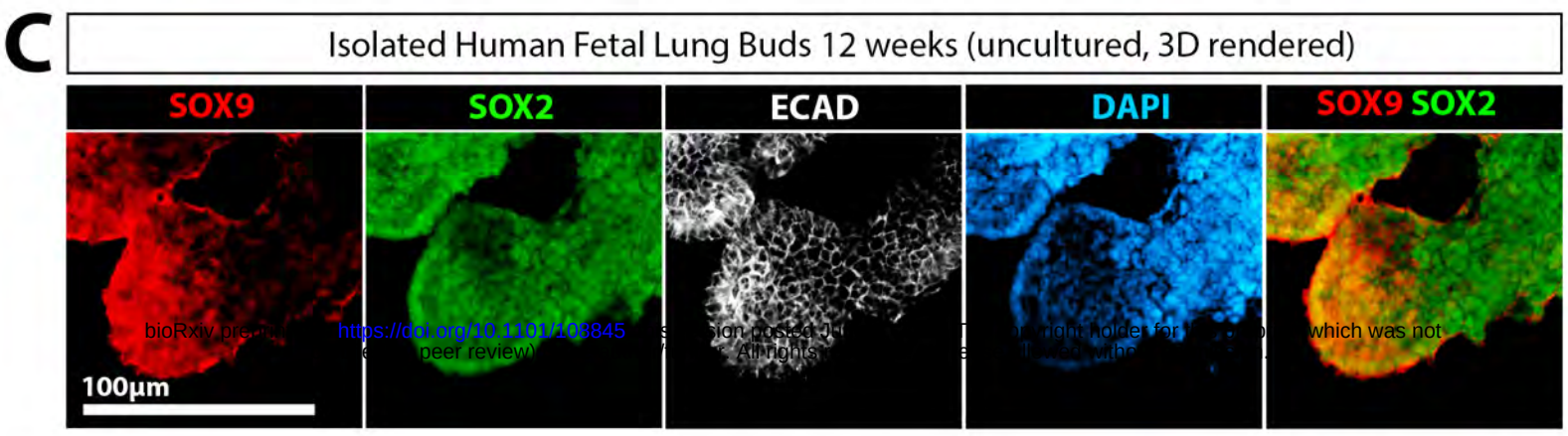

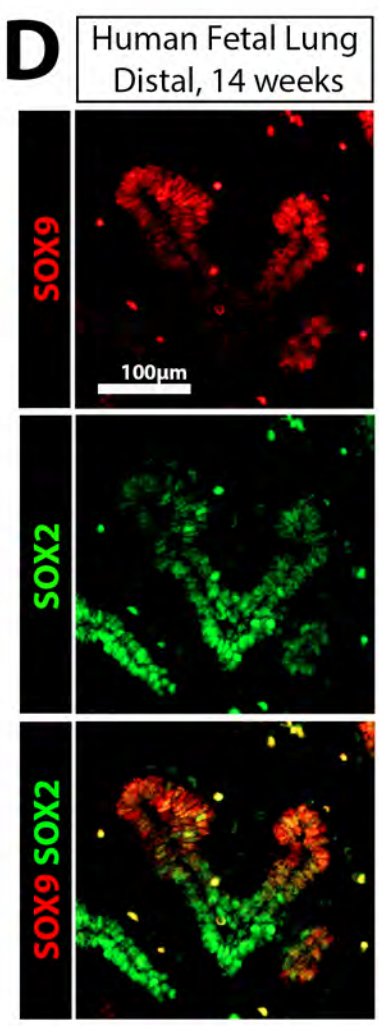

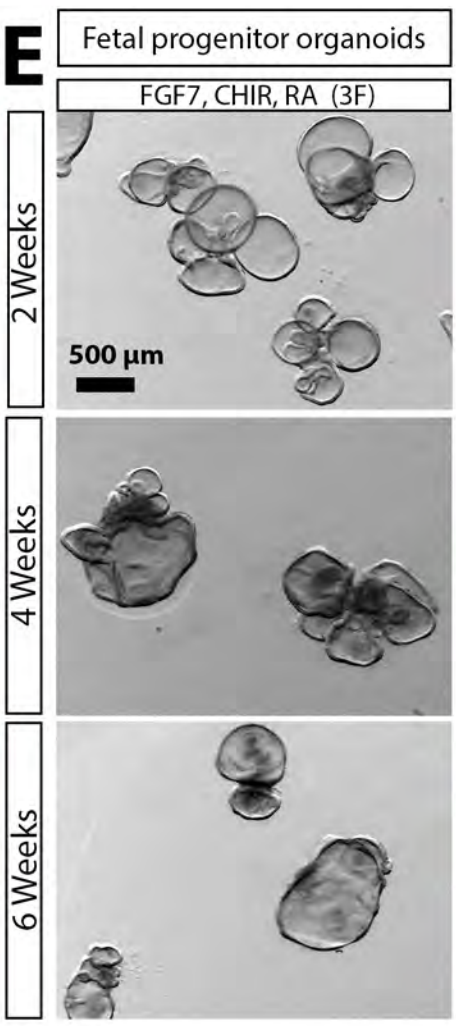

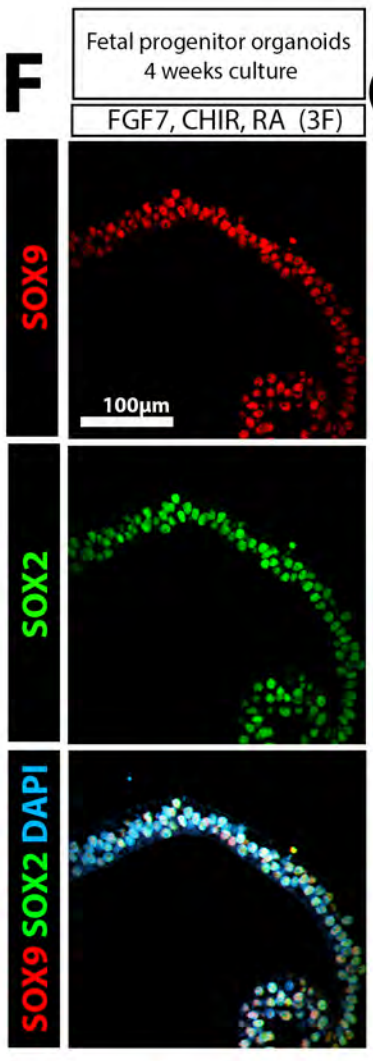

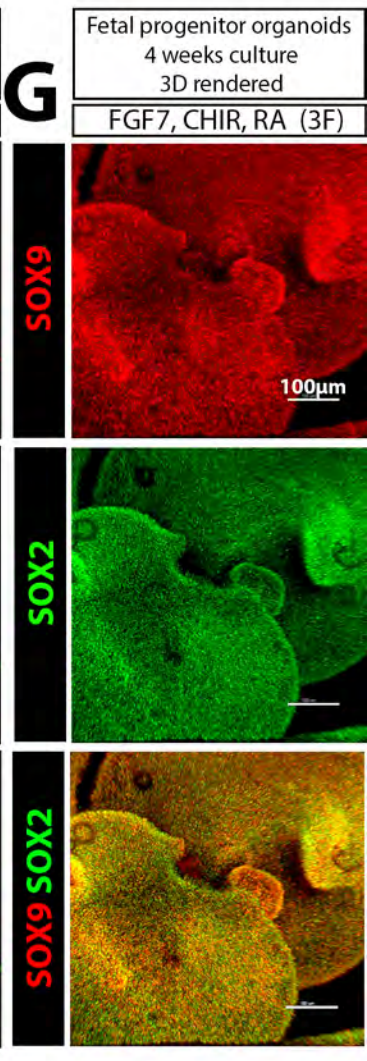

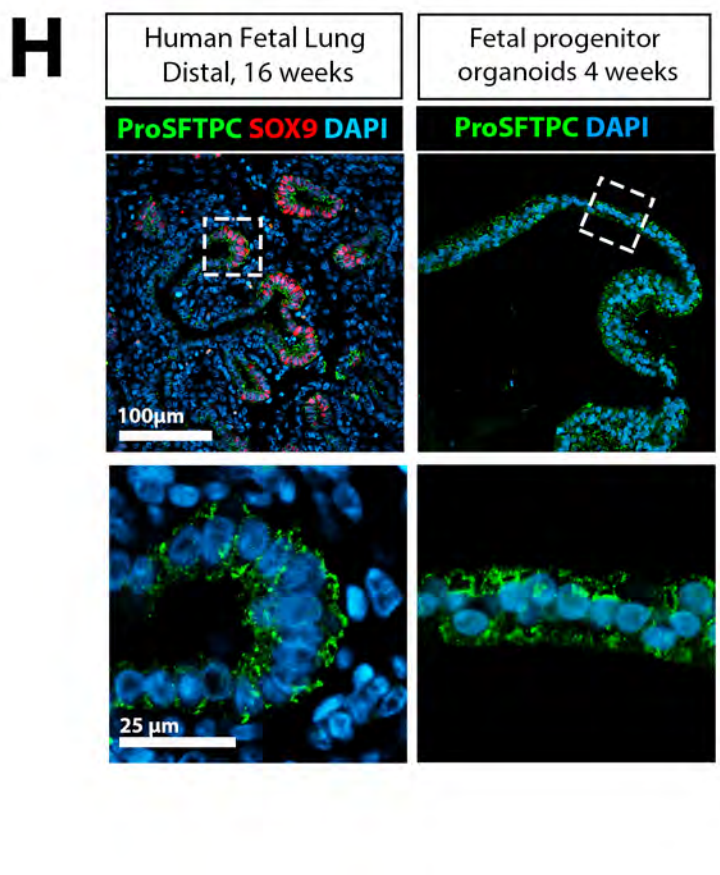

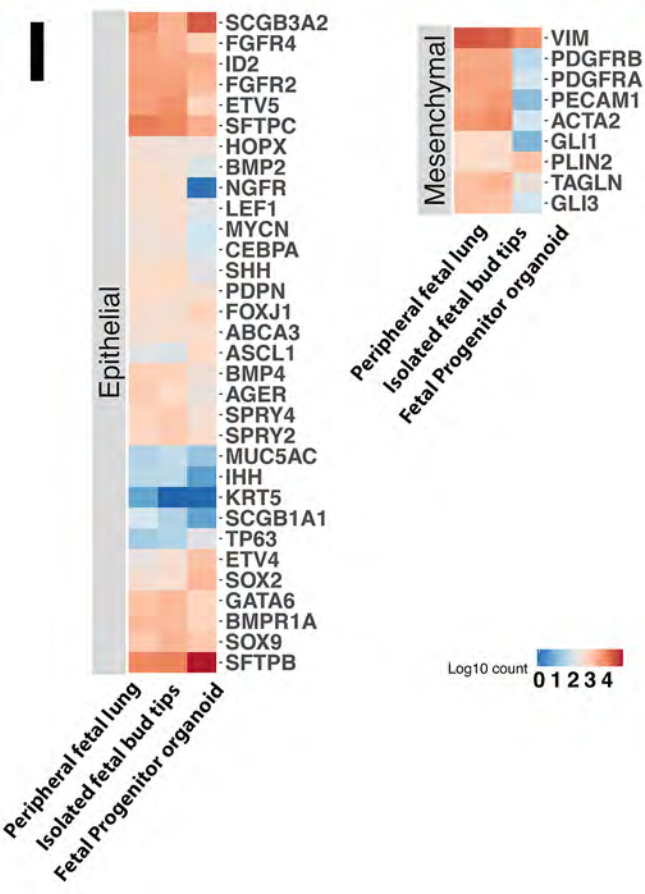

Figure 1 - Figure Supplement 1

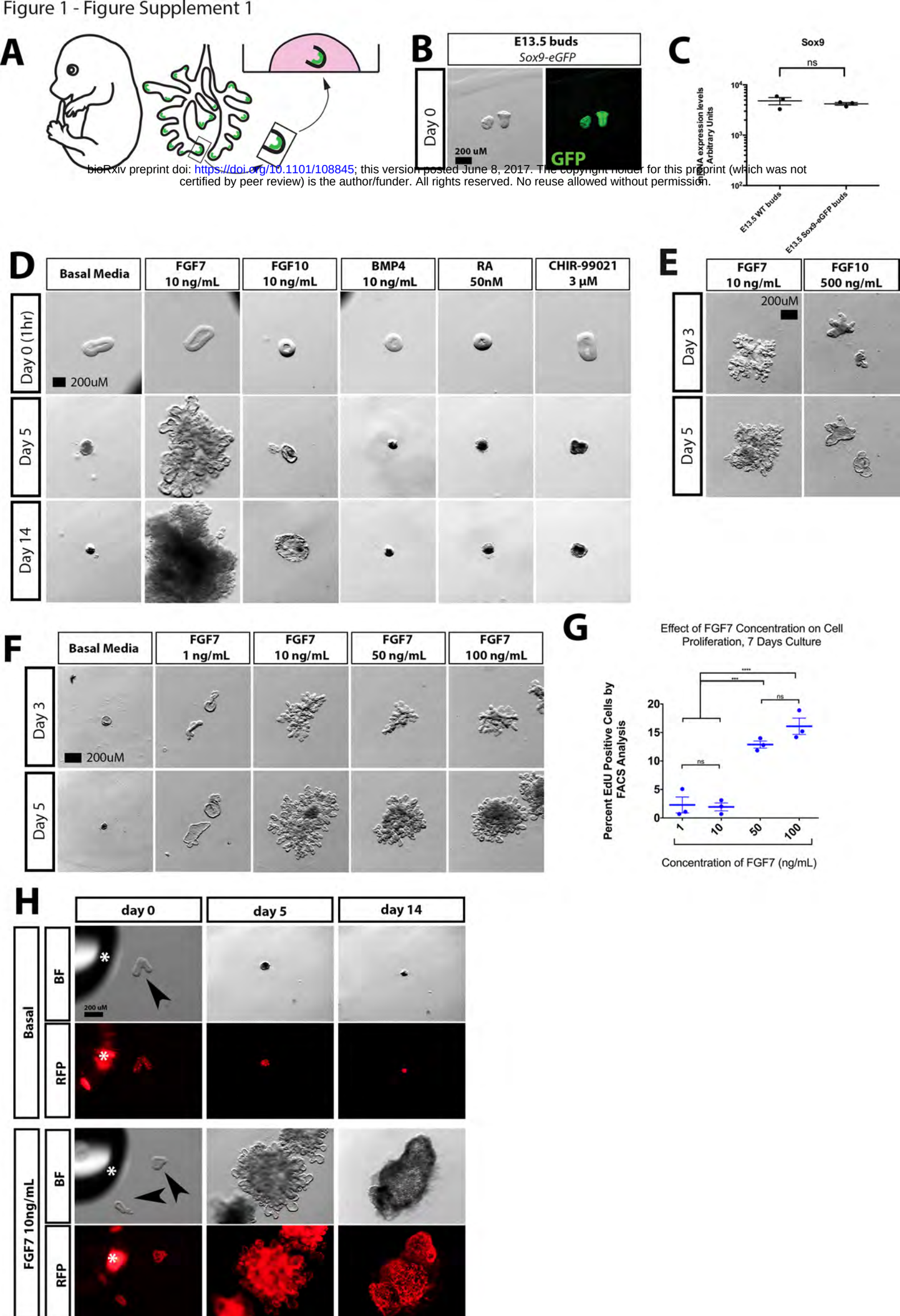

Figure 1 - Figure Supplement 2

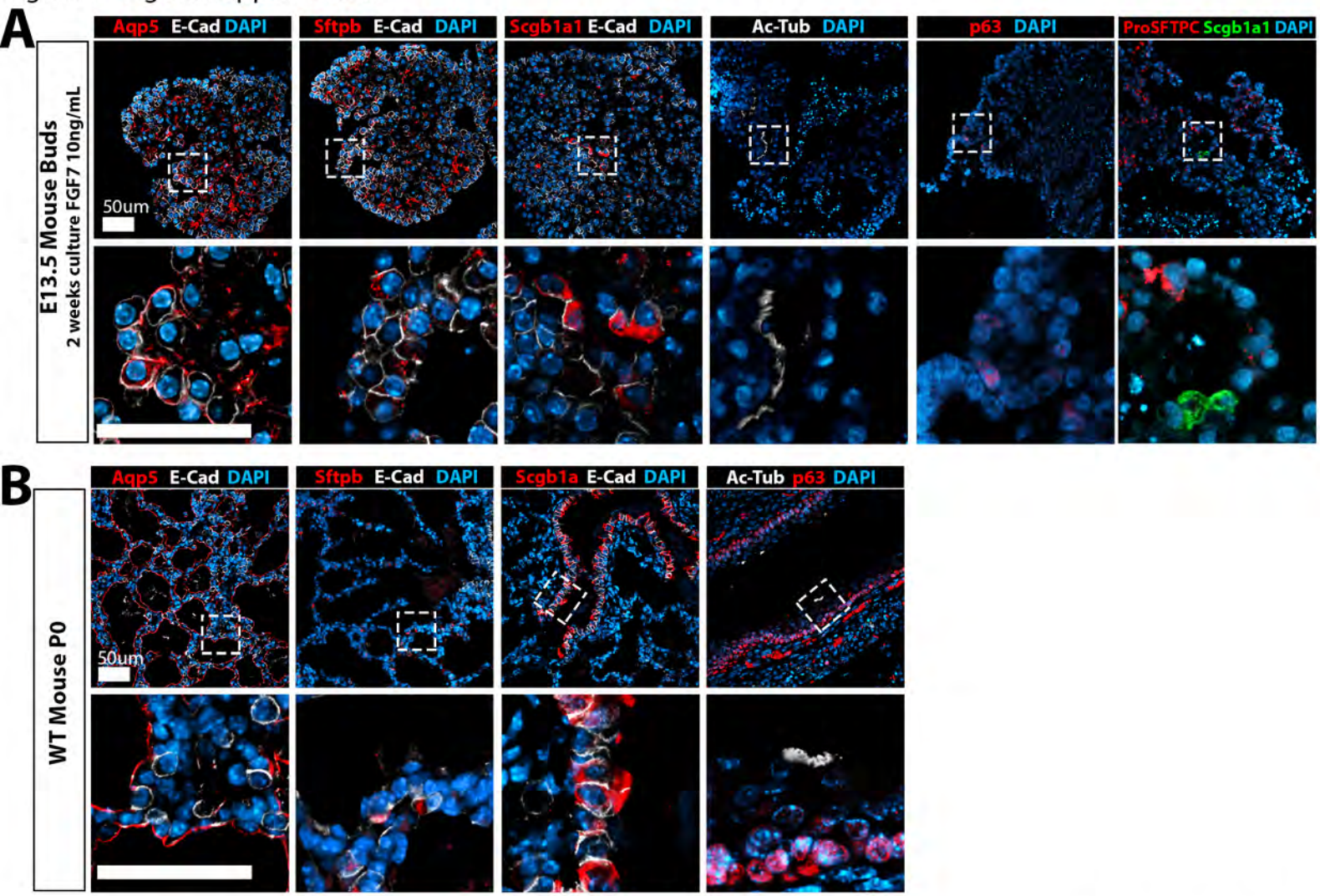

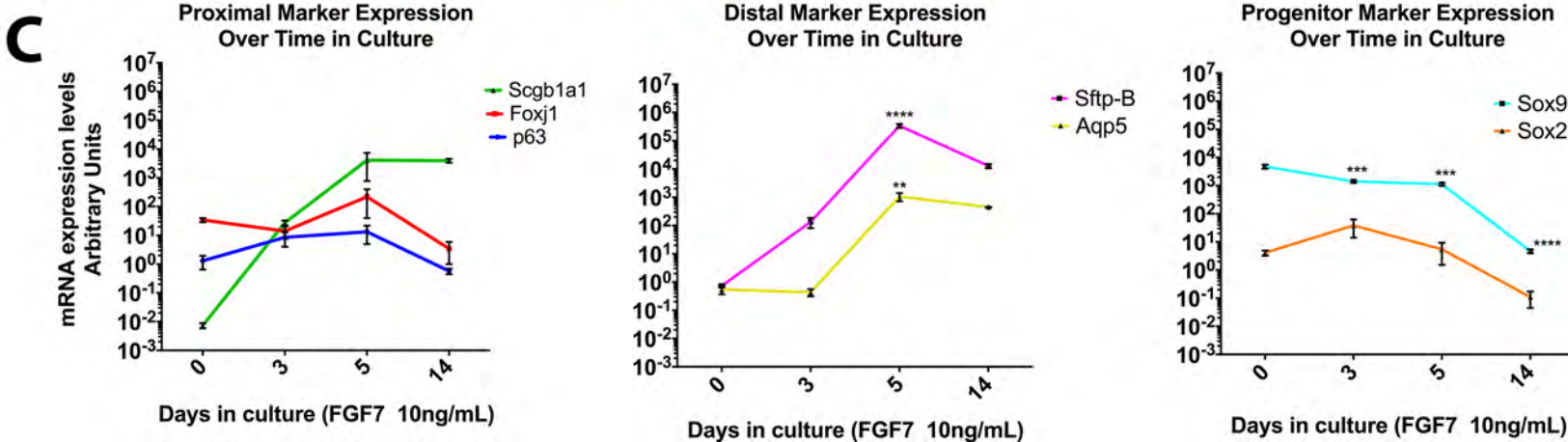

Figure 1 - Figure Supplement 3

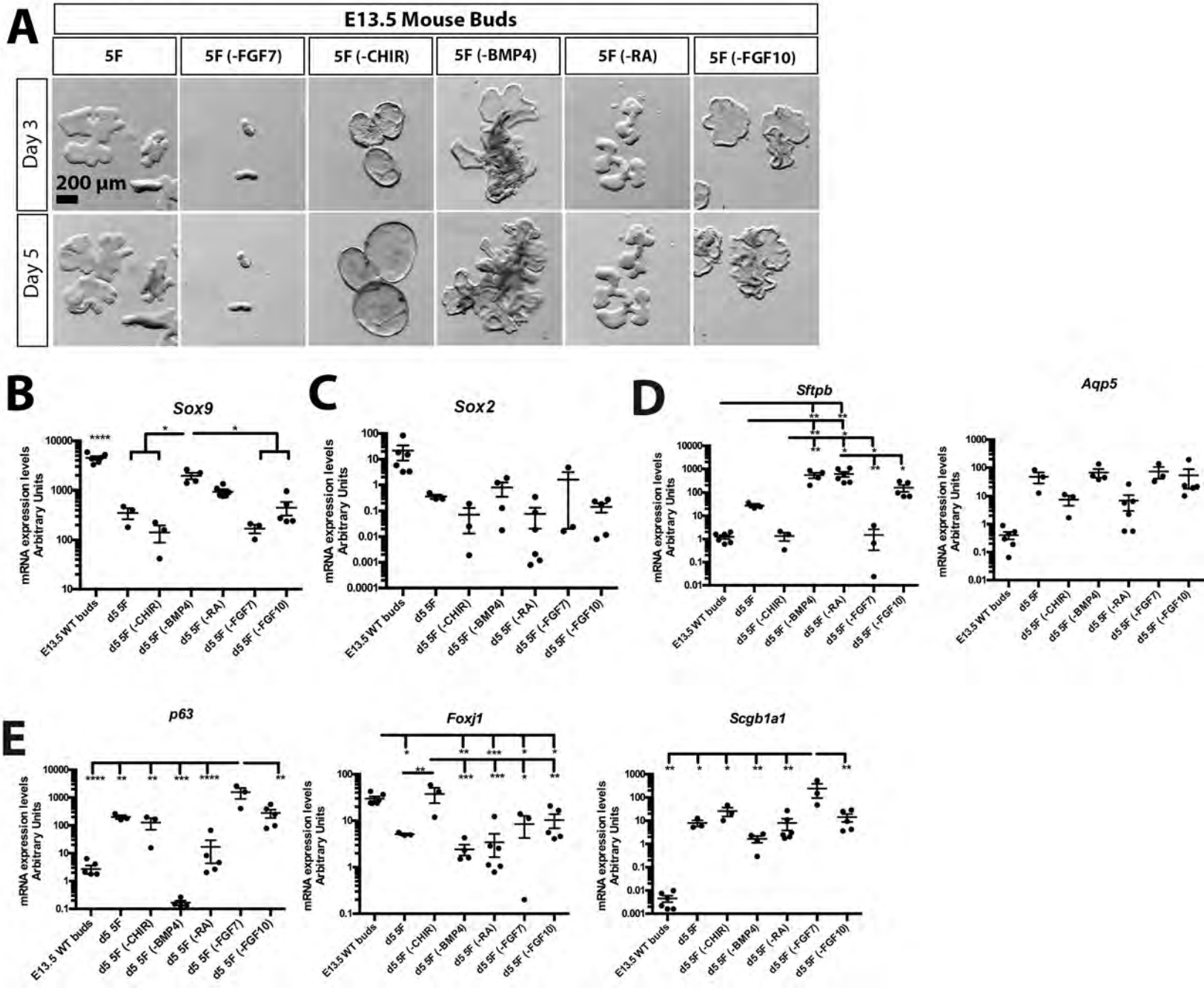

Figure 1 - Figure Supplement 4

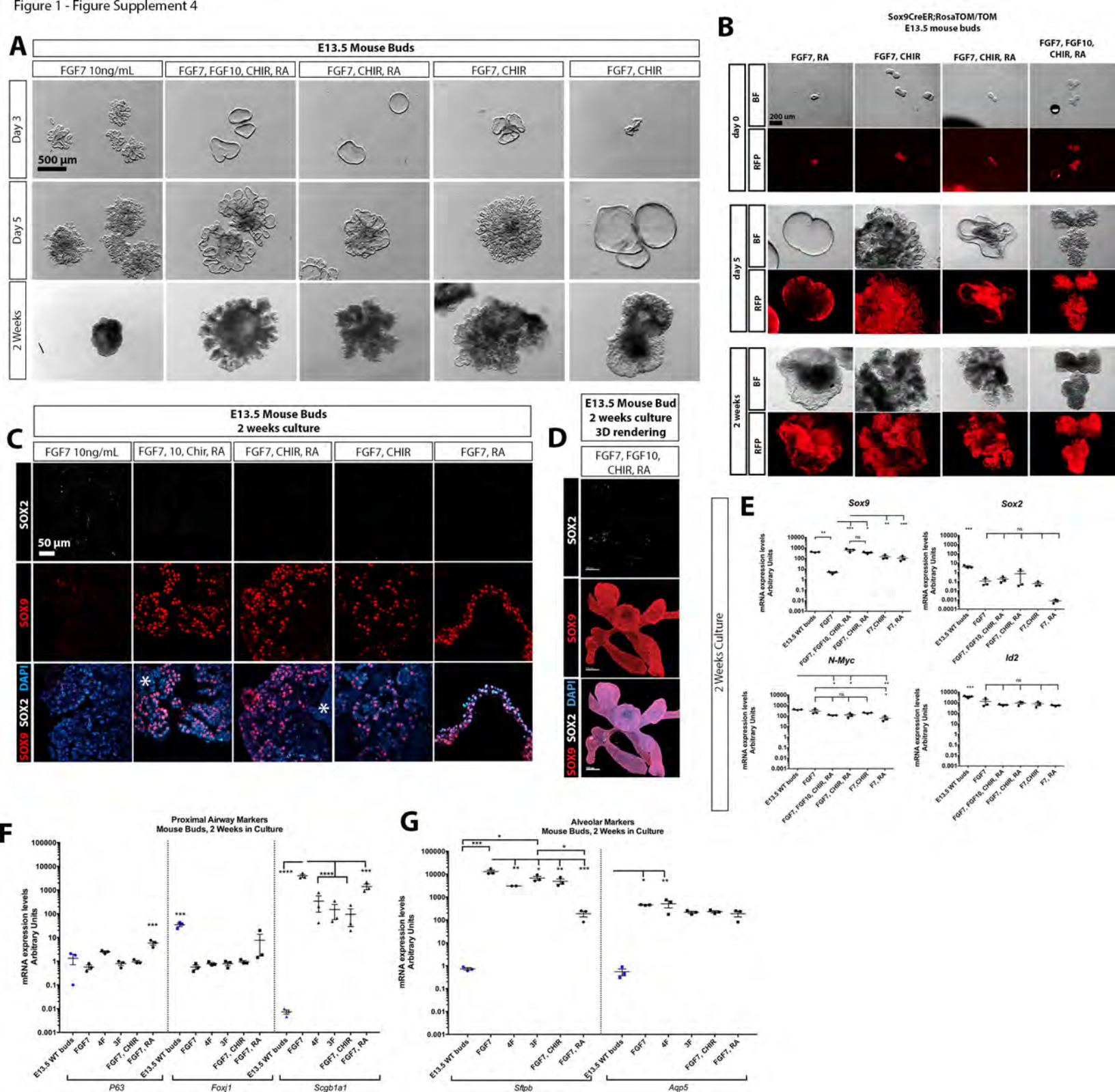

Figure 1 - Figure Supplement 5

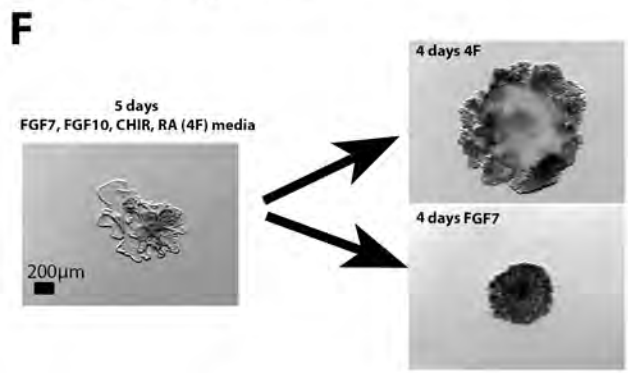

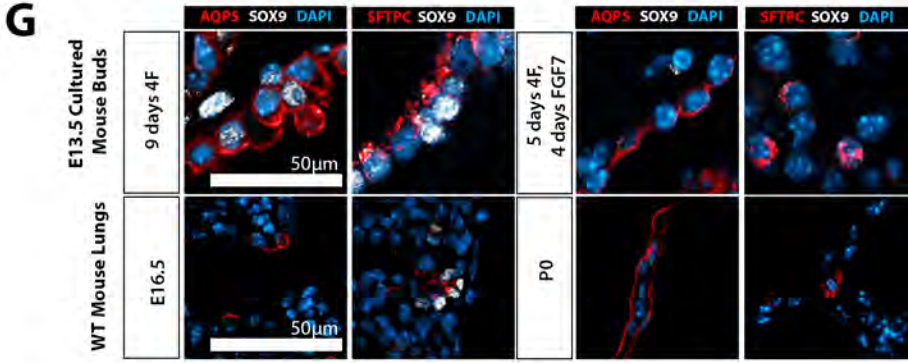

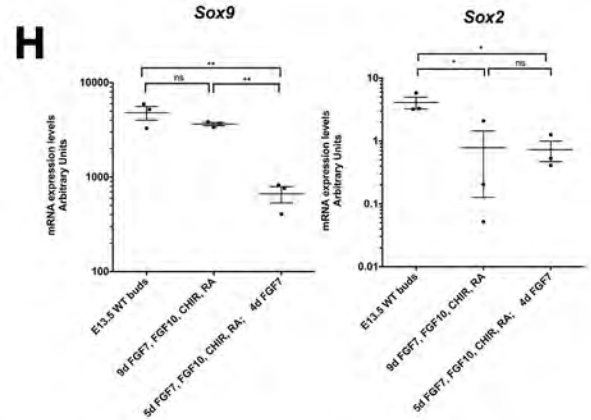

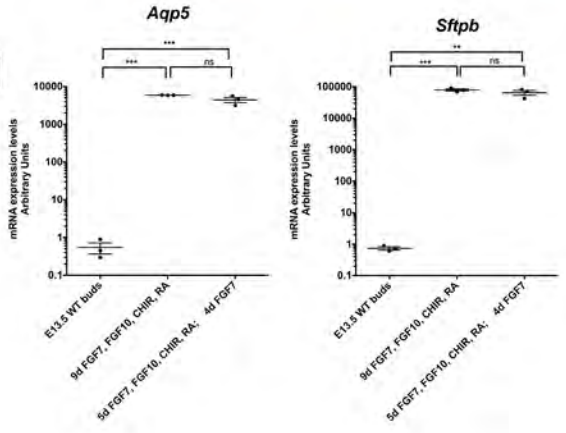

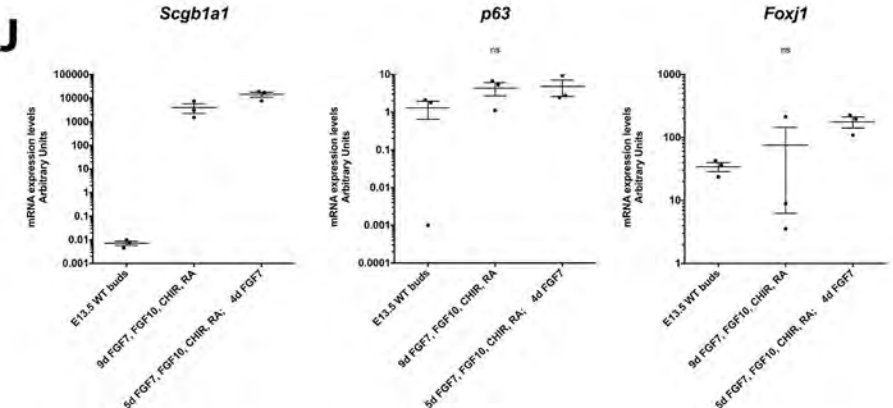

Figure 1 - Figure Supplement 6

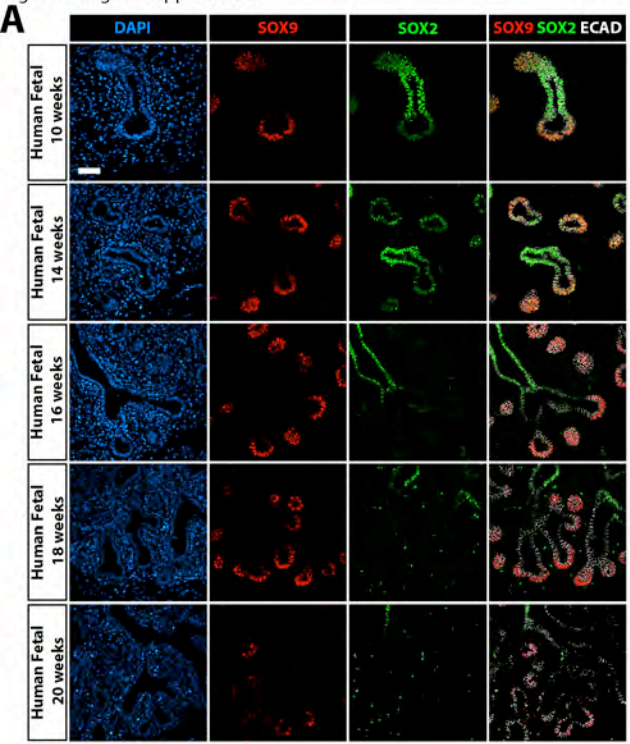

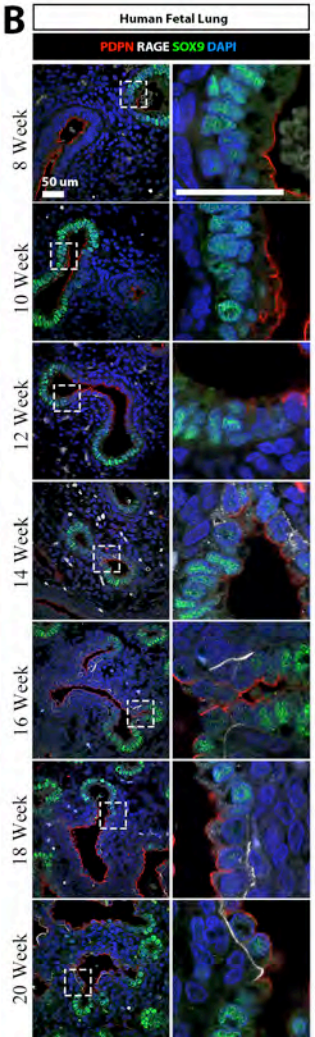

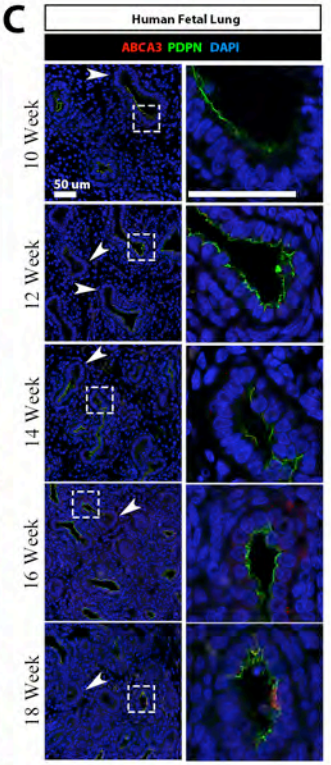

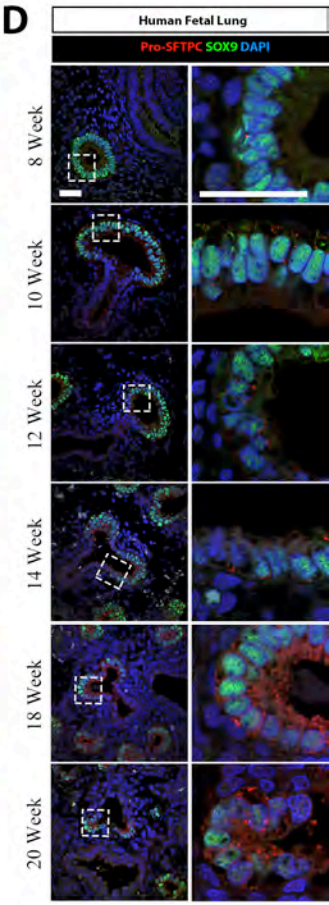

Figure 1 - Figure Supplement 7

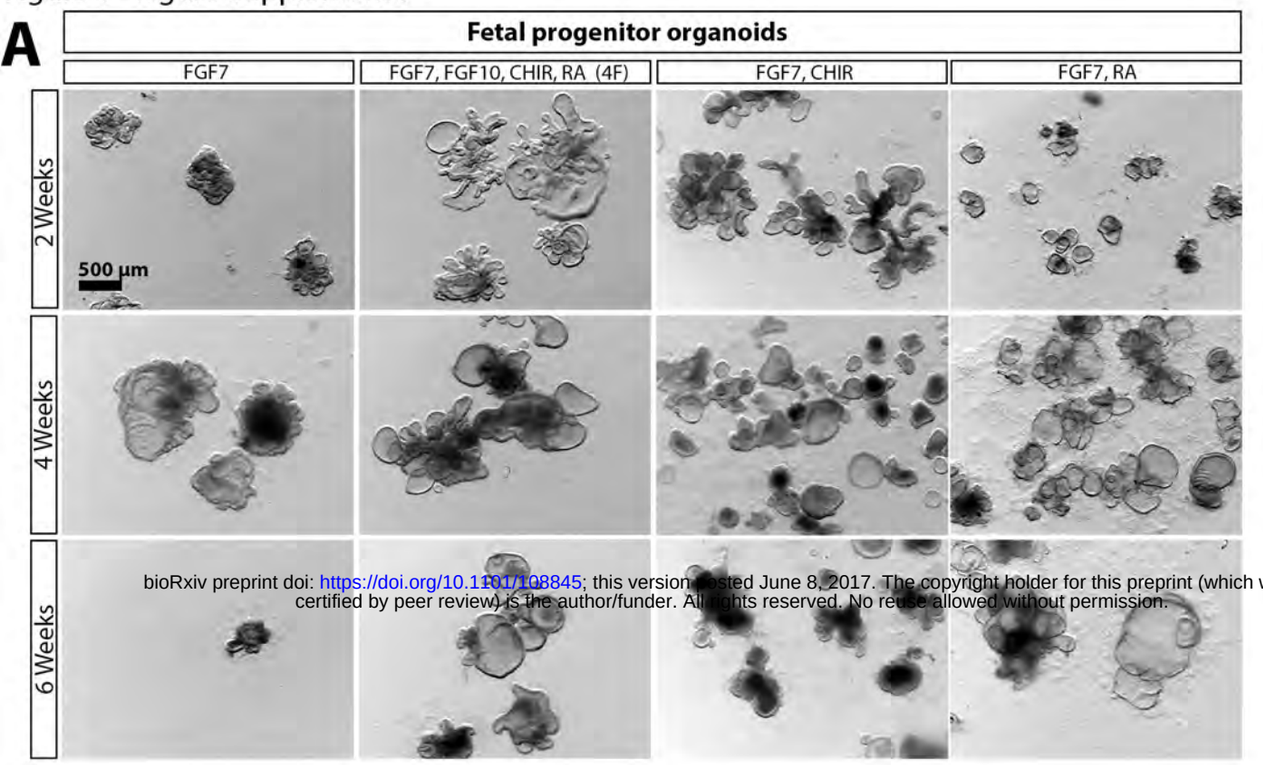

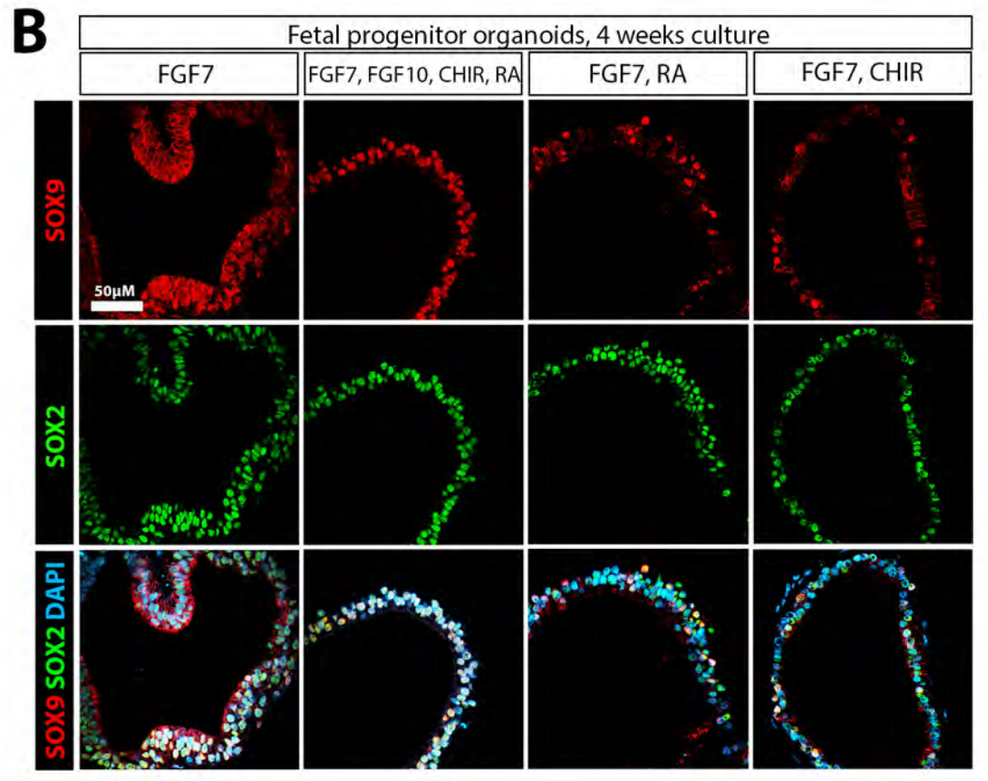

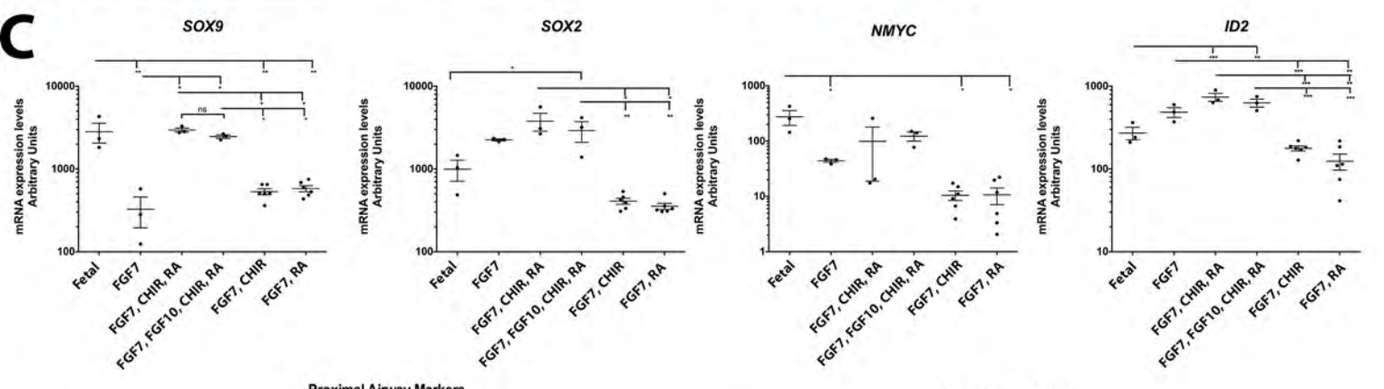

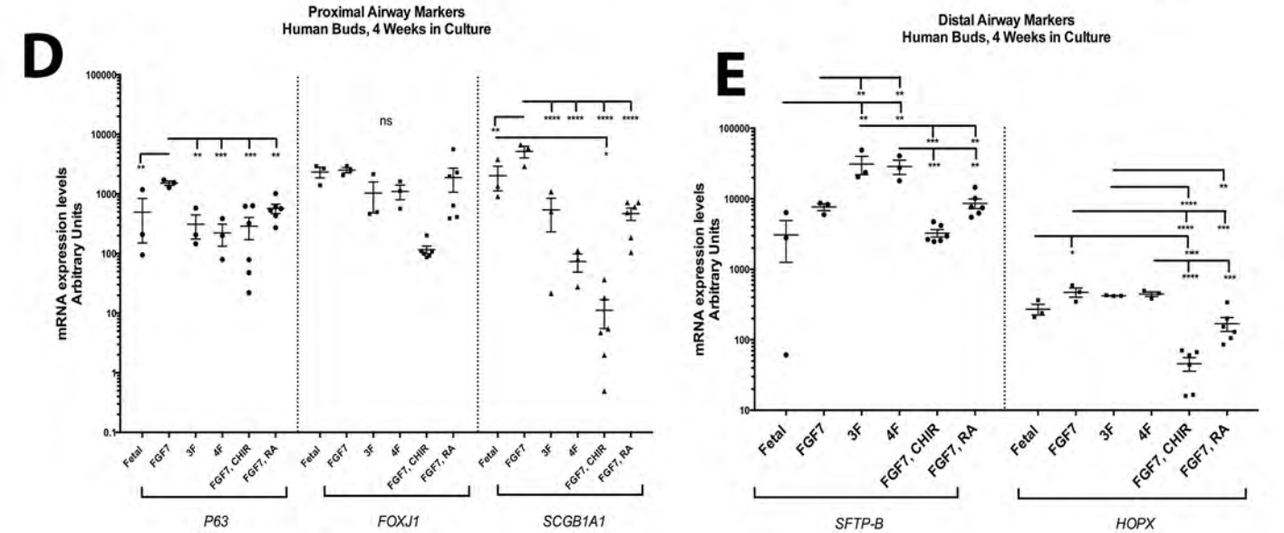

Figure 1 - Figure Supplement 8

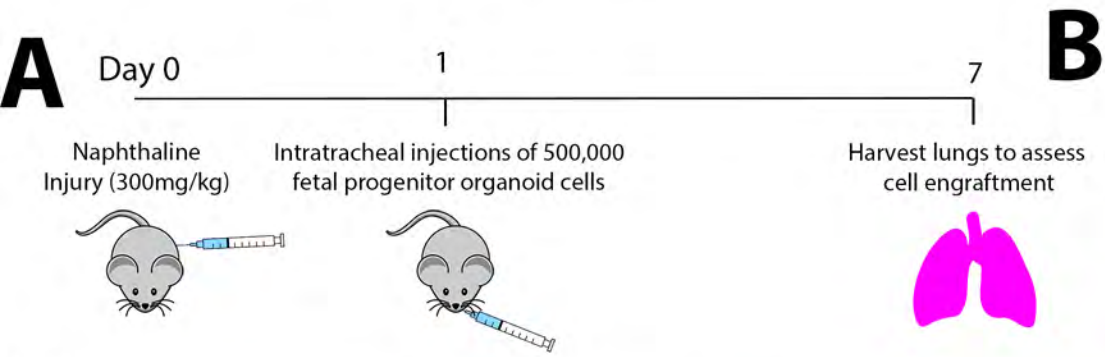

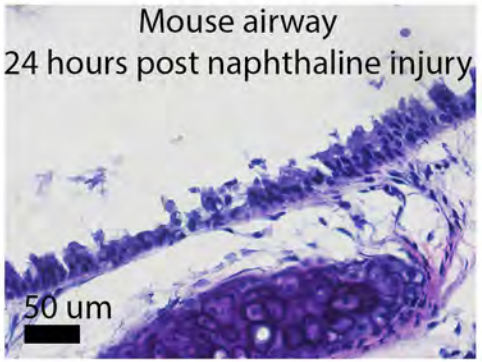

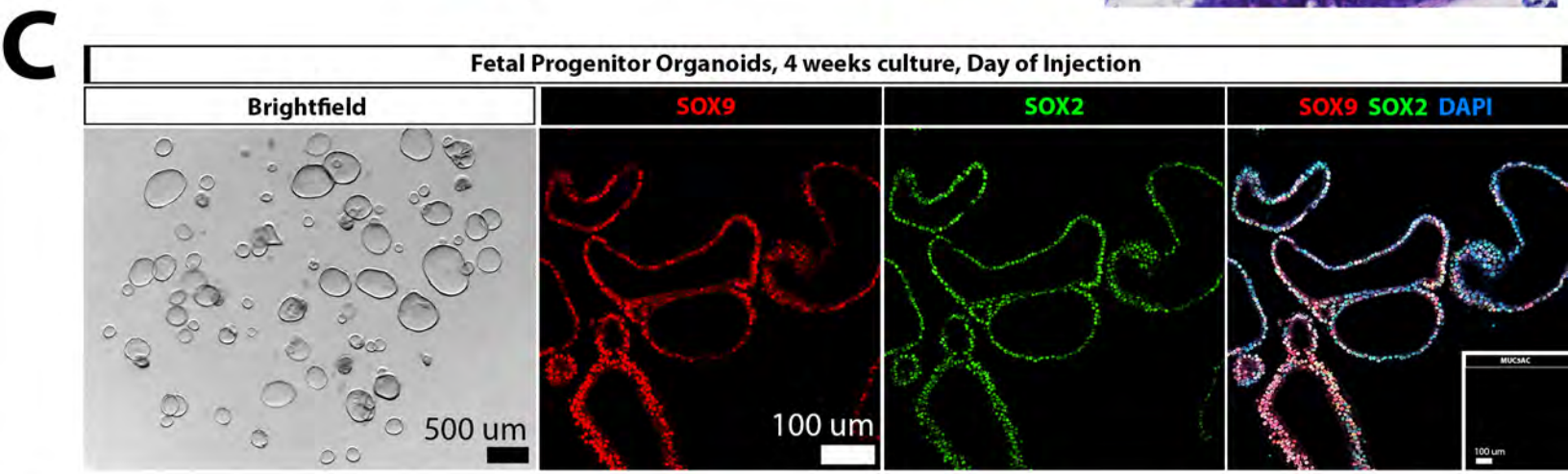

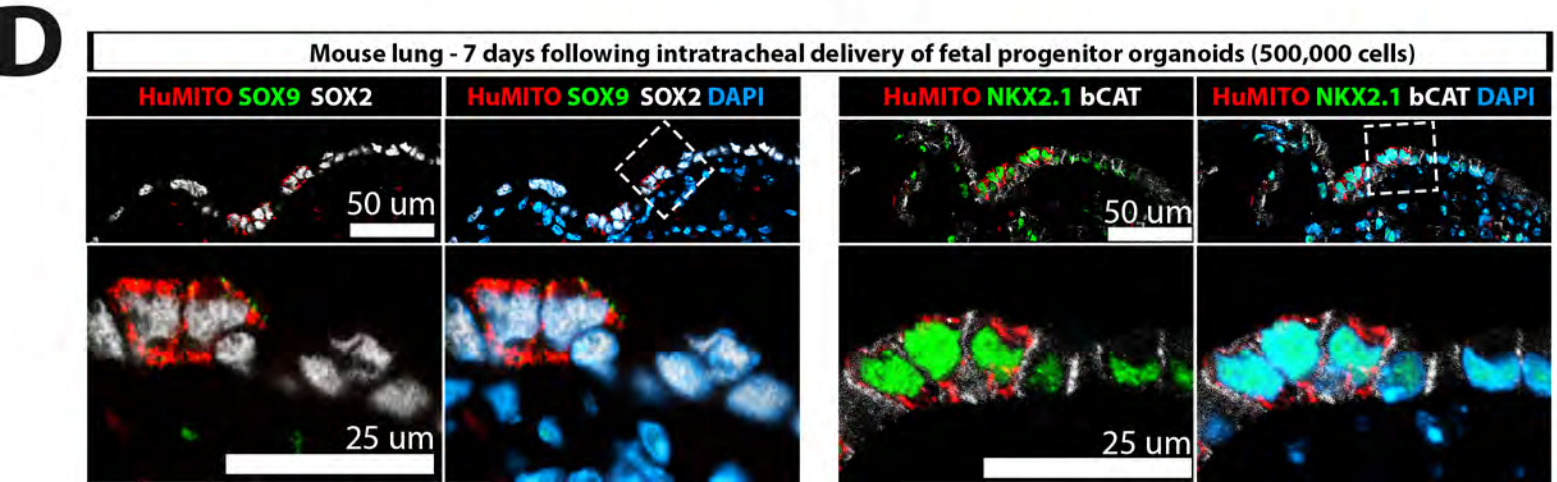

Figure 2

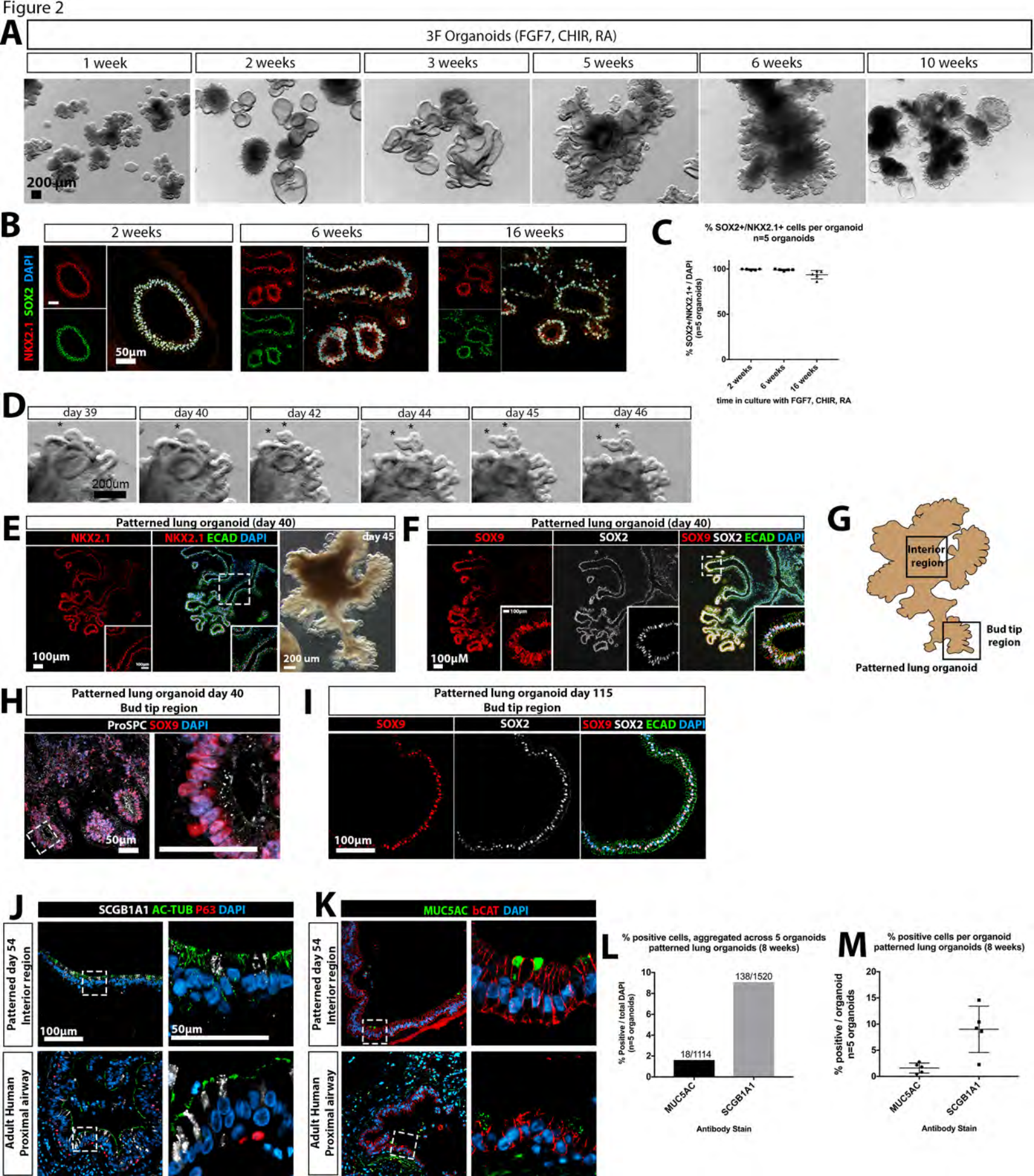
A
3F Organoids (FGF7, CHIR, RA)
1 week
2 weeks
3 weeks
5 weeks
6 weeks
10 weeks
200 µm
B
2 weeks
6 weeks
16 weeks
NKX2.1 SOX2 DAPI
50µm
C
% SOX2+/NKX2.1+ cells per organoid
n=5 organoids
% SOX2+/NKX2.1+ / DAPI
(n=5 organoids)
100
50
0
2 weeks
6 weeks
16 weeks
time in culture with FGF7, CHIR, RA
D
day 39
day 40
day 42
day 44
day 45
day 46
200um
E
Patterned lung organoid (day 40)
NKX2.1
NKX2.1 ECAD DAPI
day 45
100µm
200 um
F
Patterned lung organoid (day 40)
SOX9
SOX2
SOX9 SOX2 ECAD DAPI
100µM
G
Interior region
Bud tip region
Patterned lung organoid
H
Patterned lung organoid day 40
Bud tip region
ProSPC SOX9 DAPI
50µm
I
Patterned lung organoid day 115
Bud tip region
SOX9
SOX2
SOX9 SOX2 ECAD DAPI
100µm
J
SCGB1A1 AC-TUB P63 DAPI
Patterned day 54
Interior region
Adult Human
Proximal airway
100µm
50µm
K
MUC5AC bCAT DAPI
Patterned day 54
Interior region
Adult Human
Proximal airway
L
% positive cells, aggregated across 5 organoids
patterned lung organoids (8 weeks)
% Positive / total DAPI
(n=5 organoids)
10
8
6
4
2
0
18/1114
138/1520
MUC5AC
SCGB1A1
Antibody Stain
M
% positive cells per organoid
patterned lung organoids (8 weeks)
% positive / organoid
n=5 organoids
20
15
10
5
0
MUC5AC
SCGB1A1
Antibody Stain

Figure 2 - Figure Supplement 1

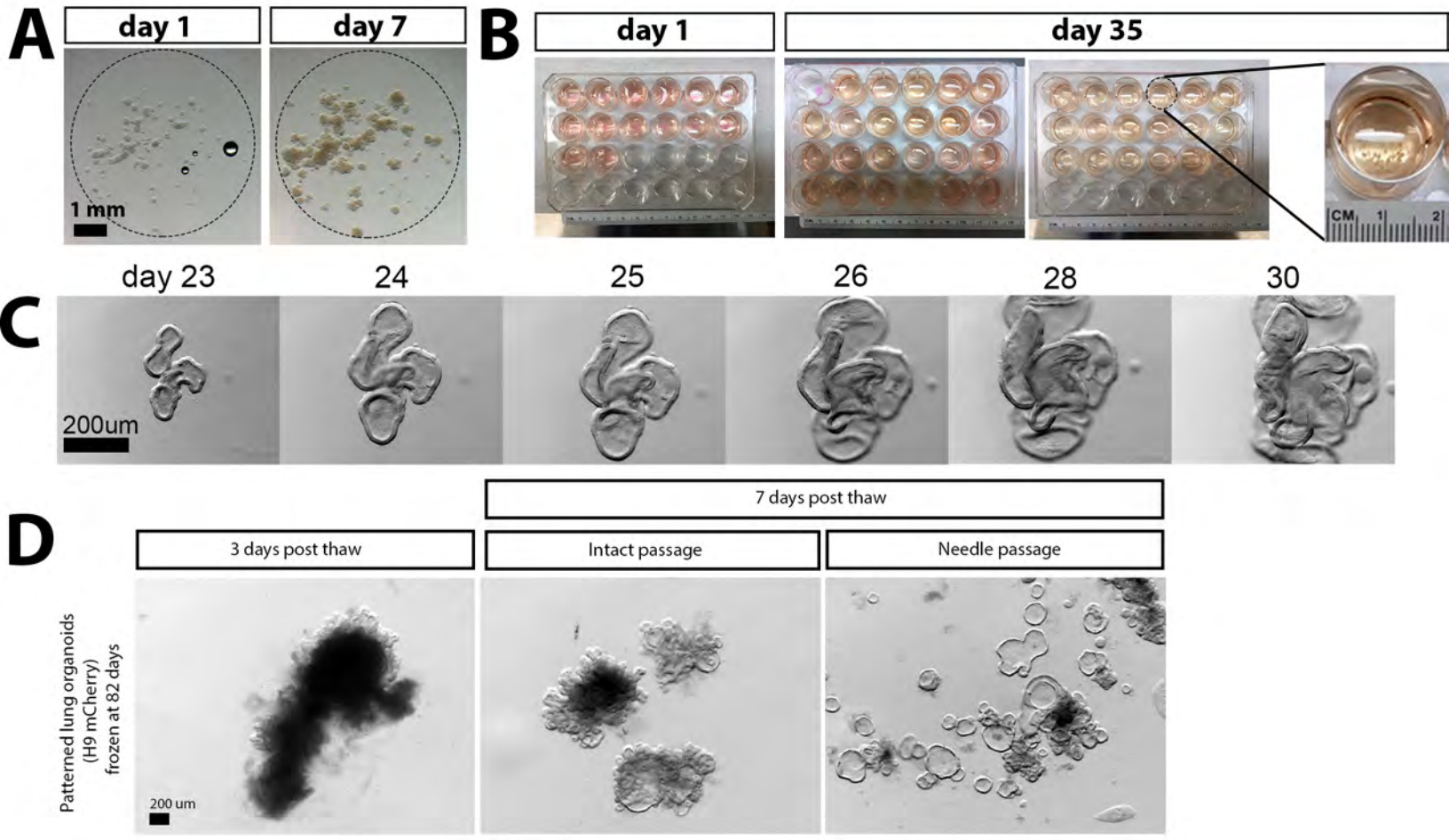

Figure 2 - Figure Supplement 2

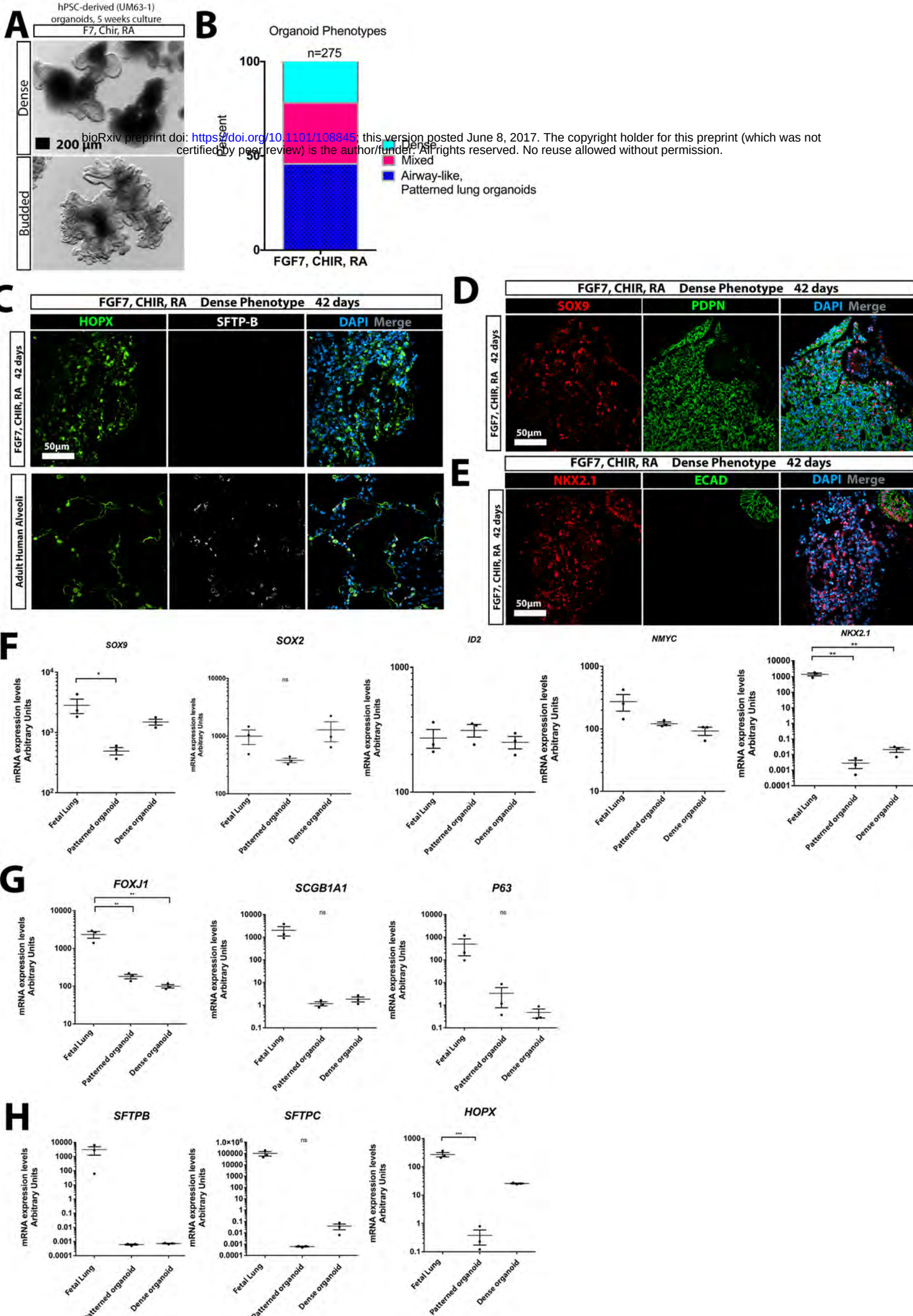

Figure 2 - Figure Supplement 3

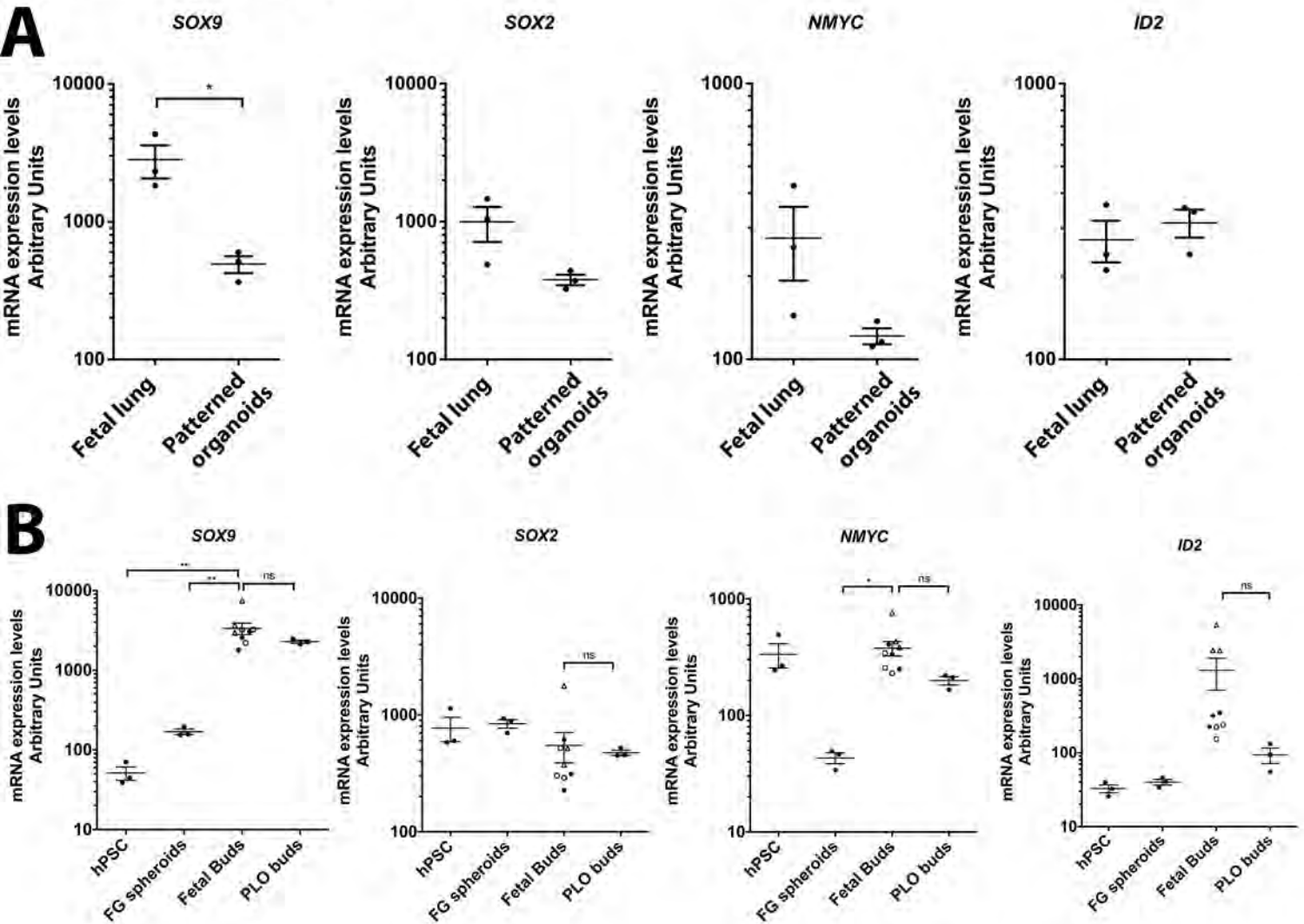

Figure 3

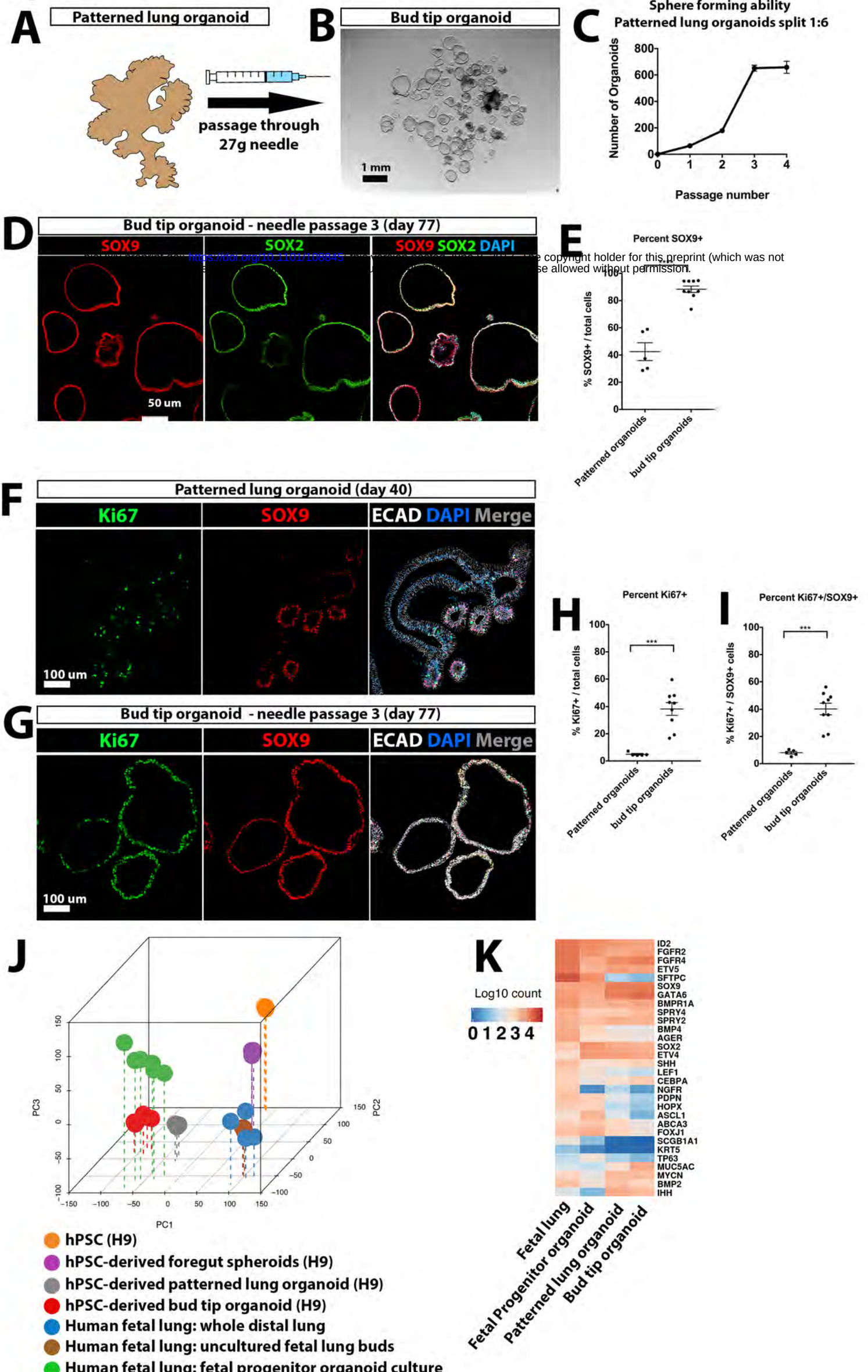

Figure 3 - Figure Supplement 1

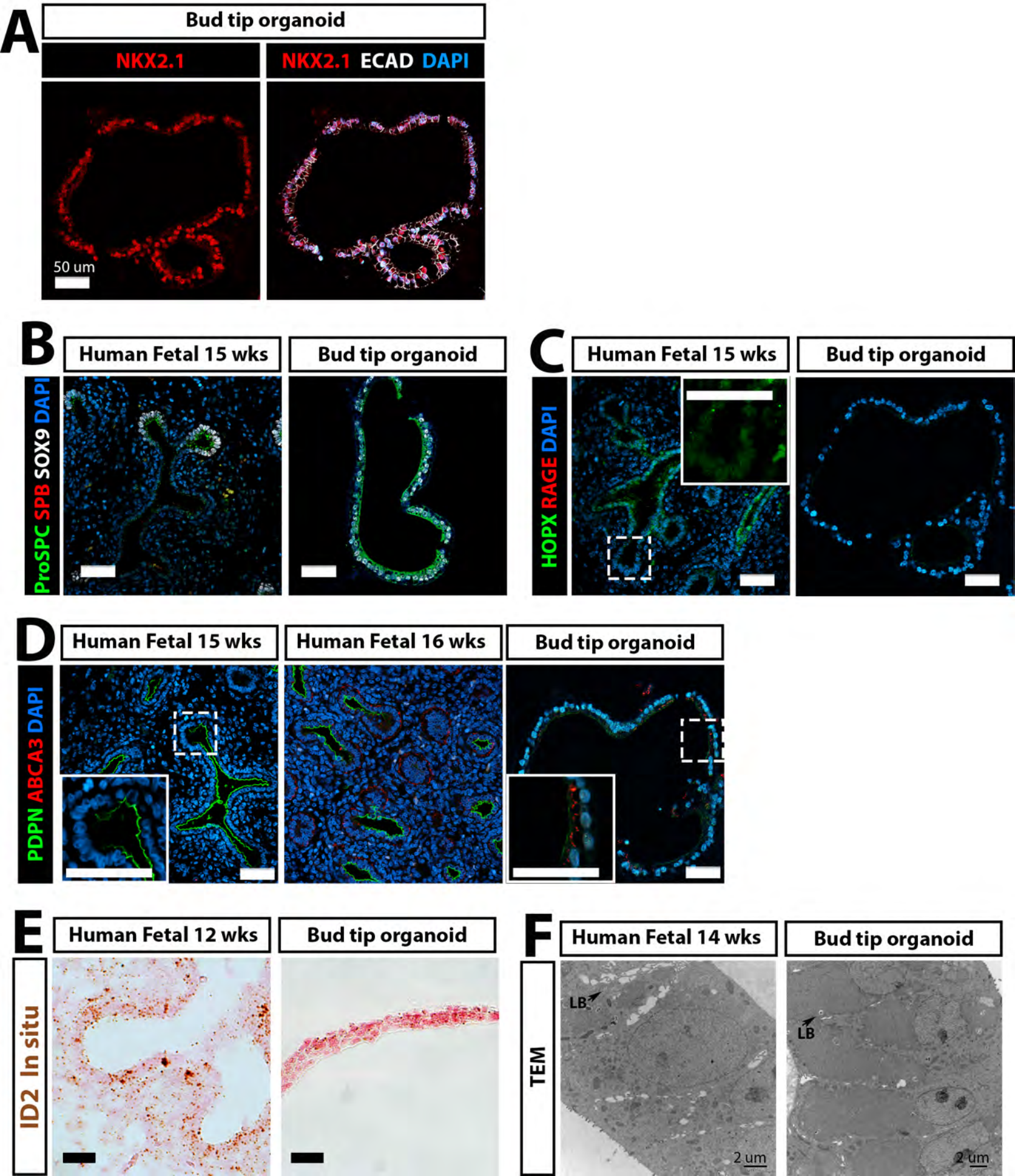

Figure 4

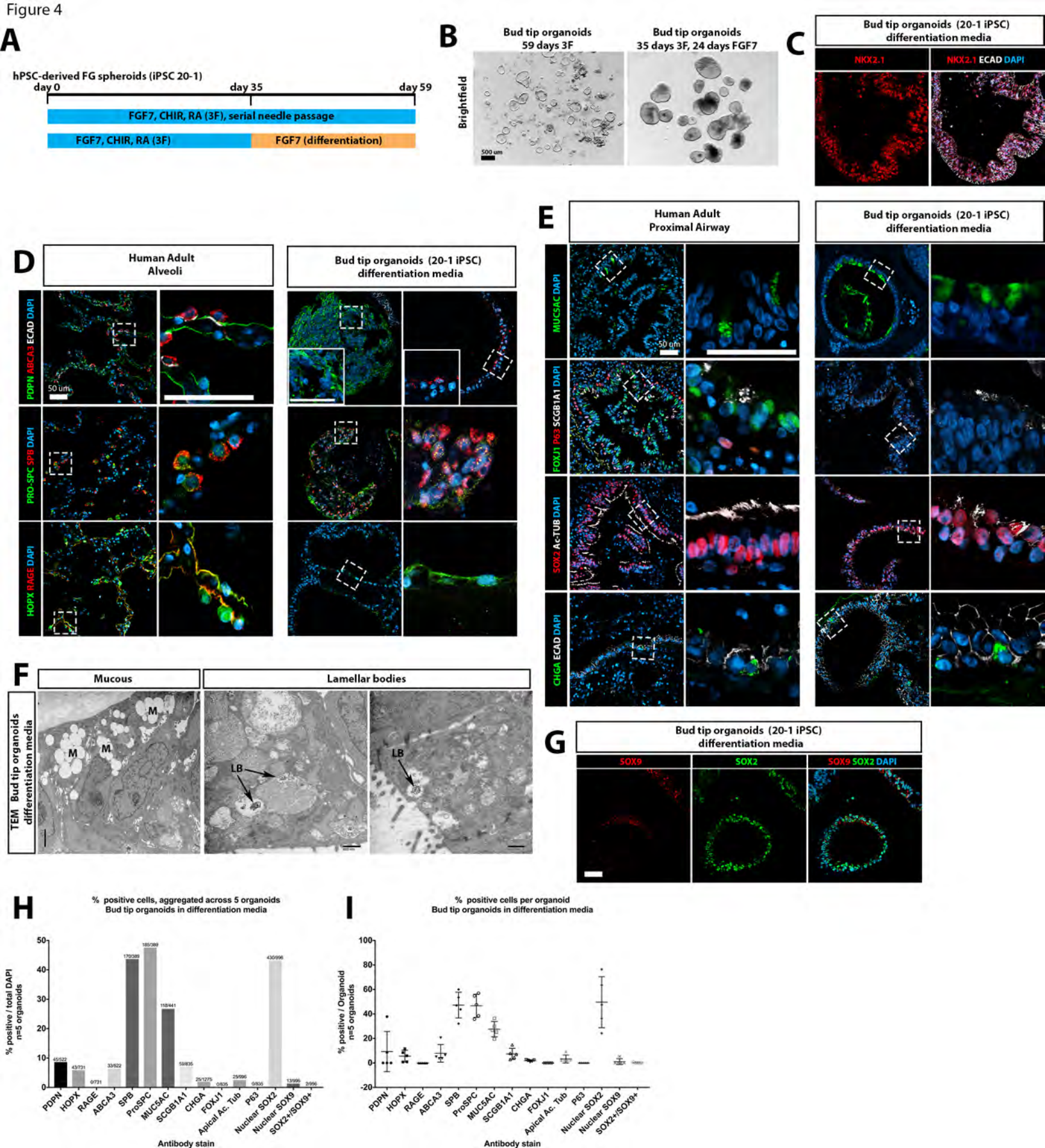
A
hPSC-derived FG spheroids (iPSC 20-1)
day 0
day 35
day 59
FGF7, CHIR, RA (3F), serial needle passage
FGF7, CHIR, RA (3F)
FGF7 (differentiation)
B
Bud tip organoids 59 days 3F
Bud tip organoids 35 days 3F, 24 days FGF7
Brightfield
500 um
C
Bud tip organoids (20-1 iPSC) differentiation media
NKX2.1
NKX2.1 ECAD DAPI
D
Human Adult Alveoli
Bud tip organoids (20-1 iPSC) differentiation media
PDPN ABCA3 ECAD DAPI
PRO-SPC SPB DAPI
HOPX RAGE DAPI
50 um
E
Human Adult Proximal Airway
Bud tip organoids (20-1 iPSC) differentiation media
MUCSAC DAPI
FOXJ1 P63 SCGB1A1 DAPI
SOX2 Ac-TUB DAPI
CHGA ECAD DAPI
50 um
F
Mucous
Lamellar bodies
TEM Bud tip organoids differentiation media
M
LB
G
Bud tip organoids (20-1 iPSC) differentiation media
SOX9
SOX2
SOX9 SOX2 DAPI
H
% positive cells, aggregated across 5 organoids
Bud tip organoids in differentiation media
% positive / total DAPI n=5 organoids
45/522
43/731
0/731
33/822
170/389
185/389
118/441
59/835
25/1275
0/835
25/996
0/835
430/996
13/996
2/996
PDPN
HOPX
RAGE
ABCA3
SPB
ProSPC
MUC5AC
SCGB1A1
CHGA
FOXJ1
Apical Ac. Tub
P63
Nuclear SOX2
Nuclear SOX9
SOX2+/SOX9+
Antibody stain
I
% positive cells per organoid
Bud tip organoids in differentiation media
% positive / Organoid n=5 organoids
Antibody stain

Figure 5

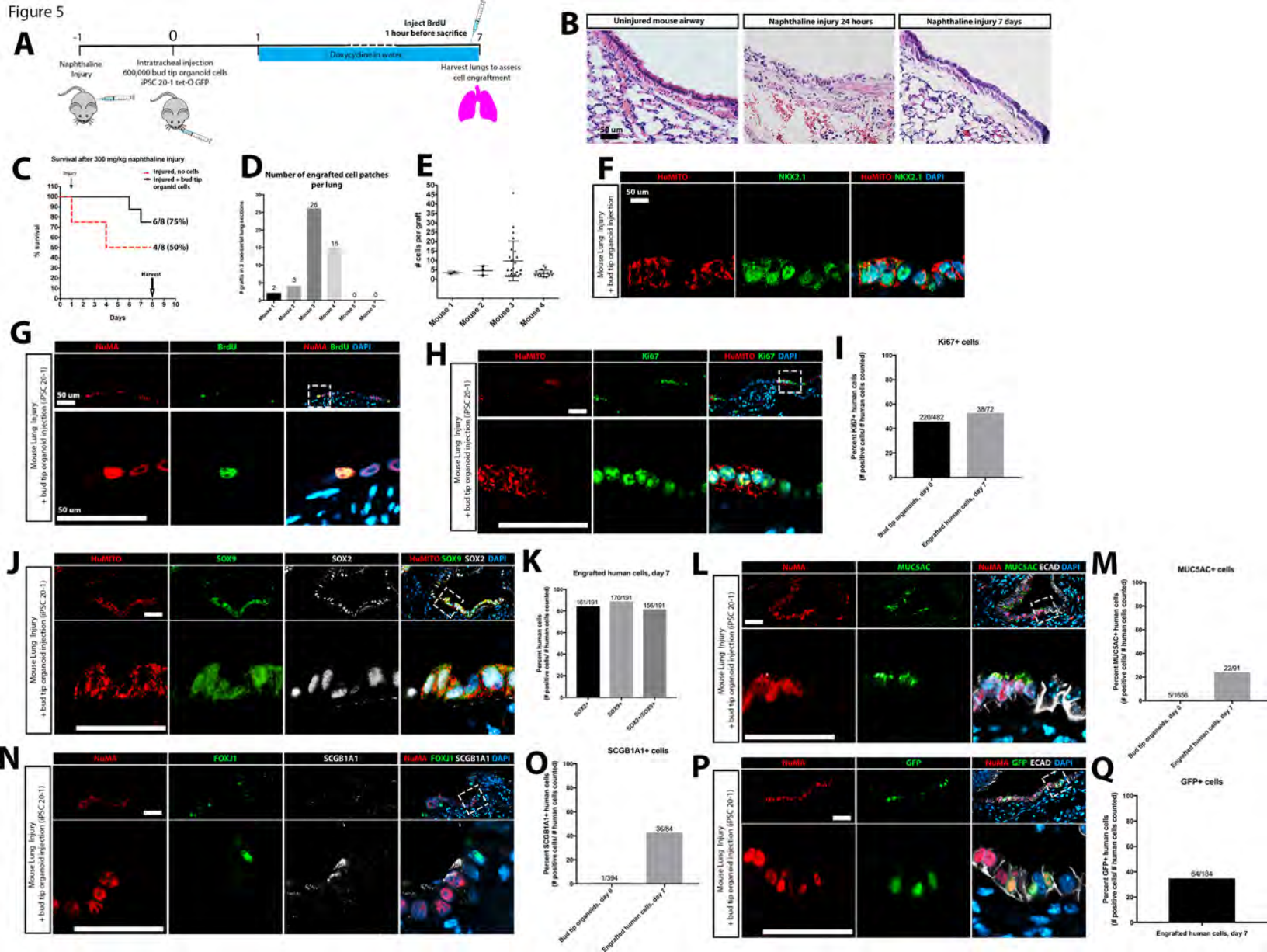
A
-1
0
1
7
Inject BrdU
1 hour before sacrifice
Naphthaline Injury
Intratracheal injection
600,000 bud tip organoid cells
iPSC 20-1 tet-O GFP
Doxycycline in water
Harvest lungs to assess cell engraftment
B
Uninjured mouse airway
Naphthaline injury 24 hours
Naphthaline injury 7 days
50 um
C
Survival after 300 mg/kg naphthaline injury
Injury
Injured, no cells
Injured + bud tip organoid cells
% survival
6/8 (75%)
4/8 (50%)
Harvest
Days
D
Number of engrafted cell patches per lung
grafts in 3 non-serial lung sections
2
3
26
15
0
0
E
cells per graft
Mouse 1
Mouse 2
Mouse 3
Mouse 4
F
HuMITO
NKX2.1
HuMITO NKX2.1 DAPI
50 um
Mouse Lung Injury + bud tip organoid injection
G
NuMA
BrdU
NuMA BrdU DAPI
50 um
Mouse Lung Injury + bud tip organoid injection (iPSC 20-1)
H
HuMITO
Ki67
HuMITO Ki67 DAPI
Mouse Lung Injury + bud tip organoid injection (iPSC 20-1)
I
Ki67+ cells
Percent Ki67+ human cells (# positive cells/ # human cells counted)
220/482
38/72
Bud tip organoids, day 0
Engrafted human cells, day 7
J
HuMITO
SOX9
SOX2
HuMITO SOX9 SOX2 DAPI
Mouse Lung Injury + bud tip organoid injection (iPSC 20-1)
K
Engrafted human cells, day 7
Percent human cells (# positive cells/ # human cells counted)
161/191
170/191
156/191
SOX2+
SOX9+
SOX2+SOX9+
L
NuMA
MUC5AC
NuMA MUC5AC ECAD DAPI
Mouse Lung Injury + bud tip organoid injection (iPSC 20-1)
M
MUC5AC+ cells
Percent MUC5AC+ human cells (# positive cells/ # human cells counted)
5/1656
22/91
Bud tip organoids, day 0
Engrafted human cells, day 7
N
NuMA
FOXJ1
SCGB1A1
NuMA FOXJ1 SCGB1A1 DAPI
Mouse Lung Injury + bud tip organoid injection (iPSC 20-1)
O
SCGB1A1+ cells
Percent SCGB1A1+ human cells (# positive cells/ # human cells counted)
1/394
36/84
Bud tip organoids, day 0
Engrafted human cells, day 7
P
NuMA
GFP
NuMA GFP ECAD DAPI
Mouse Lung Injury + bud tip organoid injection (iPSC 20-1)
Q
GFP+ cells
Percent GFP+ human cells (# positive cells/ # human cells counted)
64/184
Engrafted human cells, day 7

Figure 5 - Figure Supplement 1